PhD degree in Molecular Medicine

European School of Molecular Medicine (SEMM),

University of Milan, Faculty of Medicine

Settore disciplinare: MED/04

MicroRNA involvement in colon cancer progression

Viktorija Sokolova

IFOM-IEO Campus, Milan

Matricola n. R07952

Supervisor: **Dott. Marco A. Pierotti, PhD**

IFOM-IEO Campus, Milan

Added co-Supervisor: **Dott.ssa Manuela Gariboldi**

IFOM-IEO Campus, Milan

Anno accademico 2010-2011

TABLE OF CONTENTS

FIGURES INDEX

ABSTRACT

Loss of response to TGF-β occurs in many cancers and disruption of its regulatory circuitry appears as a central event in the genesis of colorectal cancer (CRC) malignancy. Lack of inhibitory response to TGF-β is common to most colon cancer cell lines. However, inactivating mutations at receptors and transducers occur in less than a half of neoplastic colon tissues, which underscore the significance of additional mechanisms diverting TGF-β growth suppression. In this context, abrogation of TGF-β response by some miRNAs has been recently reported.

By searching for miRNAs in regions showing copy number changes and concordant gene expression in 36 sporadic CRCs compared to their normal counterpart, we identified the miR-17-92 cluster on the 13q31 locus, which is gained and highly expressed at early stages of CRC. We hypothesized an involvement of miR-20a in the suppression of TGF-β response in CRCs and selected the TGF-β sensitive FET colon carcinoma, expressing low miR-20a levels, to investigate the relationship between enhanced expression of miR-20a and TGF-β sensitivity and address growth inhibition.

We found that miR-20a affects regulation of p21 expression, has a negative and significant effect on the cytostatic response mediated by TGF-β, as evaluated by BrdU incorporation, MTT assay, and cell-cycle analysis, but shows little effect on TGF-β untreated cells. Although CDKN1A transcript and protein are significantly decreased in cells treated or not with the cytokine, we could observe that the p21 up-regulation driven by TGF-β is twofold lower after miR-20a administration.

We confirmed that p21 down-modulation is addressed by the direct binding of its 3'-UTR by miR-20a. Moreover, we observed that miR-20a is also able to block the transactivation of the 2.3-kb CDKN1A promoter upon TGF-β stimulation, as assessed by luciferase-based assay, but not the activation of the Smad3/4-reponsive reporter. Down-modulation of c-Myc by TGF-β, crucial to regulation of CDKN1A transcription, is also subverted by miR-20a delivery into cells.

Using luciferase reporter assays we demonstrated that two of the c-MYC repressor genes, E2F5 and KLF11, are directly targeted by miR-20a thus resulting in abrogation of the TGF-β mediated repression of c-MYC.
Our experiments suggest for miR-20a an interference with the TGF-β homeostasis in colon addressing the up-regulation of p21 expression, through mechanisms involving more effectors of the TGF-β cascade. Overall, miR-20a seems to participate in the abrogation of this key regulatory response in colonic epithelium.

Finally, analysis of the effects of TGF-β stimulation on miRNAs that we found altered in CRC, identified seven miRNAs whose expression was significantly induced by the cytokine. They could be further investigated to understand the mechanisms by which miRNAs and genes from this pathway regulate each other.

1 INTRODUCTION

1.1 HALLMARKS OF CANCER

Tumor formation is a complex process that usually proceeds over several years and drives normal cells evolution into cells with increasingly neoplastic phenotype and is driven by a sequence of randomly occurring mutations and epigenetic alterations of DNA that affect genes controlling crucial cellular processes, leading to malignant growth. The genetic abnormalities that contribute to cancer pathogenesis basically take place through two main mechanisms: inactivation of negative mediators of cell proliferation (including tumor suppressor genes) and activation of positive mediators of cell proliferation (including proto-oncogenes) [1].

These genetic alterations, involving cells and tissues bring also clearly to phenotypic and morphological onset that have been well characterized and can be summarized in the eight so called “Hallmarks of Cancer”: self-sufficiency in growth signals, insensitivity to anti-growth signals, limitless replicative potentials, evading apoptosis, sustained angiogenesis, tissue invasion and metastasis, and the last two, more recently defined, reprogramming of energy metabolism and evading immune destruction [2] (Figure 1). In addition, the biology of tumors should be investigated not only focusing on the traits of cancer cells, but also considering the contributions of the “tumor microenvironment”. Cancer is also determined by individual variability provoked by hereditary predisposition, lifestyle and other variables like environmental influences, infectious agents, nutritional factors, hormonal and reproductive factors, carcinogens and radiation [3]. These predispositions could lead to

the disruption of the eight hallmarks enabling transformation of a normal cell into its neoplastic counterpart.

The conception that human tumor development is characterized by a multi-step process has been documented most clearly in the epithelia of the intestine and colon cancer providing a good model for the study of morphological and genetic stages in cancer progression.

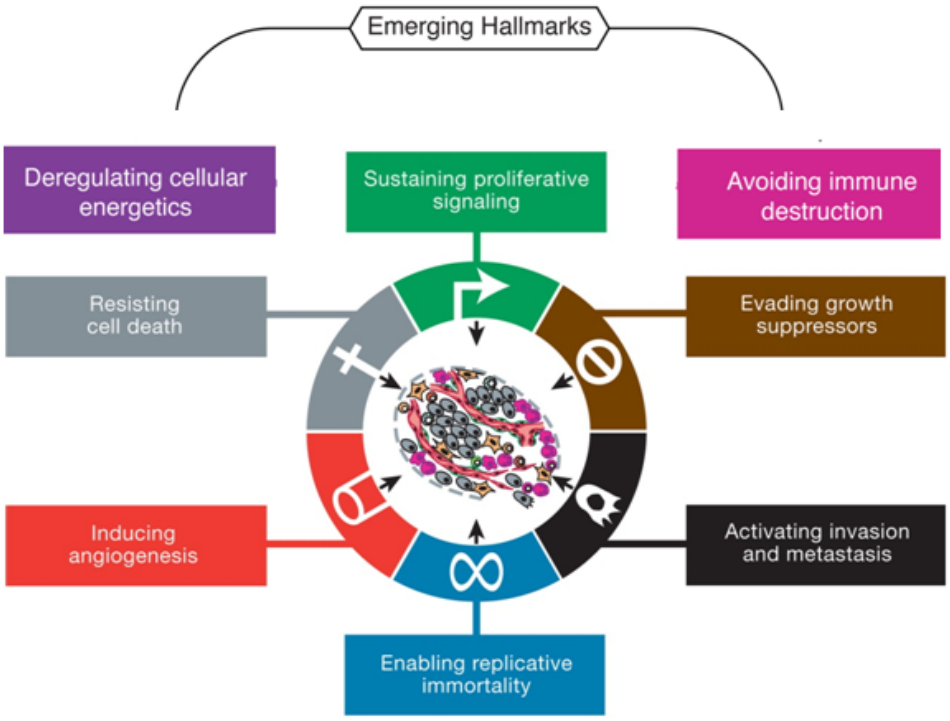

Figure 1. The hallmarks of cancer [2]

1.2 COLORECTAL CANCER OVERVIEW

Colorectal cancer (CRC) is the third most common cancer type and the third leading cause of cancer-related death in the world, with an estimated incidence of 1 million new cases and a mortality of >500000 deaths annually [4]. In the following paragraphs the morphological and histological characteristics of the colon epithelium and the changes that undergo normal tissues while developing a malignant phenotype will be described.

1.2.1 HISTOPATHOLOGICAL CHARACTERISTICS OF COLORECTAL CANCER

The intestinal epithelium is formed by a one cell depth layer in many sites, and this population of cells is in constant flux to maintain homeostasis of cell renewal process, in which cell proliferation, differentiation and apoptosis of enterocytes is highly regulated both spatially and temporally [5]. Epithelial cells are anchored on a basement membrane (basal lamina) that forms part of the extracellular matrix and is assembled from proteins secreted by both epithelial and stromal cells, mostly fibroblast, lying beneath the membrane. Other cell types including endothelial cells, which form the walls of capillaries and lymphatic vessels, and immune cells are also present. Beneath this layer of stromal cells there is a thick layer of smooth muscles responsible for intestinal peristalsis through periodic contractions [6]. Most of the pathological changes associated with the development of colon cancer occur in the epithelial layer, which undergoes transformation through a series of intermediate steps from carcinoma, where it is possible to observe a variety of tissue states with different degrees of abnormality, to mildly deviant tissues and high malignancy state, and later into multiple metastatic growths (Figure 2).

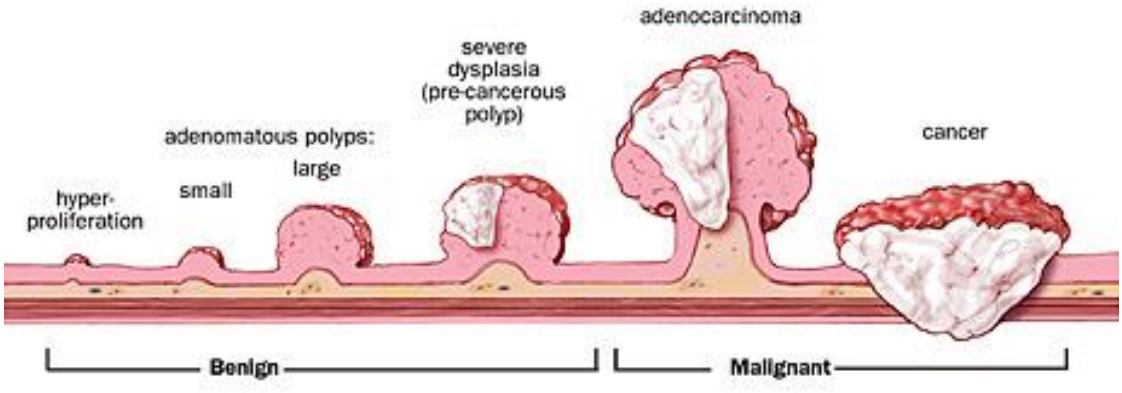

Figure 2. Progression from polyp to cancer (modified from John Hopkins Medicine Colorectal Cancer http://www.hopkinscoloncancercenter.org)

Focusing on the histopathological alterations of the colonic epithelium, there are some hyperplastic areas where epithelial cell proliferation is unusually high although the individual cells have normal phenotype. Other areas are characterized by growth with abnormal histology deviating from that of normal cells and the well ordered cell layer typical of the normal colonic epithelium is not present. During further stages of progression abnormal growth leading to adenoma formation is observed [6]. All these forms are considered benign until they pass through the basal membrane and invade the underlying tissues and the cells switch into a malignant direction. The deeper they penetrate into the stromal layers, the higher is the risk that they can migrate to anatomically distant sites in the body and metastasize.

1.2.2 GENETICS OF COLORECTAL CANCER

CRC is defined on the basis of clinical, pathological and genetic findings and can be subdivided into hereditary (< 5 %), familial (20–25 %) and sporadic (75 %) disease [7].

The inherited variants of CRCs account for a small fraction of all colorectal tumors and are well described on the basis of clinical, pathological, and genetic characteristics. The most common are hereditary nonpolyposis colon cancer (HNPCC), also named Lynch syndrome, and the familiar adenomatous polyposis (FAP) syndrome. FAP is caused by alterations of APC gene and is characterized by development of hundreds to thousands of colonic adenomas (polyps) which develop into CRC when not treated. HNPCC is caused by alterations in DNA mismatch repair genes leading to microsatellite instability (MSI) and although affected individuals can develop colonic adenomas with greater frequency that the general population, poplyposis is rare condition.

In addition to the inherited syndromes, 20-25% of CRC exhibit increased familiar risk, probable related to inheritance, but the genetic loci responsible for the risk genotype are mainly unknown. They are likely to be caused by alterations in genes that are less penetrant, but more common that those associated with the familiar syndromes. Polymorphisms in genes that regulate metabolism or in genes regulated by environmental factors could be related to familiar predisposition to CRC. Sibling studies and studies with parent/child pairs have estimated that up to 35% of all CRC cases can be attributed to genetic susceptibility [8].

In sporadic CRC genetic instability occurs either as chromosomal instability (CIN), in 85 % of all cases, or as microsatellite instability (MSI), in 15 % of the patients.

Key changes in CINs include widespread alterations in terms of gained and lost chromosomal regions, recurrently identified on chromosomes 7, 8, 13, 18 and 20 [9-11]. Although the molecular basis of CIN is unknown, mutations in p53, loss of (18q region and amplifications of 20q where multiple putative oncogenes map were reported as implementing CIN mediated tumor progression [12-14]. Direct involvement of APC in chromosomal instability was also reported [15].

MSI CRCs are characterized by defects in the DNA mismatch repair system, which result in a consequent instability of repetitive units of DNA (DNA microsatellites) [16, 17]. Genes involved and inactivated by either mutation or hypermethylation include *MSH2, MSH3, MSH6, MLH1, PMS1* and *PMS2.*

1.2.2.1 Vogelgram – a progression model for colorectal cancer

The worldwide adopted model presented by B. Vogelstein in 1990 describes the series of key genetic events that characterize colorectal cancer progression (Figure 3) [12]. The adenoma to carcinoma sequence is initiated by inactivation of APC and this event takes place in the normal epithelium. The APC gene encodes a large multidomain protein that binds to β-catenin and Axin and downregulates Wnt signaling pathway. Most of APC mutations involve the region responsible for β-catenin binding, blocking the inhibition of Wnt signaling and leading to over proliferation of cells. APC mutations can be either frameshift (68%) or nonsense (30%) and lead to the carboxy-terminal truncation of the protein. During the normal cell growth and turn-over of the colonic epithelium, normal enterocytes migrate out of colonic crypts, differentiate and die within 3 to 4 days for apoptosis. As consequence of this short life, most mutations occurring in their genome will

soon be lost. However, loss of APC function results in trapping cells within crypts and later, in the accumulation of APC-negative cell populations. Thus, because migration from crypts is blocked, the resulting mutant cells will also be retained into crypts. In this context, disruption of APC pathway may be sufficient to start small adenomatous growth [18].

The next genetic event involves hypomethylation and occurs at the state of hyperplastic polyp. Slightly larger adenomas are characterized by mutations in K-Ras gene that constitutively activate this oncogene and cause progression.

Late stage adenomas show also loss of 18q-arm; best candidate tumor suppressor gene that is lost is DPC4/MADH4, which encodes SMAD-4, involved in the transforming growth factor β (TGF-β) signaling pathway [18]. Driving progression from the intermediate stage adenoma to late adenoma, alterations in the TGF-β pathway occur and result in loss of the growth inhibitory effects of TGF-β [19].

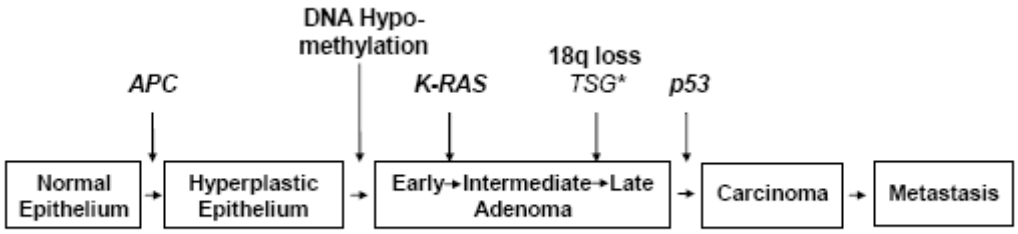

Figure 3. Vogelgram. Transformation of normal colon epithelium into malignant carcinoma by step-wise accumulation of genetic aberrations as presented by Fearon and Vogelstein in 1990 [14].

About half of the carcinomas show LOH on the short harm of Chromosome 17 (17p) where p53 (17p13) maps. p53 is a tumor suppressor gene, frequently mutated in colorectal cancer, which suppresses cell division or induces apoptosis in response to stress damage. Loss of this gene by damage of both alleles drives progression to carcinoma [19] (Figure 3).

1.2.2.2 Structural and copy number variations in colorectal cancer

Beside the gene mutations, an additional mechanism that can disrupt gene function is the copy number variation (CNV), a characteristic of sporadic CRC. These variations can include deletions, segmental duplications, insertions, inversions or complex chromosomal rearrangements and it became clear that they are actually very common events in cancer genesis [20-25]. Changes in copy number are already present in high-grade dysplasias and adenomas, but they are significantly more abundant in carcinomas causing alteration of the expression of genes directly involved in cancer.

The development of high resolution techniques has allowed to detect and catalogue CNVs and to associate them with specific biological functions and complex human genetic diseases [26]. Array-based analysis of single nucleotide polymorphisms (SNPs) is widely used for the identification of these variations. Multiple genome-wide association studies (GWAS) aimed at associate specific disease genotype to phenotype [27] have recently identified several susceptibility SNP loci that have been proposed to predispose to CRC [28-31]. Analysis of structural variations in CRC patients can provide new highlights to define further colon cancer tumorigenesis.

1.3 TGF-β SIGNALING PATHWAY

TGF-β is a pleiotropic cytokine that regulates several biological processes including tissue growth and morphogenesis during embryonic development, cell proliferation and apoptosis, epithelial-mesenchymal transition (EMT), adhesion, differentiation, migration and metastasis [32, 33]. The TGF-β superfamily of ligands includes more than 30 factors including the TGF-β isoforms, Bone morphogenetic proteins (BMPs), Growth and differentiation factors (GDFs), Anti-müllerian hormone (AMH), Activins and Nodals.

The TGF-β cytokine family is composed of the TGF-β isoforms (TGF-β1, β2 and β3) whose bioactive cytokine molecule is a dimer composed of a polypeptide chain which is cleaved from a precursor by enzymes like furin, a proprotein convertases that process latent precursor proteins into their biologically active products, and other convertases [34, 35].

The canonical signaling pathway involves the phosphorylation of Smad proteins. TGF-β ligand binds with high affinity to the TGF-β type-II receptor (TβR-II) and recruits the type-I TGF-β receptor (TβR-I) forming a hetrotetrameric complex resulting in phosphorylation of the type I receptor by the receptor type II. TβR-I subsequently recognizes and phosphorylates receptor-regulated Smad proteins (R-Smads) Smad-2 and Smad-3. Smads are intracellular proteins that transduce extracellular signals from TGF-β ligands to the nucleus where they activate gene transcription. In the basal state, the R-Smads are retained in the cytoplasm by binding to SARA (Smad anchor for receptor activation) [36]. After the phosphorylation of the Smads, their affinity to SARA decreases and Smad-2 and -3 are released. Subsequently they interact with Smad-4. This is a binding

partner common to all receptor activated Smad proteins, that is not phosphorylated, but essential for the formation of all Smads transcriptional complexes and that drives the accumulation of Smad proteins in the nucleus. The phosphorylation by TGF-β receptor I kinases at C-terminal serine residues (SXS domain) is a nuclear localization signal. Smad-2 and Smad-3 linked to Smad-4 undergo constant nucleo-cytoplasmic shuttling, determined by repeated cycles of de-phosphorylation and re-phosphorylation, involving direct interactions with both nuclear pore proteins and importins and exportins.

Once in the nucleus, there is a "sequence mediated" mechanism that regulates interactions between the Smad complex proteins and their target genes by directly recognizing target genes carrying several copies of Smad cognate sequence CAGAC [37]. However, Smad proteins have a low affinity to DNA and they need additional DNA binding co-factors to recognize and sufficiently bind Smad-responsive promoter elements containing only one copy of this sequence.

The inhibitory Smads, Smad-6 and Smad-7, negatively regulate the TGF-β signaling in response to feedback loops and antagonistic signals. Smad-7 competes with R-Smads for binding the receptor activated complex and consequently induces termination of TGF-β signaling [38] (Figure 4). Interestingly, the inhibitory Smads can be up-modulated by the TGF-β ligands which they regulate: Smad-7 by TGF-β, activin and BMP members, while Smad-6 is induced by BMP [38, 39]. Transcriptional repressors such as Ski and SnoN (Ski-like) can also inhibit the Smad signaling [40]. These findings demonstrate that the TGF-β signaling requires integration of positive and negative signals for inducing specific cellular responses: these signals are extremely variable depending on the cellular type and the stimulation context. TGF-β induces epithelial cells to undergo growth arrest and apoptosis restraining their growth, whereas it can also induce epithelial-mesenchimal transition and pro-angiogenesis promoting tumor growth and angiogenesis. The variety of the gene targets (more that 300 genes can be activated by TGF-β) and the nature and the mutability

of the cells determines the response to the cytokine and provides to TGF-β tumor-suppressing or oncogenic properties [41].

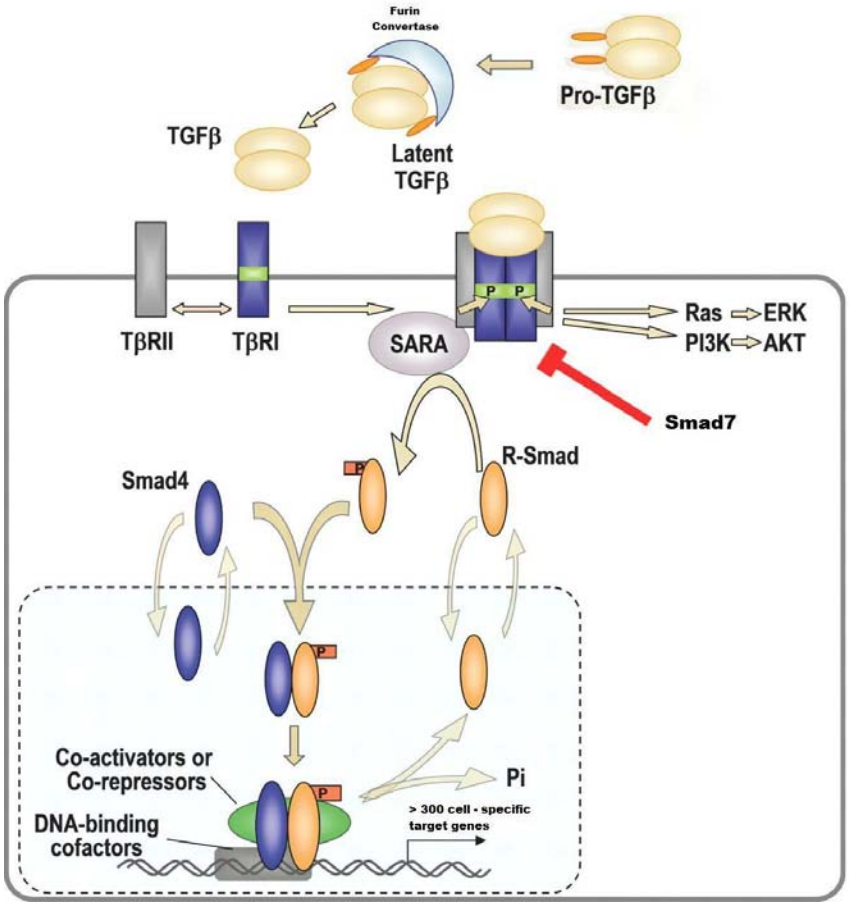

Figure 4. The TGF-β signaling pathway [42].

1.3.1 TUMOR SUPPRESSOR FUNCTION OF TGF-β

The most characterized anti-tumor response induced by TGF-β is the growth arrest. Progression of cell cycle is blocked at G1 as a result of transcriptional up-regulation of the cyclin-dependend kinase (CDK) inhibitors $p21^{Cip1/WAF1}$ (CDKN1A) and $p15^{Ink4b}$ (CDKN2B) [43, 44] and transcriptional repression of the pro-growth transcription factor c-MYC [45] (Figure 5).

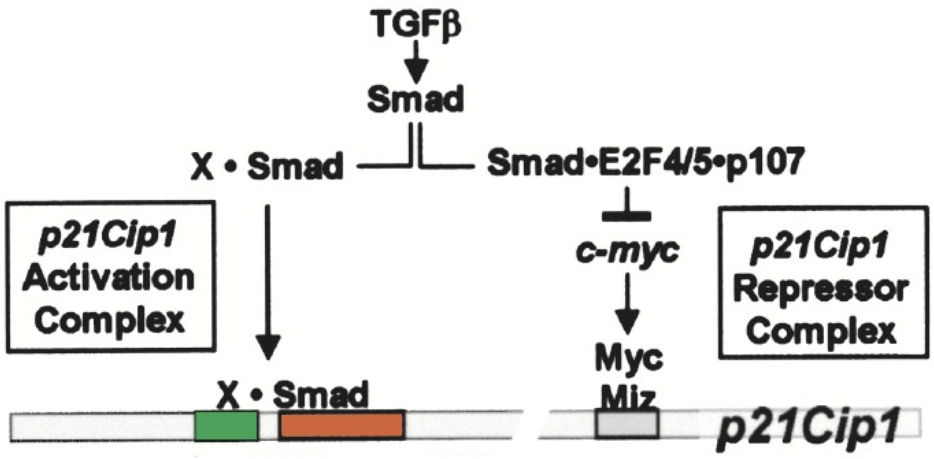

Figure 5. The TGF-β cytostatic program (modified from Seoane et al., 2004) [46]

CDKN1A (also called p21, WAF1, CAP20, Cip1, and Sdi1) contains a conserved region of sequence at the NH_2 terminus that is required for the inhibition of Cyclin/Cdk complexes, whereas the COOH terminal regions are variable in length and function. p21 binds and inhibits the Cyclin D-CDK4/6 and the Cyclin E-CDK2 complexes preventing the activation of substrates essential for the progression into S phase [44]. The mechanism by which TGF-β promotes transcription of CDKN1A and CDKN2B involves both transcriptional activation and removal of their transcriptional repression. For this aim, different transcriptional complexes are formed: activation complex provoking CDKN1A or

CDKN2B transcription and repressor complex inducing repression of c-MYC, a direct inhibitor of p21 [47] and p15 [48] (Figure 5).

The up-regulation of these cell cycle inhibitors depends not only on Smads, but also on the Smad-interacting transcriptional factors. FoxO transcriptional factors belong to the Forkhead box (Fox) family and are known to be involved in many cellular processes including cell division, metabolism and in the control of cell and organismal growth [49]. In response to TGF-β, Smad-3 and Smad-4 bind to the FoxO3 domain which includes DNA binding site and target a region of CDKN1A promoter containing Forkhead binding elements (FHBE) and Smad binding elements (SBE) inducing in this way its transactivation (Figure 6) [31].

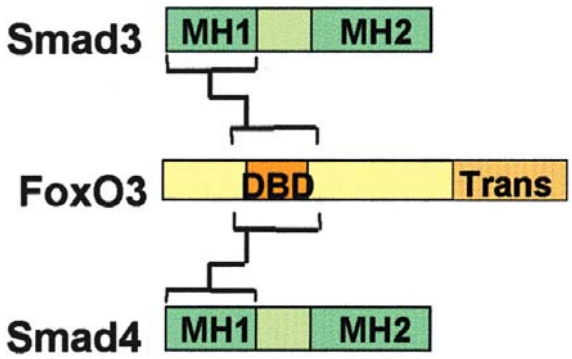

Figure 6. Schematic representation of protein-protein interactions in FoxO3-Smad-3 and FoxO3-Smad-4 complexes. The interacting domains are connected with lines [31].

Besides FoxO proteins, the members of the Runt-related DNA-binding cofactors (RUNX) family were also identified as Smad-interacting factors which up-regulate CDK inhibitors. This family consists of three DNA-binding cofactors, Runx1, Runx2 and Runx3, which play a key role in the normal development and neoplasias. All Runx family members share the central Runt domain that recognize a specific DNA sequence, but the N- and C-terminal region of each Runx factor is different from the others. Runx3 activity is closely

associated with TGF-β, and after stimulation by the cytokine Runx3 forms a complex with Smads and directly up-regulates the CDKN1A transcription [50].

In response to a variety of stress stimuli, p21 expression can be induced also by p53, which mediates the p53-dependent cell cycle G1 phase arrest [51]. The promoter contains two conserved p53-binding sites necessary for p53 responsiveness after DNA damage [52]. A variety of transcription factors induced by p53-independent mechanisms, such as Sp1, Sp3, Ap2, STATs, C/EBPα, C/EBPβ, can activate CDKN1A transcription [53].

In addition to p21 up-regulation, another critical event in TGF-β-induced cell cycle arrest is the rapid down-regulation of the pro-growth transcription factor c-Myc [54]. Myc is a basic Helix–Loop–Helix Leucine Zipper (bHLHZip) protein with the ability to regulate different events such as cell cycle, growth and metabolism, differentiation, apoptosis, transformation, genomic instability, and angiogenesis, and it is also known as a direct inhibitor of p21 [55, 56]. After forming a heterodimer with the small bHLHZip protein Max, the complex recognizes specific CACGTG and similar E-box binding sequences and regulates the expression of the target genes [57].

In proliferating cells, c-Myc is tethered to the CDKN1A and CDKN2B promoters by the zinc-finger protein MIZ1 and prevents their transcription. In this context, c-MYC downregulation in response to activation of the TGF-β signaling cascade allows the transcriptional activation of these cell cycle inhibitors.

Analysis of c-MYC promoter identified a Smad responsive element consisting of TGF-β-inhibitory element (TIE) which is directly recognized by Smads and a specific E2F binding site [58]. The TIE element, GnnTTGGnG, is located between position -92 and -63 and mediates transcriptional downregulation of c-MYC by a TGF-β-induced protein complex consisting of Smad-3, Smad-4, E2F4/5 and the transcriptional repressor p107. Smad-3 has direct contacts with specific regions of p107 and E2F4 and -5 (Figure 7). Although p107 is a member of RB family proteins and is inhibited by CDK-dependent phosphorylation in

the nucleus, the pool of p107 that is involved in c-MYC down-regulation resides in the cytoplasm and is not involved in CDK phosphorylation. The complex preexists in the cytoplasm and in response to TGF-β stimuli moves into the nucleus and binds the c-MYC promoter for repression.

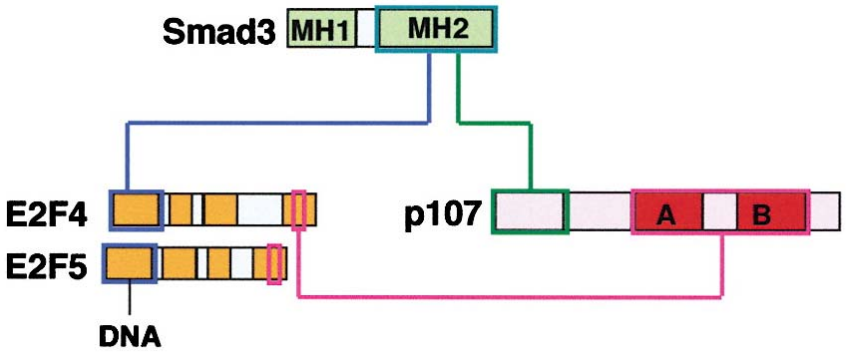

Figure 7. Schematic representation of protein-protein interactions between the members of the c-MYC repressing complex. The interacting domains are connected with lines [37].

Other works analyzing the TGF-β mediated suppression of different growth promoting transcription factors identified an alternative c-Myc repressing mechanism mediated by TGF-β. It was reported that interaction of Krüppel-like factor 11 (KLF11/TIEG2) with activated Smad-3 results in increased Smad-3 affinity for binding the TIE element on the c-MYC promoter. In addition to its effect on c-MYC promoter, KLF11 also contributes to terminate the negative TGF-β feedback loop implemented by Smad-7 by binding to GC-rich elements within the proximal Smad-7 promoter, and terminating its induction through recruitment of mSin3A corepressor complex [59]. mSin3A inhibits the transcriptional activation of target genes by histone deacetylation and subsequent remodeling of the chromatin structure [60] (Figure 8).

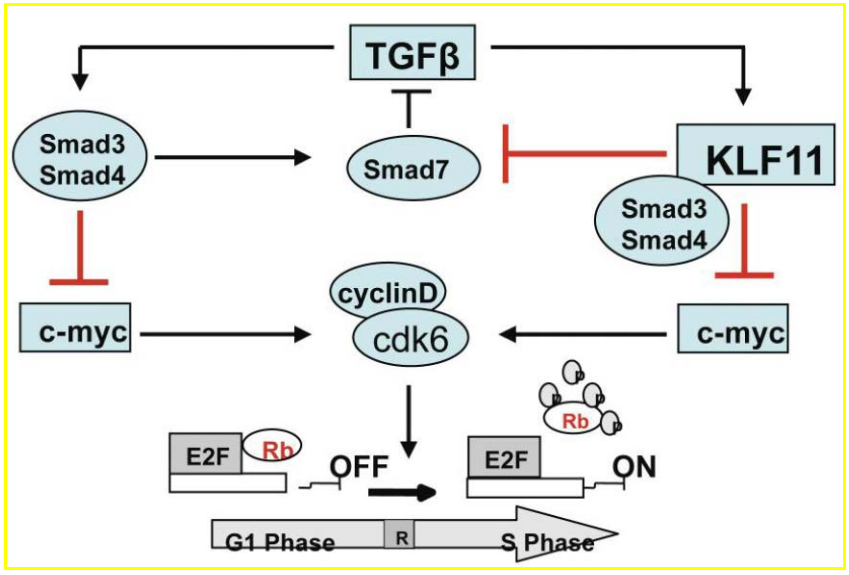

Figure 8. A schematic model of the interactions of KLF11 with the TGF-β induced cell growth inhibition. KLF11 is the key factor in the mechanism mediated by TGF-β-induced nuclear interaction of Smad-3 with KLF11, resulting in c-Myc silencing and growth inhibition.

Besides induction of p21 and repression of c-Myc, TGF-β also has other mechanisms for implementing the cytostatic program, such as repression of the inhibitors of differentiation ID1, ID2 and ID3 [61]. ID members can interact with retinoblastoma proteins (RB) and promote cell proliferation. The repression of ID1 is regulated by a complex formed of Smad-3 and activating transcription factor-3 (ATF3), and down-regulation of ID2 is a secondary effect of the TGF-β mediated repression of c-MYC [62].

Another protein which is repressed by TGF-β as part of the cytostatic program is the tyrosine phosphatase cdc25A [63]. Cdc25A downregulation by TGFβ leads to accumulation of tyrosine phosphorylation on cdk4 and cdk6 and subsequent inhibition of these kinases. Moreover, c-Myc is as a positive regulator of cdc25A expression [64], a mechanism that could also antagonize the growth suppression effect of TGFβ. This multiplicity of anti-proliferative TGFβ gene responses by regulation of high number of genes assures that the growth inhibition will be implemented efficiently. The cytostatic program mediated by TGF-β is schematically represented in Figure 9.

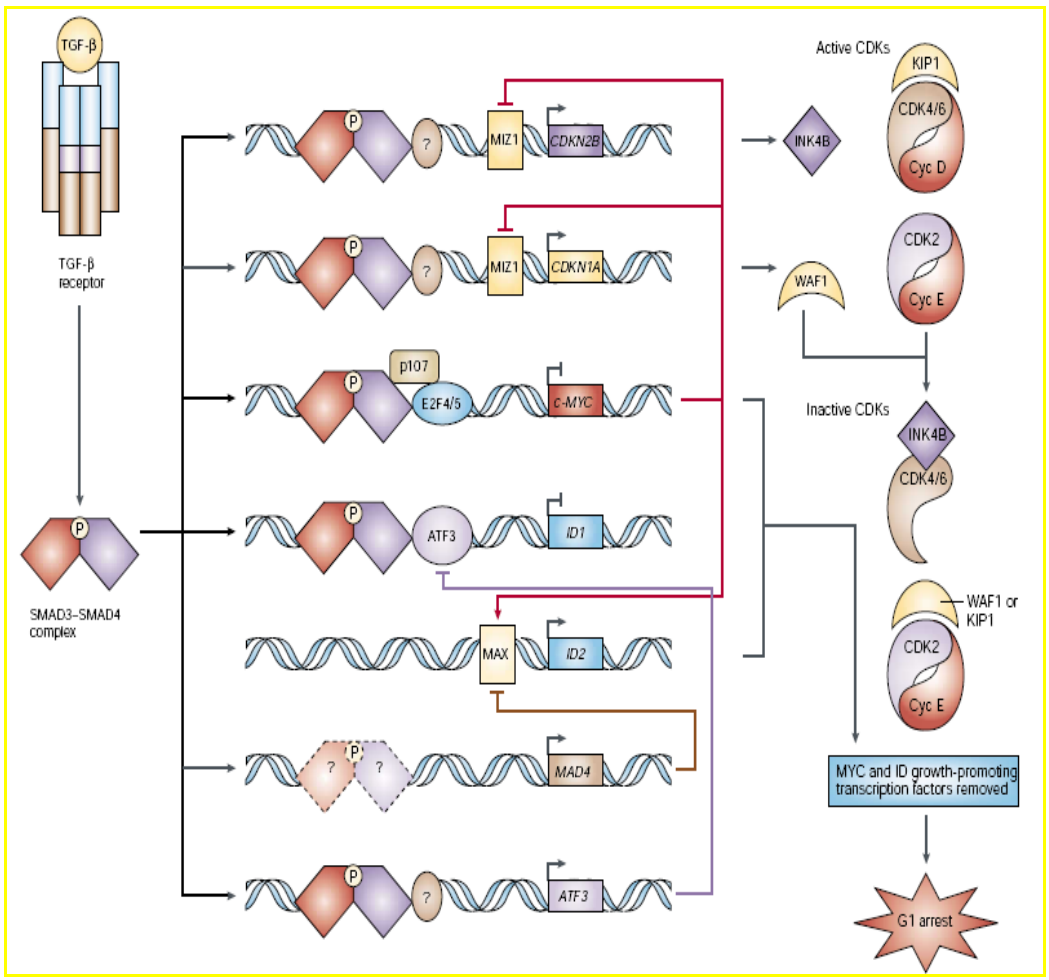

Figure 9. Schematic representation of the TGF-β cytostatic program. TGF-β induces CDK inhibitors such as CDKN1A (also named WAF1, KIP1 or p21) and CDKN2B (also named INK4B or p15); and represses growth-promoting factors such as c-MYC, ID1 and ID2 [65].

In addition to the growth arrest, TGF-β can implement its tumor-suppressor action also by activation of the apoptotic pathway [66, 67]. Smad mediated up-regulation of the Fas receptor resulting in caspase-8 activation [68] and induction of the death associated protein kinase (DAPK) was also reported [67]. TGF-β also downregulates Bcl-xL, an anti-apoptotic Bcl-2 family member, and induces up-regulation of the proapoptotic proteins Bim and Bmf [69].

1.3.2 Tumor promotion

During carcinogenesis, cells often loss the growth-inhibitory responsiveness to the TGF-β stimuli. Moreover, tumor cells can overproduce the cytokine creating a local environment that stimulates tumor growth and invasiveness. TGF-β induces epithelial-mesenchymal transition (EMT), a process of migration which requires loss of cell-cell adhesion and acquisition of fibroblastic properties through repression of the cell-cell adhesion receptor E-cadherin by Smad-3 and Snail [70].

Mouse models showed that TGF-β can facilitate the tumor growth also by repressing the host immune response [71]. Another oncogenic property of TGF-β is the ability to induce a pro-angiogenic environment by activation of angiogenic factors, such as the connective tissue growth factor (CTGF) and the vascular endothelial growth factor (VEGF) [72-74]. TGF-β can also promote distant tissue specific metastases, for example to the bones, through induction of pro-osteolytic factors such as the parathyroid hormone-related protein (PTHrP) [70, 75]. The expression of the matrix metalloproteases 2 and 9 can be stimulated by the ligand, and their activation results in enhancement of migratory and invasive properties of the endothelial cells [66, 76].

The TGF-β signaling represents a complex regulatory network which possesses tumor suppressing and oncogenic properties, and it can also interact with different oncogenic and tumor suppressor signaling cascades. Crosstalk between Smads and a wide number of proteins, such as extracellular-signal-regulated kinase (ERK1 and ERK2), p38, MAPKs, c-Jun N-terminal Kinase (JNK), PI3K-Akt or small GTPases, is commonly observed in carcinogenesis. Constitutive activation of the Ras-Mek-ERK signaling pathway (MAPK signaling pathway), due to a mutational activation of K-Ras, inhibits Smad signaling. Erk-mediated phosphorylation of MAP kinase sites within the linker region of Smad-2 and Smad-3 blocks the complex formation with Smad-4 [77]. Indeed, this pathway is a strong

antagonist of the TGF-β signaling [78]. In contrast, signaling crosstalk with JNK or MEKK1 (upstream activator of the JNK pathway) seems to facilitate the nuclear accumulation of Smad complexes [79].

Inactivating mutations in the Smad proteins or in the TGF-β receptor are present only in small part of the cases, suggesting that the switch from tumor suppressing to tumor promoting activity of TGF-β could be a result of downstream alterations of the signaling pathway, or due to a post-transcriptional modulations of its target genes.

1.4 TGF-β and colorectal cancer

The TGF-β signaling pathway is frequently altered during the carcinogenesis of CRC. It has been reported that nearly all pancreatic cancers [80, 81] and colon cancers [82] have mutations in genes from the TGFβ signaling pathway. These mutations most frequently occur in the TGFβ receptors, Smad-4 or Smad-2, but mutations affecting unknown components of the signaling pathway can not be excluded.

Mutations in the TGF-β type II receptor (TβRII) occur in approximately 30 % of all colorectal cancers [83] and are present in 80-90 % of the MSI tumors [84]. Mouse models experiments showed that mice possessing homozygous deletion of TβRII in the intestinal epithelium develop adenoma and carcinoma with increased rates, suggesting that loss of TGF-β inhibition contributes to CRC development [85]. Mutational inactivation of the TGFβ type I receptor has also been detected in human cancers, but in CRC their frequency is relatively low. Homozygosity of a common germline polymorphism, TβRI (6A), is associated with loss of TGF-β growth inhibition response and increased cancer risk [86].

Smad-2 and Smad-4 map on chromosome 18q21 which is one of the regions frequently deleted in CRC. Smad-4 is mutated in 16-38 % of colorectal tumors and alterations of this gene inculude deletions of entire chromosomal segments, small deletions or frameshift, nonsense and missense mutations [87]. Smad-2, also located on 18q21, is mutated in a small proportion of the CRCs [88, 89]. Smad-deficient mice display phenotypes which support a tumor suppressor role for these genes. Mice which have loss of one of the Smad-4 alleles develop gastric polyps which progress into tumors [90]. Furthermore, when these mice are crossed with mice defective in APC gene, their progeny develop larger polyps than mice with only APC mutations which quickly progress into carcinomas [91].

Although there are no mutations in Smad-3 found in human cancer, mice with a homozygous deletion of this gene develop aggressive metastatic colorectal cancer at an early age, which is a characteristic of the genetically predisposed CRCs [37].

In a subset of colorectal tumors loss of normal growth-inhibitory response to TGF-β is caused by mutations of TGF-β regulated genes. However, in the majority of the tumors which are not responsive to the growth inhibition stimuli by TGF-β, the signaling cascade is intact. Hence, epigenetic mechanisms of inactivation of the pathway have been proposed and the involvement of different microRNAs was also reported.

1.5 microRNAs

The microRNAs (miRNAs) are a new class of small non-coding RNAs (18-25 nucleotides long), that act as post-transcriptional regulators of gene expression, binding to the 3' untranslated regions (UTRs) of target mRNAs and promoting mRNA degradation or translational repression [92]. Although their function was originally described during normal development, nowadays it is known that the miRNAs have an important role as integral components of oncogenic and tumor suppressor networks [66].

MiRNAs derive from larger precursors (pri-miRNAs) folded into imperfect stem-loop structures. Pri-miRNAs are transcribed by RNA polymerase II (Pol II) and processed into ~70-nucleotide precursors (pre-miRNAs) which is then cleaved to generate ~21-25-nucleotide mature miRNAs. miRNAs are positioned at diverse genomic regions; for example, some pri-miRNAs map within introns of both protein-coding or non-coding genes and are therefore transcriptionally regulated through the promoters of these genes. The transcription of different miRNAs by the same promoter results in formation of microRNA clusters which are transcribed at the same time.

The sequential process of miRNA maturation is catalyzed by different multiprotein complexes; the pri-miRNA is processed by a complex called the Microprocessor, localized in the nucleus and composed by an RNase III enzyme Drosha and the double-stranded RNA-binding domain (dsRBD) protein DGCR8/Pasha. These enzymes generate 2-nucleotide-long 3' overhangs at the cleavage site. Drosha ability to process pri-miRNA into ~70-bp pre-miRNAs depends on the terminal loop size, the stem structure and the flanking sequence of the Drosha cleavage site. If shortening of terminal loop is present, disruption of the complementary within the stem sequence, or mutations of flanking sequence of the Drosha cleavage site, the Drosha processing of pri-miRNAs is significantly reduced, if not abolished.

Once the pri-miRNAs are cleaved by Drosha, they are exported from the nucleus into the cytoplasm by Exportin 5 (Exp5), a nucleo/cytoplasmic cargo transporter Ran-GTP dependent. In the cytoplasm these hairpin precursors are cleaved into a small imperfect dsRNA duplex containing both the mature miRNA strand and its complementary strand. This cleavage is performed by another RNase III enzyme, Dicer. The ability of Dicer to recognize the pre-miRNA molecules is due to the presence of a PAZ (Piwi-Argonaute-Zwille) domain that allows a low-affinity interaction with the 3' end of ssRNAs. For this reason, the dsRNA that presents 2-nucleotide 3' overhangs, such as those resulting from Drosha cleavage, can be easily recognized and processed by Dicer.

Dicer cleavage generates mature miRNAs ~21-25-nucleotide long. Once that the dsRNA duplex is formed, the target specificity and the functional efficiency of a miRNA, requires that the mature miRNA strand from the imperfect duplex is incorporated into the RNA-induced silencing complex (RISC).

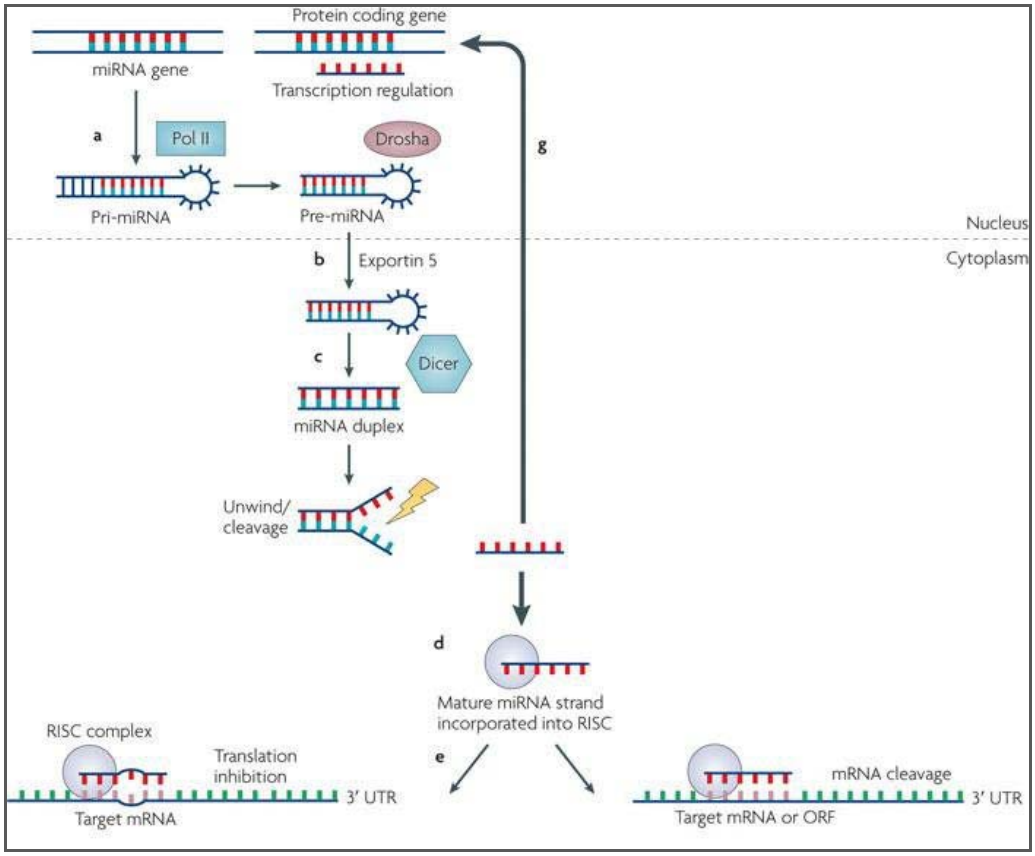

Figure 10. MicroRNA biogenesis [93].

The mechanism by which the RISC complex incorporates the mature miRNA strand of the dsRNA duplex is driven by the different stability of the 5' ends of the two arms of the miRNA duplex. Potentially the mature miRNA strand can reside on either strand of the hairpin stem, but because of thermodynamic reasons it mostly derives from the strand with the less stable 5'. Once incorporated into the RISC, the miRNA drives this complex to its RNA target by base-pairing interactions. If mRNA/miRNA complementary is perfect or near-perfect, the target mRNA can be cleaved and degraded; otherwise the translation is repressed and mRNA remains intact [94].

The target recognition is determined by base-pairing of nucleotides in a particular region of the microRNA, called the "seed sequence". The seed sequence is a conserved heptametrical sequence which is mostly located at positions 2-7 from the miRNA 5′-end and is essential for the binding of the miRNA to the mRNA. The miRNA seed sequences are used for developing of computational approaches for target predictions. The microRNA target site is positioned at the 3'-UTR region, probably because the movement of the ribosomes occurring during translation will contrast the RISC binding [95]. Different reports about "non 3' interactions" are emerging recently. It was reported that some miRNAs can bind to the open reading frame (ORF) sequences or to the 5'-UTR region of the target genes, determining gene activation rather than repression [93]. The RISC action on target mRNA is determined by the character of the Ago protein which is incorporated in the complex with the miRNA and by the grade of complementarity between the miRNA strand and its mRNA target as well.

1.5.1 microRNAs involvement in TGF-β signaling

The first reported microRNA cluster involved in the TGF-β signaling was miR-106b-25 localized on chromosome 7 [96]. This cluster of miRNAs regulates the expression of p21 and Bim and makes gastric cancer cells insensitive to TGF-β mediated cell-cycle arrest [66, 97]. The miR-106b-25 cluster contains three members: miR-106b, miR-93, and miR-25 which share seed region homology with the members of two other clusters, which are referred as its paralogs: miR-17-92, positioned on 13q31 and miR-106a-363, located on chromosome X. Probably the similarity between the clusters is a result of ancient gene duplications during early vertebral evolution [98]. Unlike the miR-17-92 and miR-106b-25 clusters, which are both abundantly expressed in different types of malignancies [99], the expression of the miR-106a-363 cluster is undetectable or at trace levels [100].

The miRNAs encoded by the three clusters can be classified into four separate miRNA families according to their seed sequences: the miR-17 family (miR-17, miR-20a, miR-20b, miR-106a, miR-106b, and miR-93), the miR-18 family (miR-18a and miR-18b), the miR-19 family (miR-19a, miR-19b-1, and miR-19b-2) and the miR-92 family (miR-92a-1, miR-92a-2, miR-383, and miR-25). All microRNAs in one family have the same seed sequence and consequently could recognize the same target genes (Figure 11). Indeed, the regulation of p21 by miR-17 and miR-20a from the miR-17-92 cluster was also reported (previously shown as target of miR-106b) [101, 102].

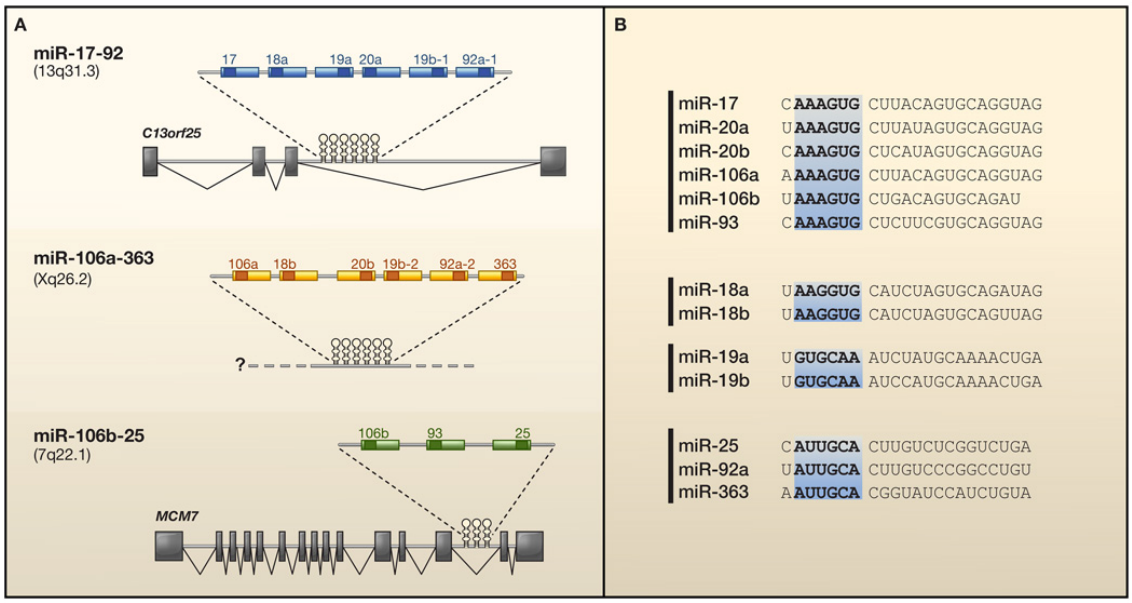

Figure 11. Organization of the miR-17-92 cluster and its paralogs [103]. The seed regions are highlighted in blue. The classification in four groups (right panel) is according to the seed region shared between different members.

The involvement of miR-17-92 in TGF-β signaling was demonstrated also by reports showing that miR-20a modulates the expression of the TGFβRII [99] and miR-18 that of Smad-4 [104]. miR-34a and miR-373 were also identified as TGFβRII regulators [105].

Interestingly, modulation of the microRNA expression by TGF-β was also reported. It was demonstrated that Smads can facilitate the cleavage reaction by Drosha by direct association with a specific binding element within the miRNA sequence (Figure 12). The consensus sequence is similar to the Smad binding element in the promoter of TGF-β regulated genes and was named R-SBE (RNA-Smad binding element). Mutations in R-SBE impair the miRNA induction by the cytokine, and introduction of this element in pri-miRNAs previously not modulated by TGF-β allows their up-regulation [106]. MiR-21 and miR-199a were the first two microRNAs identified as induced by TGF-β [107].

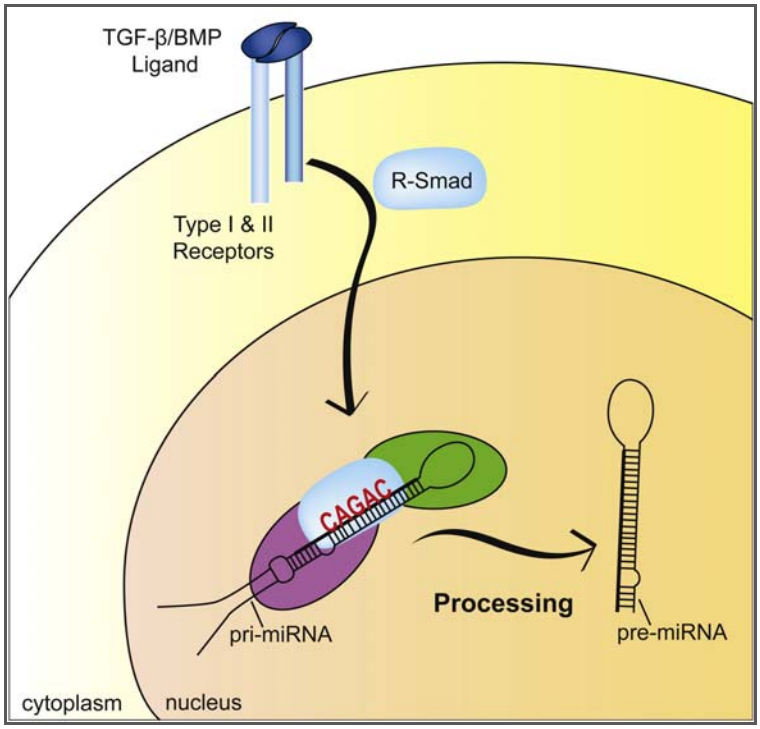

Figure 22. Schematic representation of the Smad binding element (R-SBE) within the pri-miRNA stem region. Smad binding to R-SBE facilitates the pri-miRNA processing by Drosha.

1.5.2 The miR-17-92 cluster

MiR-17-92 is a polycistronic miRNA cluster also named oncomir-1 and located in *chromosome 13 open reading frame 25 (C13orf25)* on 13q31.3, which encodes six microRNAs: miR-17, miR-18a, miR-19a, miR-20a, miR-19b-1 and miR-92a-1. Expression profiling studies have revealed that miRNAs included in the miR-17-92 cluster are overexpressed in diverse tumor subtypes including both hematopoietic malignancies and solid tumors such as those derived from breast, lung, pancreas, prostate and colon [99].

The transcription of the miR-17-92 cluster is directly transactivated by the oncogene c-Myc which binds directly to the cluster locus and activates its expression [108]. The transcriptional factors E2F1, -2 and -3 activate genes involved in the cell cycle progression and drive the cell into S phase. c-MYC and E2F factors could activate one another's transcription. E2F1, -2 and -3 are negatively regulated by miR-17-5p and miR-20a from the cluster and this will consequently result in decreasing of c-Myc levels or also was proposed inhibiting the proapoptotic function of E2F1 [109-111]. This complex regulatory network in which c-Myc, E2Fs and miR-17-92 members regulate their levels by both positive and negative feedback loops suggested that miR-17-92 can regulate the expression of different types of genes, probably depending of the cellular context and resulting in oncogenic or tumor suppressive (Figure 13).

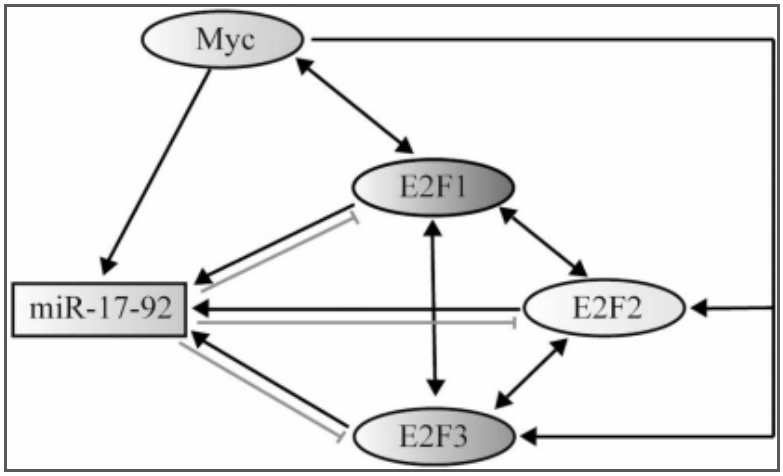

Figure 33. The interactions among c-Myc, e2Fs and the miR-17-92 cluster [112].

Additionally, it is known that c-Myc is a potent inducer of tumor angiogenesis through downregulation of antiangiogenic proteins like thrombospondin-1 (Tsp1) and connective tissue growth factor (CTGF). Both Tsp1 and CTGF are negatively regulated by miR-17-92 cluster, whose expression is enhanced by c-Myc [113].

The oncogenic properties of the cluster were confirmed also by mice model experiments. A mouse line that selectively overexpresses miR-17-92 in the lymphocytes was generated, and as a result these mice developed lymphoproliferative disease and died prematurely [114]. miR-17-92 also stimulates proliferation of the lung epithelium [115] and can affect tumor angiogenesis [113].

Even that accumulating evidences indicate the oncogenic role of miR-17-92, it was also reported that in some circumstances the cluster can act as tumor suppressor. The tumor suppressive activity of this cluster, as mentioned before, is attributed to the downregulation of E2Fs operated by miR-17-92 which results in decreasing of the c-Myc levels.

A reverse correlation between the levels of miR-17/miR-20a and Cyclin D1 was found in breast cancer cell lines, where Cyclin D1 has an oncogenic function [116].

Study performed by high-resolution array-based comparative genomic hybridization reported deletion of the miR-17-92 in 16,5% in ovarian cancers, 21,9% of breast cancers and 20% of melanomas suggesting a tumor suppressive role for the cluster [117].

1.5.3 Involvement of microRNA in colorectal cancer pathogenesis

To date, different studies have reported aberrant miRNA expression in colon cancer specimens. Expression of miRNAs in colon tumors can be influenced by numerous clinical variables such as tumor grade and location, and also by the mutational status of genes crucial for the colorectal cancer genesis [118]. Several microRNAs have consistently emerged as deregulated in colon cancer. Among these, miR-31, promotes cell migration and invasion in colon cancer cells, is frequently upregulated [119], while the microRNA cluster miR-143/145, inhibit cell growth, are found down-regulated in colon cancer [120]. Among the miRNAs with higher expression in CRC tumors, *APC* is a validated target of miR-135b [121]. miR-21 is the microRNA most frequently upregulated in most solid tumors and it was reported as associated with the progression of CRC [122].

2 MATERIALS AND METHODS

2.1 Colorectal cancer specimens

Tissue specimens from 76 consecutive sporadic CRCs were obtained from previously untreated patients lacking family history and high-frequency microsatellite instability (MSI) who underwent surgical resection at the Foundazione IRCCS Istituto Nazionale dei Tumori Milano (INT) between 1998 and 2000. Tumor specimens containing more than 70% neoplastic cells and their surrounding normal mucosa were selected by an experienced pathologist from cryopreserved tissue.

2.2 Cell lines

SW837, HT 29, Fs74, COLO 205, SW 480, SW 620, T 84, HCT 116, SW 1116, SW 1463 and Caco 2 cell lines were derived from the collection available at IFOM (Istituto Firc di Oncologia Molecolare, Milano) and grown in appropriate media as described in ATCC [123].

FET, colon carcinoma cell line, was provided by Michael G. Brattain [124]. Cells were grown in D-MEM/F-12 Media - GlutaMAX™ (Invitrogen) + 10% fetal bovine serum +1% Sodium Pyruvate.

HEK293T, a specific cell line originally derived from human embryonic kidney cells, derived from the collection available at IFOM (Istituto Firc di Oncologia Molecolare, Milano). Cells were grown in Dulbecco's Modified Eagle Medium (DMEM) (Invitrogen) + 10% fetal bovine serum + 1% Glutamine.

All cell lines were maintained as a monolayer in a humidified incubator at 37°C with a supply of 5% CO_2.

2.3 Nucleic Acids Extraction and Molecular Analysis

Total RNA containing small RNA was extracted using the Trizol reagent (Invitrogen) and the miRNeasy Mini Kit (Qiagen) according to manufacturer's protocol. DNA was extracted using the QIAamp DNA Mini Kit-Tissue Protocol (Qiagen).

2.4 High-Density DNA Copy Number and RNA Expression

Microarray production was done following standard protocols by AROS Applied Biotechnology AS (Aarhus, Denmark). All 51 DNA samples were hybridized to Affymetrix GeneChip® Human Mapping 250K NspI (SNP arrays). Three samples were excluded because of poor quality hybridizations resulting in 48 samples. All 36 RNA samples hybridized to Affymetrix GeneChip® Human Exon 1.0 ST arrays passed quality controls. All samples hybridized to the exon arrays were also hybridized to the SNP arrays.

2.5 Statistical analysis

TaqMan Array MicroRNA Cards v.2 were used to quantify the level of mature miRNAs according to the manufacturer's instructions. The analysis of the miRNA profiles were performed by bioinformaticians using nonparametric or parametric methods.

Bioinformaticians also performed meta-analysis of gene expression microarray datasets following the guidelines from [125]. Briefly, data were extracted from seven studies of normal and tumor tissue of CRC patients available at the NCBI GEO archive [126], annotated and analyzed. Using an FDR rate of 5%, 7629 differentially expressed genes were found.

2.6 Quantitative Real-Time Polymerase Chain Reaction (qRT-PCR) of genes and miRNAs

Gene expression analysis was done using TaqmanR assays. Briefly, 500 ng of total RNA in a final volume of 20 µl was reverse transcribed to cDNA using High-Capacity cDNA Reverse Transcription Kit (Applied Biosystems) according to the manufacturer's instructions. qRT-PCR was performed using the FAST chemistry (Applied Biosystems) with the manufacturer provided gene-specific assay in ABI PRISM 7900 Real-Time PCR system (Applied Biosystems). The cycle threshold (Ct) is defined as the number of cycles at which the fluorescence passed the fixed threshold in qRT-PCR. The ΔCt value represents the difference between the Ct value of the gene used for normalizing (house-keeping gene), and the Ct value of the gene of interest. Data are represented as -ΔCt or as $2^{-\Delta Ct}$ (values are directly related to expression levels). For microRNA expression analysis cDNA was synthesized from 30 ng of total RNA using miRNA–specific primers, then qRT-PCR was performed with miRNA-related specific assay and the expression levels of miRNAs were normalized to RNU6B. Data analyses for gene and miRNA expression were done using the Sequence Detector version SDS 2.1.

2.7 microRNA precursor transfection

For transient transfection, FET cells were seeded one day prior to the experiment to achieve 30-40% of confluence at the time of transfection. Transfection was done using Lipofectamine RNAiMAX (Invitrogen) according to the manufacturer's instructions. Pre-miR-20a and pre-miR negative control#1 (scramble) (Ambion) were transfected at a final concentration of 50nmol/L. Twelve hours after transfection cells were treated with 5 ng/mL of recombinant human TGF-β1 (R&D Systems), in combination with 10µM U0126 MEK1 inhibitor (Sigma-Aldrich).

2.8 Western Blotting analysis

After transfection and treatments, cells were collected by trypsinisation and whole cell lysates were resuspended in 300 µl of 1X SDS sample buffer (50 mM Tris-HCl pH 8.5, 0.15 mM NaCl, 1% Triton-X, 0.2% SDS, 0.05% Sodium deoxycholate, 2 mM EDTA, 2 mM EGTA, 1mM PMSF, 5 mM Glycerolphosphate, 10% glycerol, 50 mM NaF, 10 mM NaPP) supplemented with protease inhibitors cocktail (Calbiochem). The suspensions were then sonicated for 5 seconds (two cycles) to shear DNA and reduce viscosity. For separating the nuclear and cytoplasmic fraction, cells were lysed with hypotonic buffer (10 mM HEPES, pH 7.9, 2.5 mM MgCl2, 0.2% NP40, 1 mM EDTA, 0.5 mM DTT, 0.5 mM PMSF) and protease inhibitors cocktail. After centrifugation for 10 minutes at 4000 rpm at 4°C the supernatant representing the cytoplasmatic fraction was removed and supplemented with 0.15 M NaCl and 1% Triton-X. The remaining pellet was resuspended in RIPA buffer and sonicated for 5 seconds (two cycles).

Protein quantification was performed using the BCA protein assay (Thermo Scientific). For each sample 40 µg of protein lysate was precipitated using 100% cold acetone for 20 minutes at -20°C, then centrifuged at 8000 rpm for 7 minutes and dried in the speed vacuum for 10 minutes. The pellets were resuspended in 20 µl of 1X loading buffer (200 mM Tris HCl pH 6.8, 8% SDS, 0.4% Bromophenol blue, 40% Glycerol) and then boiled at 98°C for 5 minutes. Samples were loaded onto gels made with different polyacrylamide concentrations: 12% for p15 and p21, and 8% for all other proteins analyzed. Proteins were then transferred on Nitrocellulose membranes with porosity of 0,2 µm. The primary antibodies used for Western blotting are showed in Table 1.

Antigen	Antibody	Type	Species	Dilution	Supplier
CDKN1A (p21)	C-19 sc-397	Polyclonal	Rabbit	1:1000	Santa Cruz
CDKN1B (p15)	#4822	Polyclonal	Rabbit	1:1000	Cell Signaling
c-Myc	D84C12	Monoclonal	Rabbit	1:1000	Cell Signaling
E2F5	E-19 sc-999	Polyclonal	Rabbit	1:300	Santa Cruz
Smad 2/3	#3102	Polyclonal	Rabbit	1:1000	Cell Signaling
Phospho-Smad 2/3	#3108 138D4	Monoclonal	Rabbit	1:1000	Cell Signaling
p44/42 MAPK (Erk1/2)	#4695 137F5	Monoclonal	Rabbit	1:1000	Cell Signaling
Phospho-p44/42 MAPK (Erk1/2)	#9106 E10	Monoclonal	Mouse	1:1000	Cell Signaling
Actin	691002 5029J	Monoclonal	Mouse	1: 5000	MP Biomedicals
Lamin B	C-12 sc-365214	Monoclonal	Mouse	1:500	Santa Cruz

Table 1. The antigen, dilution and source of antibodies used for Western Blotting.

2.9 MTT viability assay

Twelve hours after pre-miR-20a or scramble oligonucleotide transfection, cells were collected by trypsinization and seeded into a 96 well plate at a density of 5000 cells per well in six replicates, and then treated with 5ng/ml TGF-β. 36 hours later the cell proliferation rate was measured using an MTT assay, a colorimetric test for measuring the activity of enzymes produced by viable metabolically active cells that reduce MTT (3-[4,5-Dimethylthiazol-2-yl]-2,5-diphenyltetrazolium bromide) substrate to formazan, giving a purple colour. In more detail, MTT powder (Sigma) was dissolved in the growth medium at the concentration of 1 mg/2 ml and added to each well. The cells were incubated at 37°C and after two-three hours Lysis buffer (10% SDS, HCl 0.01 M) was added to the MTT

solution. Plates were then re-incubated at 37°C overnight under light protected conditions and the following day were read on a microplate reader (Infinite M200 TECAN) at a wavelength of 570 nm.

2.10 BrdU proliferation assay

Cells were seeded in 8well Lab-Tek chamber slide (ThermoScientific) at 30-40% of confluence. 12 hours later transfection with pre-miR-20a or pre-negative control treatment with 5ng/ml TGF-β was performed. After 30 hours, cells were incubated for 6h in presence of 100 μM BrdU (R&D Systems). The bromodeoxyuridine (BrdU) incorporation was evaluated by immunofluorescence staining with anti-BrdU antibody. Images were acquired by florescence.

2.11 Cell cycle analysis

Cell-cycle was evaluated in arrested-restimulated cells. Following transfection with miRNA duplexes, cells at 60% confluence were serum-deprived for 24 h. Then, the cells were re-stimulated to grow in medium containing 10% serum and Nocodazol mitotic blocker (100ng/mL) for additional 24 hours. Cells were scraped and fixed in ice-cold ethanol and stained with RNAse/propidium iodide protocol. The effect of the TGF-β treatment on cell-cycle progression was evaluated by flow-cytometric analysis of cellular DNA content via FACS instrument (Beckton & Dickinson).

2.12 c-MYC and CDKN1A silencing

A siRNA pool of four oligonucleotides (ON-TARGETplus SMARTpool) targeting different portions of the c-MYC gene were bought from ThermoScientific Dharmacon. The c-MYC siRNAs pool was transfected into cells at the final concentration of 25 nM using Lipofectamine RNAiMAX (Invitrogen). ON-TARGETplus SMARTpool targeting CDKN1A was also provided, and the transfection was performed following the same conditions. The sequences of the siRNAs against c-MYC and CDKN1A are shown in Table 2. The control siRNA (siGENOME non targeting siRNA#1) containing a mixture of four scrambled oligonucleotides sequence with no significant homology to any known human mRNA was also obtained from ThermoScientific Dharmacon.

Name	Sequence
c-MYC #1	5'- ACGGAACUCUUGUGCGUAA -3'
c- MYC #2	5'-GAACACACAACGUCUUGGA -3'
c- MYC #3	5'-AACGUUAGCUUCACCAACA -3'
c- MYC #4	5'-CGAUGUUGUUUCUGUGGAA -3'
CDKN1A #1	5' –CGACUGUGAUGCGCUAAUG -3'
CDKN1A #2	5' –CCUAAUCCGCCCACAGGAA-3'
CDKN1A #3	5' –CGUCAGAACCCAUGCGGCA-3'
CDKN1A #4	5' –AGACCAGCAUGACAGAUUU-3'

Table 2. Sequences of the individual siRNAs from the pools targeting c- MYC and CDKN1A (p21).

2.13 DNA constructs

The luciferase reporter vectors used in our experiments contain the following promoter regions:

1) pWAF1Luc containing the 2.2-kb CDKN1A promoter region

2) p(CAGA)^{9}luc containing SMAD3/4 responsive promoter

3) p(c-MYC -367/+16)luc containing -367/+16 from the c- MYC promoter

4) p(c-MYC -367/+16) E2Fm luc containing mutation in the E2F binding site.

The cells were transfected with 200 ng of the reporter vector and 40 ng of pRL-TK co-reporter, and then cotransfected with miR-20a synthetic precursor or negative control using transfection mix of Lipofectamine 2000 and Lipofectamine RNAiMAX (Invitrogen). Following the co-transfections, the cells were treated with 5 ng/ml of TGF-β for 36 hours and the luciferase activity was measured using the Dual Luciferase Assay kit (Promega).

2.14 Luciferase assay

According to the protocol, cells were firstly resuspended in 100 µl of passive lysis buffer and then analysed using a Veritas luminometer (Turner Biosytems). Briefly, 100µl of Luciferase Assay Reagent II (LARII) was added to 20µl of the cell lysate to measure the firefly luciferase reporter activity. After quantifying this luminescence, 100 µl of the Stop &Glo Reagent was added to the same samples to determine the activity of the Renilla Luciferase used for normalization.

2.15 Cloning of the ID4 3'UTR into the pGL3-promoter vector

The fragments of the 3'- UTR regions of CDKN1A, E2F5 and KLF11 containing the predicted miR-20a binding site, were amplified by PCR reaction using the following primers (Table 3), flanked by the restriction sites for the *Xba*I enzyme (TCTAGA) that was also added with the sequence GCATAT to enhance the stability at the end of the sequence for E2F5 and KLF11.

Oligo	Sequence	Amplified fragment (bp)
CDKN1A FW	5'-TCTAGAATGAAATTCACCCCCTTTCC-3'	174
CDKN1A RV	5'-TCTAGACTGTGCTCACTTCAGGGTCA-3'	
E2F5 FW	5'-GCATATTCTAGATCCAAACAGACGTTCACTGC-3'	206
E2F5 RV	5'-GCATATTCTAGATGTACAGGCATTGGCACATT-3'	
KLF11 FW	5'-GCATATTCTAGATTCTGAGAACCACAAACCTTG-3'	150
KLF11 RV	5'-GCATATTCTAGAAAAAGGCTCAAAGTCACAAAAGA-3'	

Table 3. List of the oligonucleotides used for amplification of the 3'-UTRs of the indicated genes.

The cDNA used as template for the amplification reaction was synthesized by reverse transcription of 2 μg of total RNA extracted from the FET cell line (expressing high levels of CDKN1A, E2F5 and KLF11) using the High Capacity cDNA Reverse Transcription Kit (Applied Biosystems) according to the manufacturer's instructions. The PCR amplification was performed using GoTaq DNA polymerase (Promega) with the conditions of the reaction listed in Table 4.

	CDKN1A	E2F5	KLF11	HMBS	Cycles
Initialization	95°C for 2 min			95°C for 5 min	1
Denaturation	95°C for 30 sec			95°C for 30 sec	35
Annealing	60 °C for 20 sec	56 °C for 20 sec	56 °C for 20 sec	60°C for 20 sec	
Extension	72°C for 20 sec	72°C for 25 sec	72°C for 20 sec	72°C for 20 sec	
Final Extension	72° C for 5 min			72°C for 5 min	1

Table 4. PCR reaction conditions used for amplification of the 3'-UTRs of the indicated genes.

The amplification product was visualized by UV-illumination on a 1.5% agarose gel, excised and extracted from the gel, subjected to automated sequencing by ABI PRISM 3100 genetic Analyser (Applied Biosystems) using BigDye® Terminators kit v3.1 (Applied Biosystems) and analyzed with the Sequencing Analysis 5.2 software (Applied Biosystems). After validation we used TOPO TA Cloning® Kit Dual Promoter pCR® II-TOPO® (Invitrogen) for direct insertion of the 3'-UTR fragments of CDKN1A, E2F5 and KLF11 3'UTR into pCR II-TOPO vector which was characterized by single 3'-thymidine (T) overhangs for cloning PCR products. The vectors were digested with the *Xba*I enzyme (New England Biolabs) for 2 hours at 37°C and then purified using Wizard SV Gel and PCR Clean-Up System kit (Promega) before being cloned into the pGL3-Promoter vector (Promega) which had previously been digested with the same enzyme. Ligation reaction was performed incubating CDKN1A, E2F5 and KLF11 3'UTR fragment and pGL3-Promoter vector with T4 DNA ligase (New England Biolabs) overnight in water at 16°C.

3 RESULTS

3.1 Identification of miRNAs positioned on regions frequently altered during colon cancer progression

3.1.1 Analysis of Molecular Markers Linked to Colon Cancer

We analyzed a consecutive cohort of sporadic colon cancer specimens including 43 tumors belonging to stages II to IV (Cohort 1) for copy number and gene expression profiles. Affymetrix 250K NspI arrays (copy number analysis) and Affymetrix Exon 1.0 ST arrays (gene expression) were used for the analyses. All samples were MSS and CIN and were previously characterized for mutations in APC, KRAS, TP53 and LOH of 18q, all known to be involved in colon cancer progression (Table 5) [14, 127].

		APC	KRAS	TP53	18qLOH
Total cases	43	33	24	20	22
Stage II	10	7	4	6	7
Stage III	10	8	5	3	4
Stage IV	23	18	15	11	11

Table 5. Distribution of mutations in APC, KRAS, TP53 and 18q LOH in 43 CRC samples (Cohort 1). Samples belonged to consecutive series of sporadic CIN colon cancer cases diagnosed at IRCCS INT Foundation (1998-2000) (Cohort 1).

Only two cases had none of the described genetic alterations whereas most patients had two (18 samples), followed by triplets (12 samples), singletons (9 samples) and seven samples carried all four genetic alterations. The comparison of our cohort of samples with data from literature [128, 129] highlighted that our specimens resemble the characteristics of colon cancer case series (mutation frequencies of *APC*, *KRAS*, *TP53*, and 18q LOH are 77, 56, 44, and 50%, respectively), thus minimizing any selection bias.

Copy number analysis highlighted substantial chromosomal instability in all patients. Aberrations that were present in at least 15% of the samples were amplifications on

chromosome arms 7, 8q, 12, 13q, and 20 and deletions on chromosome arms 1p, 5q, 8p, 9q, 10p, 14q, 15q, 16p, 17, 18, 19, 20p, and 22q (Table 6). These regions are frequently altered during the colon adenoma to carcinoma progression.

Chromosome arm	Gain	Lost
1p	2	27
5q	6	17
7p	58	0
7q	42	0
8p	6	40
8q	38	0
9q	6	19
10p	4	38
12p	25	4
12q	17	4
13q	**56**	**4**
14q	4	27
15q	0	35
16p	8	48
17p	0	83
17q	8	35
18p	2	54
18q	6	52
19p	2	65
19q	6	54
20p	33	21
20q	**69**	**10**
22q	0	67

Table 6. Frequencies of gained and lost regions found in 43 CRC samples (Cohort 1). Gain or loss of an arm of a sample was attributed if it contained more than 20% gain or loss over all SNPs found on the arm. Regions with highest concordance between copy number alterations and gene expression are labeled in red.

By integrating the copy number analysis data with the expression patterns of 2774 genes performed on the same samples, we found a predominantly positive correlation (74%) between the chromosomal alterations (gain and loss of specific regions) and the expression levels of the genes located on them. Gained regions containing genes with increased expression were found on chromosomal arms 7, 8q24, 12p, 13q, and 20; whereas genes

with decreased expression and lost were found on chromosomal arms 6p21, 8p, 18q, and 20p. The highest number of genes with expression levels correlated to the copy number of the regions where they map was observed on the chromosomal arms 20q and 13q with 182 and 118 genes respectively (Table 6, labeled in red) [127].

3.1.2 Identification of miRNAs positioned on frequently altered regions

We hypothesized that miRNA expression could also be linked to chromosomal gain and losses. To demonstrate this, we searched for miRNAs positioned in the regions that we found frequently gained or lost in our samples. Chromosomal locations of the miRNAs were obtained from the miRBase database v.11.0 [130] and gain and losses were defined by scanning our copy number dataset with a 100kb window. A total of 609 miRNAs were analyzed: 96 of them fell in regions with poor coverage or no SNPs and 274 were localized on altered regions (60 miRNAs in regions with over 20% gain and 214 in regions with over 20% loss), and the remaining 239 miRNAs mapped on regions with no alterations. We focused on the miRNAs positioned on 13q and 20q, where highest correlation with the gene expression was observed (Table 6). We identified nine miRNAs on chr13q including six miRNAs belonging to the cluster miR-17-92, and 13 miRNAs on 20q (Table 7). Over-expression of the miR-17-92 cluster was reported in different types of tumors, suggesting its oncogenic characteristics and co-involvement in crucial regulatory mechanisms. Therefore, we concentrated our further study on the miR-17-92 and its association with CRC.

miRNA name	Band
hsa-miR-1297	13q21.1
hsa-miR-622	13q31.3
hsa-miR-17	**13q31.3**
hsa-miR-18a	**13q31.3**
hsa-miR-19a	**13q31.3**
hsa-miR-20a	**13q31.3**
hsa-miR-19b-1	**13q31.3**
hsa-miR-92a-1	**13q31.3**
hsa-miR-1267	13q33
hsa-miR-644	20q11.22
hsa-miR-1259	20q13.13
hsa-miR-645	20q13.13
hsa-miR-1302-5	20q13.13
hsa-miR-296	20q13.32
hsa-miR-298	20q13.32
hsa-miR-646	20q13.33
hsa-miR-1257	20q13.33
hsa-miR-124-3	20q13.33
hsa-miR-941-1	20q13.33
hsa-miR-941-2	20q13.33
hsa-miR-941-3	20q13.33
hsa-miR-647	20q13.33

Table 7. MicroRNAs located on 13q and 20q, regions previously identified with highest correlation between copy number and gene expression. The chromosomal positions of the miRNAs were obtained from the miRBase database. MicroRNAs labeled in red belong to the miR-17-92 cluster.

3.1.3 miR-17-92 maps on a gained region and is over-expressed in CRC specimens

To confirm if concordant amplification of 13q13 region results in overexpression of miRNAs from the 17-92 cluster in colon cancer specimens, we analyzed the expression levels of the 6 miRNAs belonging to the cluster (miR-17, miR-18a, miR19a, miR-19b-1, miR-20a and miR-92a-1) in a second CRC cohort of 40 pairs of primary colon tumor and adjacent non-tumor tissues (Cohort 2). The group is representative of the first test cohort

according to age, gender, cancer type and stage and the cases were collected in the same timeframe. The second cohort was also characterized for presence of mutations in APC, KRAS, TP53 and 18qLOH analyses and their frequencies resembled that found in the first cohort. With respect to their paired non-tumor tissues, the tumor specimens exhibited higher expression levels of all six miRNAs from the cluster miR-17-92 (Figure 14). MiR-18a, miR-92a, and miR-20a showed the highest fold difference, and therefore we looked for their predicted target genes using the Targetscan database [131]. After excluding miR-18a (very few putative gene targets) and miR-92a (its commercially available expression assay was shown to recognize also other miRNAs [132], we focused our further studies on miR-20a.

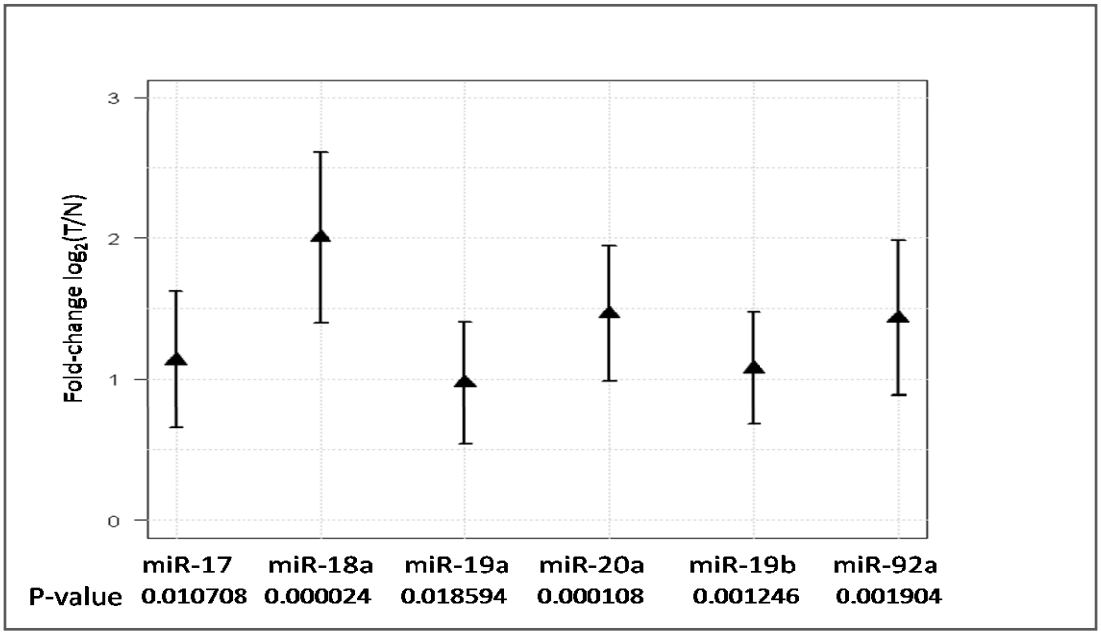

Figure 44. qRT-PCR expression levels of miR-17-92 cluster in 40 CRC patients (Cohort 2). The expression of each miRNA from the miR-17-92 cluster is shown as a $\log_2$ of the ratio of its expression level in the tumor samples versus its matched normal tissue.

We also analyzed the expression levels of miR-20a in 22 samples for which RNA was still available from the patient cohort 1, used previously for copy number and gene expression

analysis, and we confirmed a trend of difference between the expression levels of miR-20a in tumor tissue versus its normal counterpart (Figure 15).

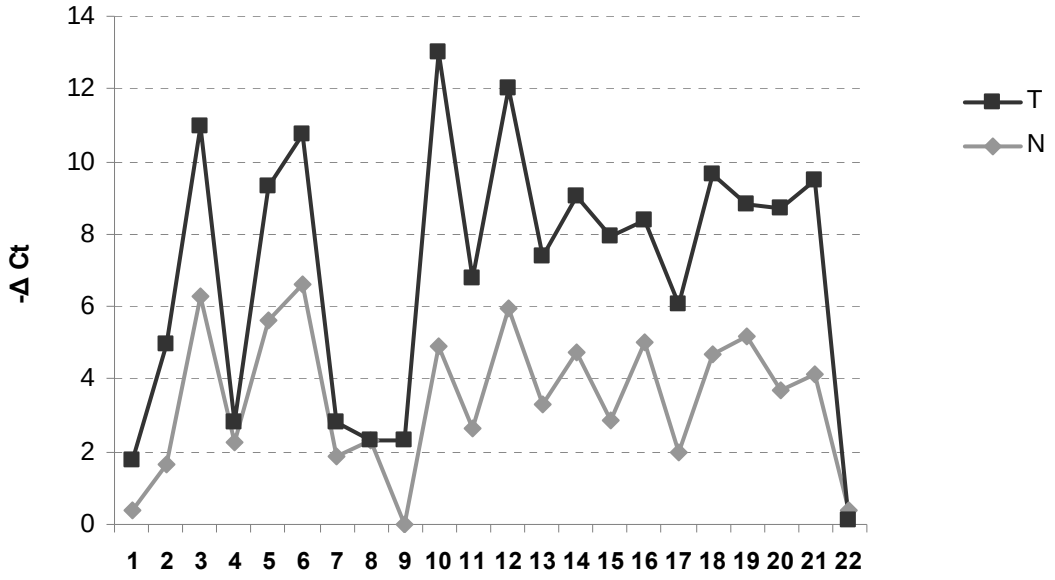

Figure 55. qRT-PCR expression levels of miR-20a in 22 CRC patients from Cohort 1. The expression levels of miR-20a in tumor or normal specimens are shown as –ΔCt obtained by normalization with the endogenous control RNU6B.

3.1.4 miR-20a putative target genes

It was recently reported that miR-106b, a paralog of miR-20a, from the cluster miR-106-25 targets p21 and abrogates the cytostatic effect of TGF-β in gastric cell lines. Based on the homology between the seed regions of the members belonging to these polycystron microRNA clusters, we hypothesized a potential involvement of miR-17-92 in the inactivation of the TGF-β mediated growth suppression in CRC and next, we searched for genes predicted as targets of miR-20a involved in this signaling pathway. The screening using the TargetScan program identified about 1,000 genes with a complementary binding site in their 3'-UTR for this miRNA. To categorize functionally

the obtained predicted genes, we used the database for annotation, visualization and integrated discovery DAVID [133] and the classification by the KEGG database. We enriched the list with other genes found in the literature as regulated by the cytokine, but not classified in this category by KEGG and we finally selected eight genes with the highest probability to be targeted by miR-20a and involved in TGF-β signaling, listed in Table 8.

Gene name and predicted miRNA binding region	Predicted consequential pairing of target region (top) and miRNA (bottom)	Seed match
Position 468-474 of **CDKN1A** 3' UTR hsa-miR-20a	5' ...AGAAGUAAACAGAUGGCACUUUG... 3' GAUGGACGUGAUAUUCGUGAAAU	7mer-m8
Position 508-514 of **E2F5** 3' UTR hsa-miR-20a	5' ...GUGCCUUCUGUUUUAGCACUUUA... 3' GAUGGACGUGAUAUUCGUGAAAU	8mer
Position 25-31 of **RBL1** (p107) 3' UTR hsa-miR-20a	5' ...GUUUCUAUGAUAAAAGCACUUUC... 3' GAUGGACGUGAUAUUCGUGAAAU	7mer-m8
Position 2144-2150 of **KLF11** 3' UTR hsa-miR-20a	5' ...GUGGGCUCCCCUCGUGCACUUUA... 3' GAUGGACGUGAUAUUCGUGAAAU	8mer
Position 749-755 of **RUNX3** 3' UTR hsa-miR-20a	5' ...GACCGGCUCCUCCAUGCACUUUA... 3' GAUGGACGUGAUAUUCGUGAAAU	8mer
Position 971-977 of **SKI** 3' UTR hsa-miR-20a	5' ...CGUAUAUUUAGAACUGCACUUUG... 3' GAUGGACGUGAUAUUCGUGAAAU	7mer-m8
Position 1365-1371 of **SMAD7** 3' UTR hsa-miR-20a	5' ...AAAUAAAGAAAAGAUGCACUUUG... 3' GAUGGACGUGAUAUUCGUGAAAU	7mer-m8
Position 268-274 of **TGFBR2** 3' UTR hsa-miR-20a	5' ...UAGCCAAUAACAUUUGCACUUUA... 3' GAUGGACGUGAUAUUCGUGAAAU	8mer

Table 8. Putative miR-20a target genes co-involved in TGF-β signaling pathway. Consequential pairing shows the complementary sequence between miR-20a and its putative gene targets, and the seed match shows the number of the nucleotides involved in the pairing: 7mer-m8 represents an exact match to positions 2-8 of the mature miRNA (the seed + position 8) and 8mer is an exact match to positions 2-8 of the mature miRNA (the seed + position 8) followed by an 'A' [131].

3.1.5 miR-20a is differentially expressed in colorectal cancer cell lines

To study the involvement of miR-20a in the TGF-β-mediated regulatory network, we searched for a cell line showing an intact TGF-β/Smad signaling and expressing low endogenous levels of this miRNA. For this aim, we evaluated the expression levels of miR-20a in a panel of 12 colorectal cell lines by qRT-PCR (Figure 16), and using the information from public databases [134] we characterized the cell lines from our panel for mutations in genes involved in TGF-β signaling pathway (SMAD-4, TGFβR).

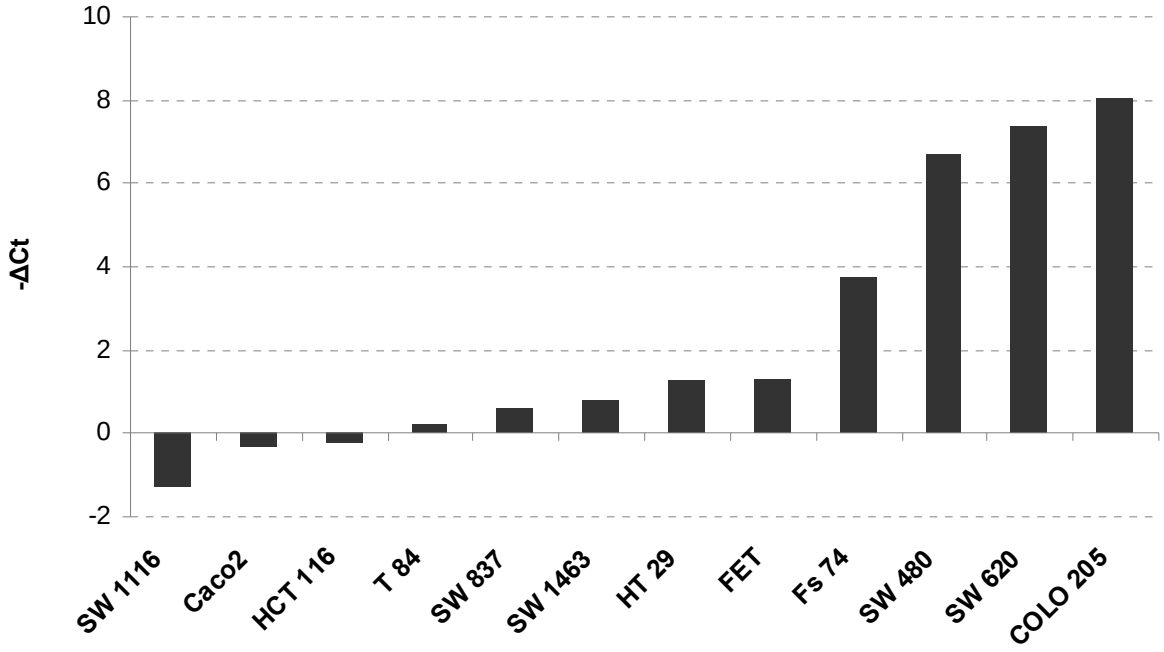

Figure 66. MiR-20a shows a broad expression range in CRC cell lines. The expression levels of miR-20a are shown as -ΔCt values, following normalization with an endogenous control RNU6B.

The four cell lines showing lowest endogenous miR-20a expression were SW1116, Caco2, HCT116 and T84. In three of them we found mutations in genes crucial for the TGF-β signaling: SW1116 (del SMAD-4 -/-), HCT116 (del TGFBR2 -/-) and Caco2 (functionally

inactive SMAD-4 [134, 135], and the cell line T84 we found as not responsive to the growth suppression effect of TGF-β (data not shown). Among the other cell lines analyzed, we found that SW837 and FET cell lines express relatively low endogenous miR-20a levels and possess intact TGF-β signaling, thus making them suitable for experiments requiring overexpression of miR-20a and studying its interactions with the TGF-β signaling network. We analyzed the growth rates of FET and SW837 cells in response to TGF-β treatment by performing MTT viability assay. For this aim, cells were treated with 5ng/ml TGF-β ligand for 48 hours and then the cell proliferation was measured. We found that both cell lines showed reduced proliferation rates after TGF-β treatment. The stimulation with the cytokine decreased of 36% cell growth in SW837 cells, and twice stronger effect was observed in FET cells (about 72%) (Figure 17).

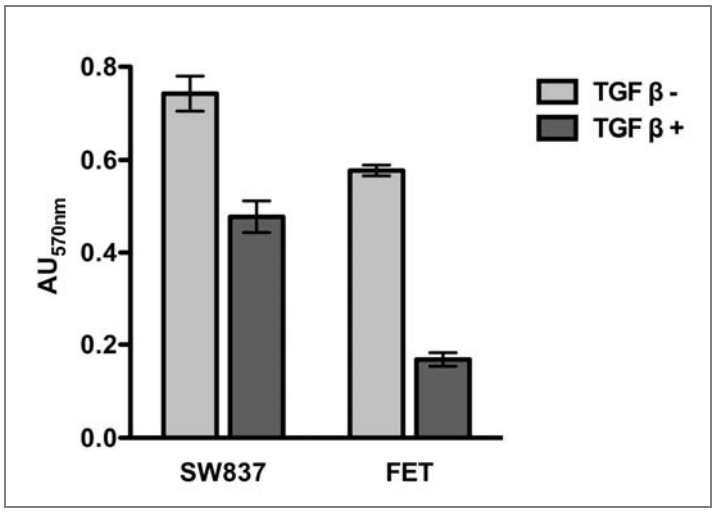

Figure 77. MTT assay showed reduced cell viability of SW837 and FET cells after TGF-β treatment. Both cell lines showed reduced growth rates after stimulation. Cells were seeded in six replicates in 96well plate, treated with TGF-β (5 ng/ml) for 48 hours and then the absorbance was measured. Averages and standard deviations are calculated from the six measurements.

Next, we optimized the transfection conditions in FET and SW837 by testing several concentrations of the oligonucleotide and different transfection reagents. Transfection using RNAiMAX and Lipo2000 gave effective results for FET cells. Regarding SW837

cells, we were not able to reduce the toxicity of the transfection reagents (used both in combination for transfection of microRNA precursors and plasmid vectors concurrently) to not toxic levels. For this reasons, we continued our work only with the FET colon carcinoma cell line. This cell line has been isolated from a well-differentiated early stage CRC, is unable to generate progressive tumor growth in vivo and retains many normal growth controls including growth inhibitory responsiveness to TGF-β [124]. As we observed, the endogenous expression levels of miR-20a are relatively low in this cells which makes the FET cell line a suitable in-vitro model for our study.

3.1.6 Over-expression of miR-20a leads to decrease of p21 mRNA and protein levels

Rapid activation of cyclin-dependent kinase inhibitors (p21 and p15) is crucial for implementing the TGF-β mediated growth suppression. CDKN1A (p21) is predicted as a putative target of miR-20a, and other groups confirmed that it is repressed by this miRNA family. To investigate if miR-20a modulates p21 levels and represses its induction by TGF-β in our cellular model, we transfected FET cells with synthetic RNA duplexes of miR-20a or with a control sequence (scramble) and treated them with the cytokine for 36 hours. CDKN1A mRNA expression was analyzed by qRT-PCR and protein levels were quantified by western blotting. Overexpression of miR-20a resulted in a significant decrease of p21 protein compared to the negative control in cells not stimulated with TGF-β. This effect was even stronger when the cells were treated with the cytokine, showing that miR-20a causes a remarkable attenuation of the p21 up-regulation provoked by TGF-β (Figure 18A). The down-modulation of the p21 protein was paralleled by a reduction of mRNA, suggesting that the regulation caused by miR-20a occurs also at transcriptional

level (Figure 18B). Actually, the induction of CDKN1A mRNA by the cytokine in presence of mir-20a is twofold lower when compared with the scramble (Figure 18C).

A

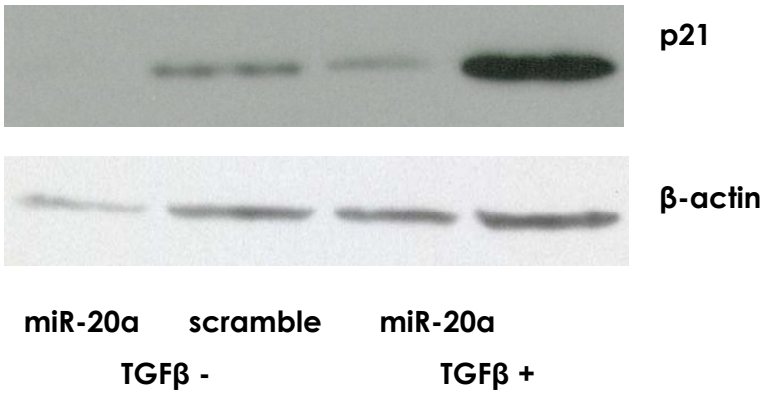

B

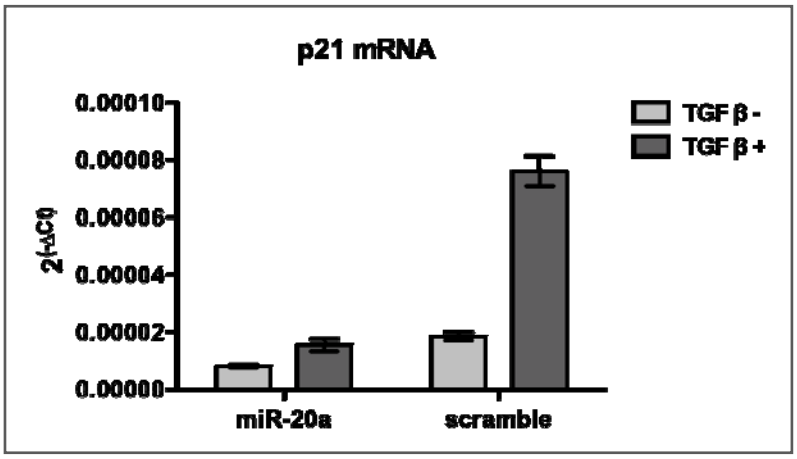

C

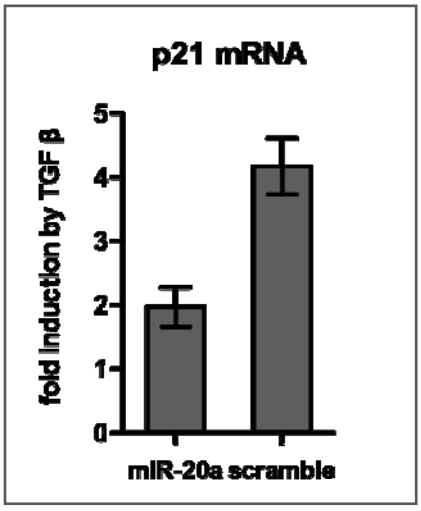

Figure 88. MiR-20a modulates p21 at mRNA and protein level. (A) p21 protein levels were determined by Western blotting after miR-20 overexpression and 36 hours treatment with TGF-β. 40 µg of total protein were loaded and β-actin was used as a control of equal loading. (B) The expression levels of CDKN1A mRNA were analyzed by qRT-PCR under the same conditions. The presented values are calculated as $2^{(-\Delta Ct)}$ and normalized to GAPDH. RNA from two separated experiments was used and for each sample the qPCR reaction was performed in triplicate. (C) Induction of CDKN1A mRNA provoked by TGF-β was calculated as a ratio of TGF-β treated versus TGF-β non treated cells.

3.1.7 CDKN1A is a direct target of miR-20a

The 3'-UTR of CDKN1A mRNA possess a binding site complementary to the miR-20a seed region. In order to validate the direct effect between CDKN1A and miR-20a, a 150 bp fragment of the CDKN1A 3'-UTR was cloned downstream of the luciferase reporter gene into PGL3-Promoter vector (pLuc CDKN1A WT 3'-UTR). The cloned region extends from nucleotide 401 to nucleotide 567 and contains the miR-20a complementary site at position 470-477 (Figure 19).

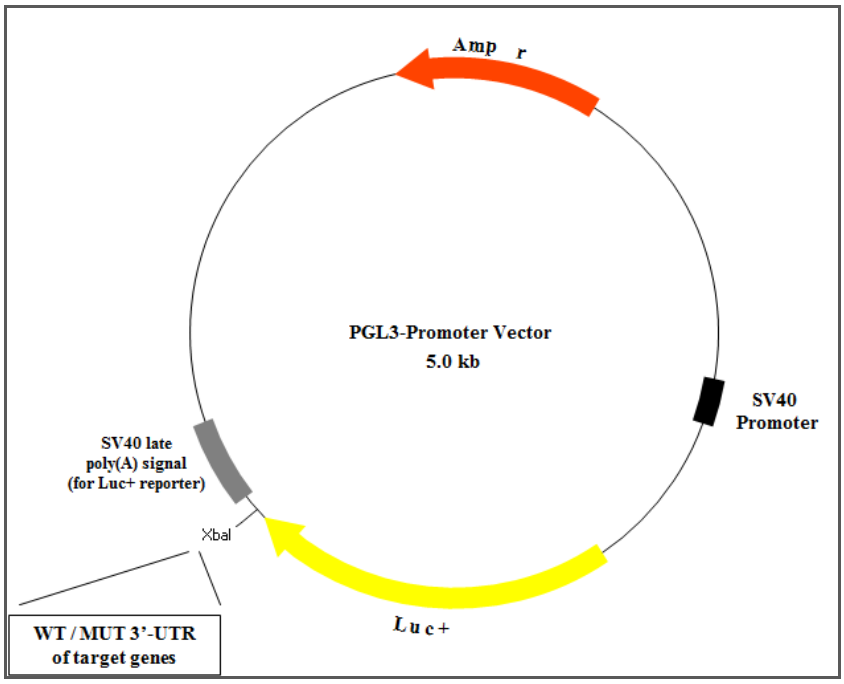

Figure 19. Scheme of the CDKN1A WT 3'-UTR/ CDKN1A MUT 3'-UTR luciferase reporter vector. The 3'-UTR of CDKN1A (containing WT or mutated binding site for miR-20a) was cloned downstream of the luciferase (Luc+) reporter gene into PGL3-Promoter vector (5.0 Kb).

The pLuc CDKN1A MUT 3'-UTR reporter vector in which two nucleotides from the miR-20a binding region were mutated was generated using the QuickChange II XL Site-Directed Mutagenesis Kit. In this way the complementarity to miR-20a was removed and the vector was used as a control of the miR-20a/CDKN1A interaction (Figure 20).

miR-20a	**3'**	**GAUGGACGUGAUAUUCGUGAAAU**
		I I I I I I I
p21 WT 3'UTR	**5' ...**	**AGAAGTAAACAGATGGCACTTTG**
p21 mut 3'UTR	**5' ...**	**AGAAGTAAACAGATGGCCCTGTG**

Figure 90. Mutagenensis of the miR-20a complementary region in the 3'-UTR of CDKN1A. The miR-20a seed sequence GCACTTT was mutated into GCCCTGT.

To confirm the direct effect of miR-20a on the CDKN1A transcript, HEK293T cells were transfected with pLuc CDKN1A WT 3'-UTR/ pLuc CDKN1A MUT 3'-UTR, and co-transfected with pre-miR-20a. The basal luciferase activity of the pLuc CDKN1A WT 3'-UTR/ pLuc CDKN1A MUT 3'-UTR plasmids (without miR-20a transfection) was used for normalization. 24 hours after transfection, cells were lysed and the luciferase activity was detected. After miR-20a transfection, decrease of 30 % (p-value = 0.001) in the luciferase activity of the pLuc CDKN1A WT 3'-UTR reporter compared to the pLuc CDKN1A MUT 3'-UTR was observed confirming the direct interaction between miR-20a and CDKN1A (Figure 21).

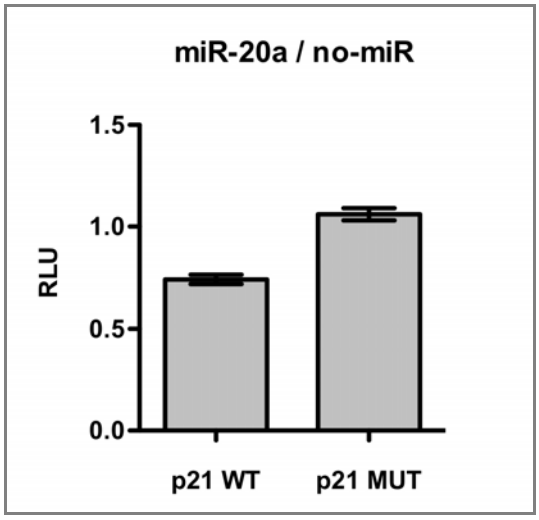

Figure 10. MiR-20a modulates the CDKN1A mRNA 3'-UTR reporter plasmid. Co-transfection of the pLuc CDKN1A WT 3'-UTR construct with miR-20a duplexes resulted in down-regulation of luciferase activity, compared to a construct in which the miR-20a complementary sites were mutated (pLuc CDKN1A MUT 3'-UTR). Averages and standard deviations are calculated from three independent experiments.

3.1.8 Inhibition of MAPK signaling did not influence the effect of miR-20a on p21

The FET cell line harbors hyperactive k-Ras allele and constitutively active MAPK/ERK signals, which can contribute to attenuate the TGF-β suppressive response. We used the MEK1/2 inhibitor U0126 in our assays in order to down-regulate MAPK/ERK cascade and prevent the phosphorylation of ERK. Treatment with 10μM U0126 significantly decreased the pERK protein levels (Figure 22A).

We observed a significant p21 up-regulation induced by the cytokine, and the mechanism mediated by miR-20a that suppresses this TGF-β effect on p21 is still operative, as evidenced by the remarkable reduction of p21 in miR-20a FET-transfected cells (Figure 22B).

A

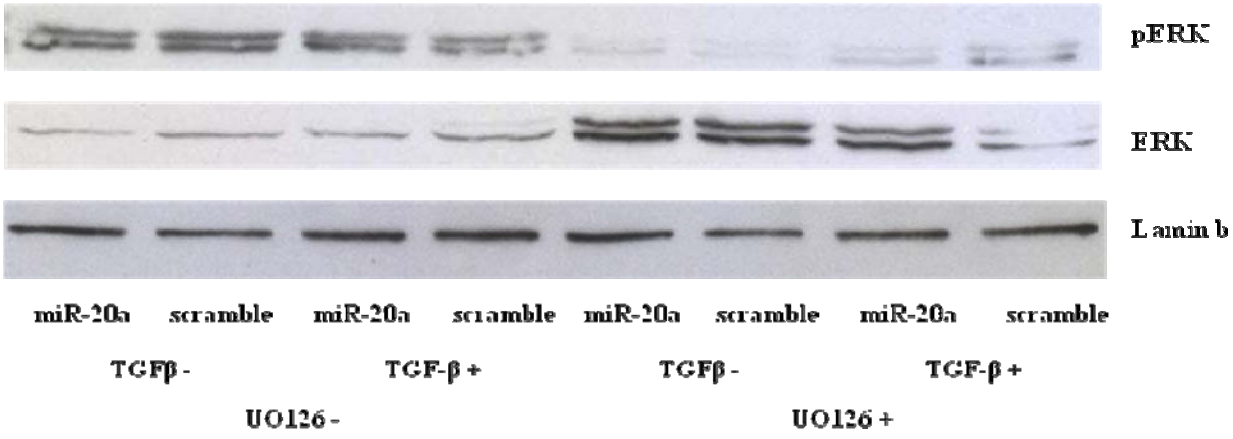

B

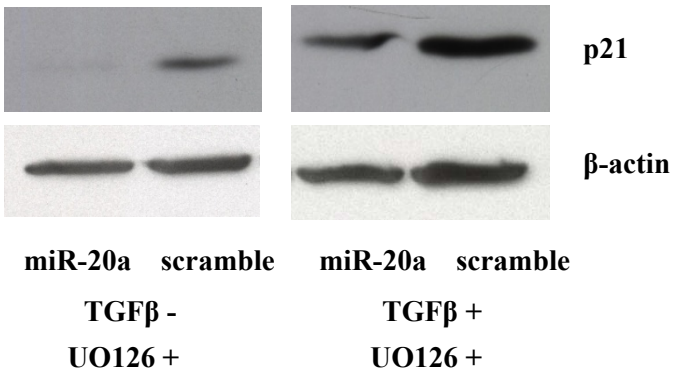

Figure 112. The modulation of p21 and c-Myc protein levels by miR-20a was maintained after inhibition of the MAPK signaling pathway. (A) The efficiency of the inhibition of the MAPK pathway was confirmed by analyzing the protein levels of pERK and ERK proteins. (B) p21 protein levels were determined by western blotting after transfection with miR-20a or negative control precursors, treatment with TGF-β and U0126 addition.

3.1.9 miR-20a significantly decreases TGF-β induced growth inhibition

In order to analyze if the cytostatic function of TGF-β is implemented after overexpression of miR-20a and consequent reduction of the CDK inhibitor p21, the proliferation rates of FET cells were analyzed following miR-20a transfection and TGF-β treatment by BrdU incorporation and MTT-based viability assay experiments. We observed that miR-20a overexpression has a slight effect on TGF-β non stimulated cell proliferation increasing by about 20% the portion of BrdU-marked nuclei. As expected, following TGF-β treatment growth suppression was induced and the population of proliferating cells was strongly reduced in control cells (about 70%), while the cells transfected with miR-20a precursor showed only a moderate reduction of BrdU incorporation (about 25%) (Figure 23A). This finding was confirmed by MTT assay which showed similar results: no significant growth inhibition due to miR-20a transfection was observed, and the inhibition of the cell growth was twofold higher in control cells (about 33%) than in miR-20a transfected (about 17%) (Figure 23B).

A

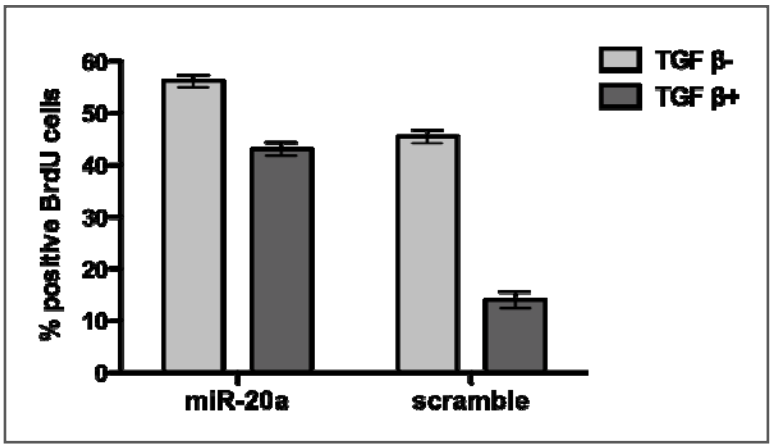

B

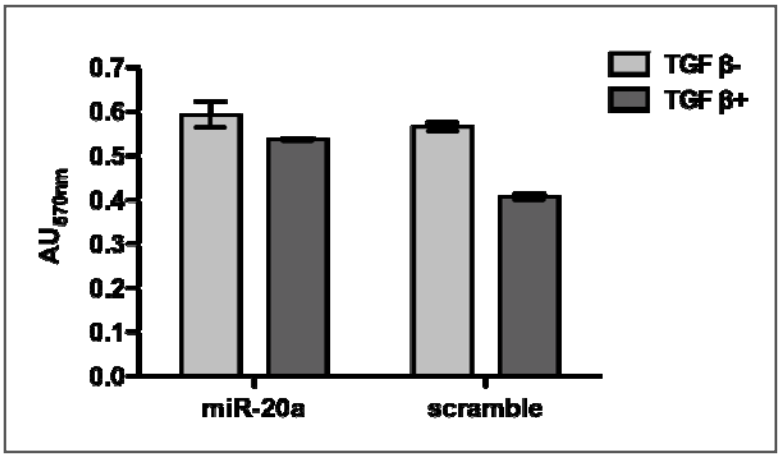

Figure 23. Exogenous miR-20a abrogated the growth arrest induced by TGF-β. (A) BrdU incorporation assay was performed 48 hours after transfection with miR-20a or with negative control and 36 hours after TGF-β treatment. Averages and standard deviations are calculated from three independent experiments, for each condition at least six fields were counted. (B) MTT assay performed following the same conditions as for BrdU assay. After transfection and TGF-β treatment, the cells were seeded in six replicates and the absorbance was measured. The represented values are calculated from the six measurements performed.

3.1.10 Knockdown of CDKN1A abolishes TGF-β induced growth inhibition in FET cells

We observed that in FET cells the TGF-β mediated cytostatic program is present, and stimulation with the cytokine resulted in growth arrest. The growth suppression effect is implemented by rapid activation of CDK inhibitors, such as p21 and p15. To understand if the observed effect of TGF-β in our cellular model is due to activation of p21 or p15, we decided to knock down the expression of endogenous p21 in FET cells and to analyze subsequently the proliferation rate of the cells. For this aim, cells were transfected with siRNA duplexes targeting p21 (siCDKN1A) or with a control unspecific siRNA sequence (siCNTR), and treated with TGF-β for 36 hours. In the control cells, TGF-β stimulation

reduced the cell growth for about 80%, while after siRNA mediated depletion of p21 the cell proliferation rates were decreased for only about 40% (Figure 24). This result suggested that in our cellular model the growth inhibition induced by TGF-β is achieved by induction of the CDK inhibitor p21.

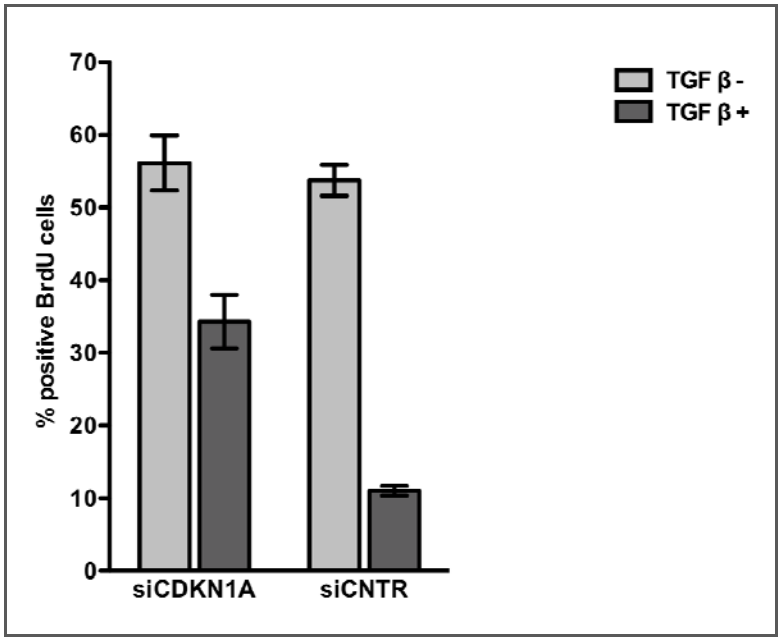

Figure 124. Growth inhibition induced by TGF-β is impaired upon depletion of CDKN1A. FET cells were transfected with siCDKN1A duplex or with a negative control siCNTR, treated with TGF-β for 36 hours and stained for BrdU incorporation assay. Averages and standard deviations are calculated from two independent experiments, for each condition at least six fields were counted.

We analyzed also the induction of p15 after stimulation with the cytokine and its eventual regulation by miR-20a. FET cells were transfected with miR-20a precursors and stimulated with TGF-β for 36 hours. CDKN1B (p15) does not possess a complementary seed region for miR-20a, therefore a direct modulation was not expected and indeed was not observed (no difference between miR-20a and scramble transfected cells). Neither induction by TGF-β was found (Figure 25). This result indicates that in the FET cell line, the cytostatic effect of TGF-β is achieved by induction of CDKN1A (p21).

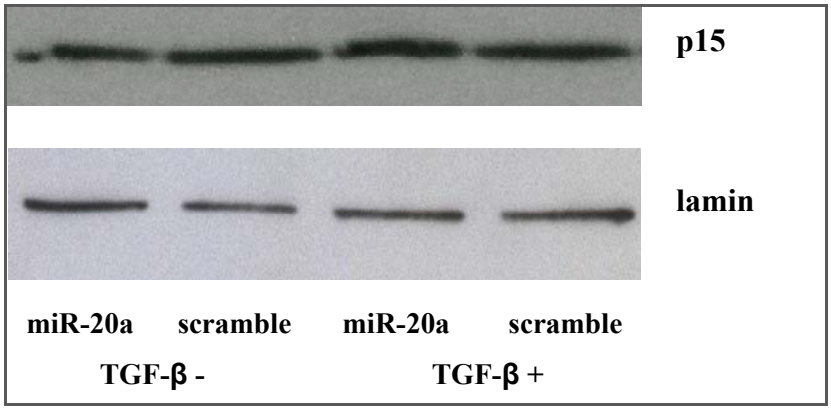

Figure 135. CDKN1B (p15) protein is not modulated by mir-20a and is not induced by TGF-β in FET cells. p15 protein levels were evaluated by Western Blot in the nuclear fraction after miR-20 overexpression and treatment with TGF-β. 40ug of nuclear protein were loaded and the nuclear protein lamin was used as a control of equal loading.

3.1.11 miR-20a affects cell cycle progression

To study if the effect of miR-20a on p21 expression also affects cell cycle progression, we transfected FET cells with miR-20a precursor and cultured them in serum free medium for 24 hours (cells enrichment in the G_0/G1 phase). The cell cycle progression was then re-stimulated by adding serum-containing medium, in absence or presence of TGF-β. Nocodazole, a mitotic blocker, was also included in the medium to prevent entry into second phase G1 (G1'). Following RNAse treatment/propidium iodide staining, the distribution of cells in cell-cycle phases was determined by analyzing their DNA content via FACS. The relative DNA profiles of mock- and miR-transfected cells, harvested 24 after re-stimulation with serum showed that, in absence of TGF-β most of the cells (about 85%) escaped the G_0/G1 block operated during the serum-deprivation step and progress through the cell-cycle (Figure 26A). Following TGF-β addition, a significant delay of G1/S transition was observed both in scramble and miR-transfected cells. However, this delay appears significantly attenuated in miR-20a-transfected cells (32% cells in G1 phase

in miR-20a transfected cells *vs.* 52.3% in control, Figure 26B), suggesting that miR-20a interferes with the TGF-β signaling by subverting the G1/S arrest induced by the cytokine.

A

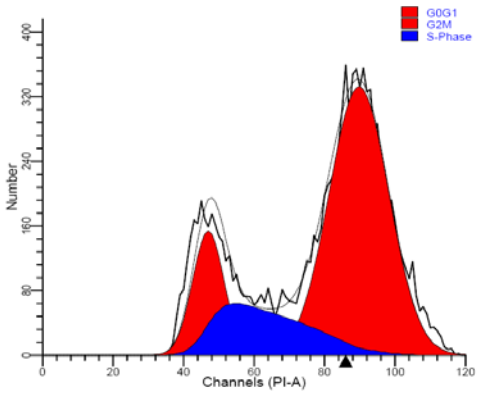

scramble

G0/G1 15.8%

S 18.8%

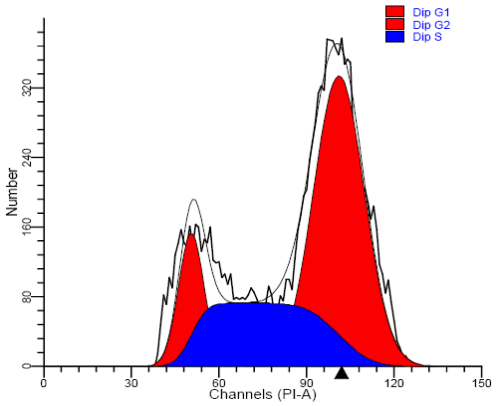

miR-20a

G0/G1 13.4%

S 29.1%

B

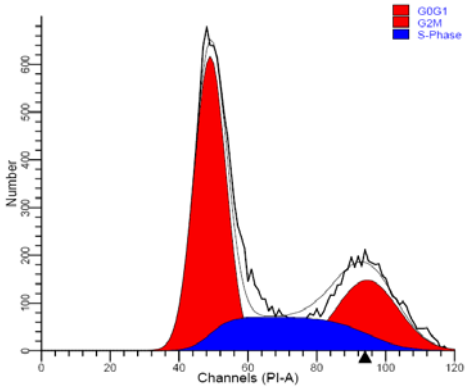

scramble TGF-β

G0/G1 52.3%

S 23.4%

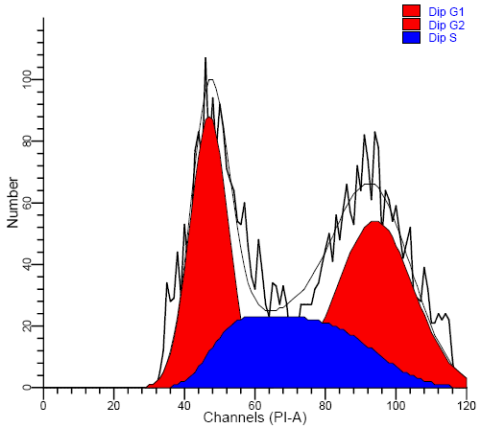

miR-20a TGF-β

G0/G1 32%

S 29.2%

Figure 146. The block of G1/S transition induced by TGF-β is rescued by mir-20a. The cells were transfected with miR-20a, left not treated with TGF-β (Figure 26A) or stimulated with the cytokine (Figure 26B) and with nocodazole. The cell cycle profiles were analyzed by flow cytometry. The presented data derives from one of the three experiments performed.

3.1.12 mir-20a decreases the CDKN1A promoter transactivation induced by TGF-β

We found that many of the miR-20a predicted target genes are transcriptional factors forming complexes that bind directly to the CDKN1A promoter and induce its transcription (RUNX3), or regulate the repression of the p21 inhibitor c-Myc (E2F5, p107, KLF11) in response to TGF-β stimulation. We suggest that a potential repression of these genes caused by direct binding of miR-20a to their 3'-UTR can destabilize them, thus resulting in decrease of the TGF-β induced CDKN1A promoter activity. To investigate this hypothesis, we transfected FET cells with a reporter vector containing the 2.2-kb CDKN1A promoter upstream of the luciferase gene. Co-transfection experiments with the miR-20a precursor or scramble were performed and treatment with TGF-β was carried out for 36 hours. As expected, upon stimulation with the cytokine we observed a 2- to 2.2-fold induction of the CDKN1A promoter activity in the control cells, while in cells overexpressing miR-20a this activation was significantly reduced. Not significant modulation of the basal response (TGF-β untreated cells) was observed in presence of miR-20a (Figure 27). These results indicate that miR-20a does not affect the basal CDKN1A promoter activity, but reverses its induction mediated by TGF-β.

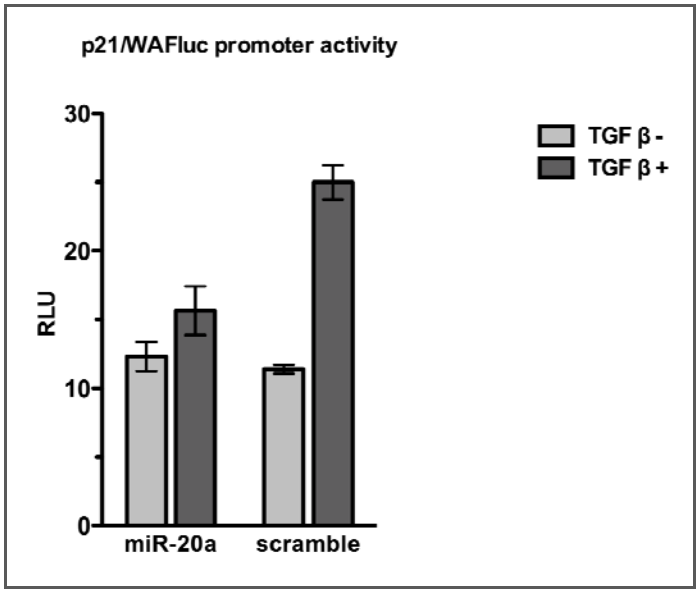

Figure 27. mir-20a decreases CDKN1A promoter transactivation driven by TGF-β. FET cells were co-transfected with miR-20a precursor or scramble and CDKN1A luc vector and treated with TGF-β for 36 hours. Averages and standard deviations are calculated from three independent transfections.

3.1.13 SMAD-dependent promoter activation is not modified by miR-20a

After observing inhibition of the TGF-β mediated CDKN1A promoter induction by miR-20a, we tested whether this microRNA interferes also with the Smad-mediated signaling. Smad-3 and Smad-4 bind to the TGF-β inducible DNA element named CAGA box and drive TGF-β dependent CDKN1A transcription. A reporter p(CAGA)^{9}luc vector composed of nine repeats of the CAGA box upstream of the luciferase gene was transfected into FET cells. Following co-transfection with miR-20a or scramble, cells were treated with TGF-β for 36 h and assayed for luciferase activity. FET cell line is responsive to TGF-β mediated growth inhibition, and as expected we observed increased p(CAGA)^9 promoter activity for about 15 fold after TGF-β stimulation (Figure 28, scramble). We found that the promoter transcativation by TGF-β was not significantly altered when the cells were co-transfected with miR-20a precursor (Figure 28, miR-20a) showing that miR-20a has no effect on the activity of the Smad-responsive reporter and does not affect the

Smad signaling cascade to the nucleus, confirming that its effect is downstream of the core Smad-3/-4 TGF-β signaling.

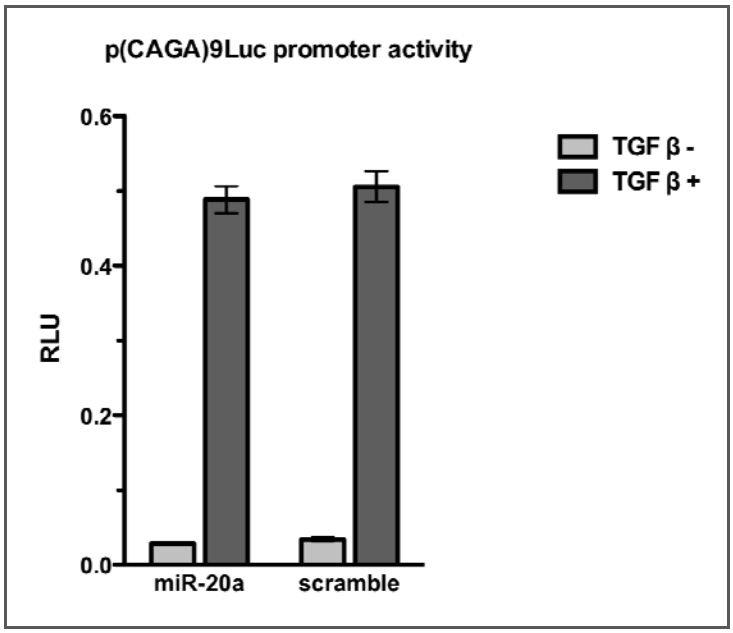

Figure 158. The Smad-3/-4 promoter activity is not affected by miR-20a. FET cells were co-transfected with miR-20a precursor or scramble and p(CAGA)^{9}luc vector and treated with TGF-β for 36 hours. Averages and standard deviations are calculated from two independent transfections. For each condition the luciferase activity was measured in triplicate.

3.1.14 c-Myc repression is necessary for TGF-β mediated p21 activation

c-Myc down-regulation is required for implementing of the cytostatic program regulated by TGF-β, but is not uniformly present in cells that are grow inhibited by this cytokine. c-Myc via the zinc finger protein Miz-1 binds to the CDKN1A promoter and directly inhibits its transcription [45, 46]. Decreasing of c-Myc levels enables trans-activation of p21 by a TGF-β activated complex, and consequently initiation of the growth suppression program. To confirm that this mechanism is operating in our cellular model, FET cells were co-transfected with a reporter vector containing the 2.2-kb CDKN1A promoter upstream of the luciferase gene (p21/WAFluc vector) and siRNA duplexes targeting c- MYC or with a

control siRNA. The efficiency of the c- MYC knockdown was confirmed by qRT-PCR and western blotting, showing a reduction in c- MYC mRNA and protein levels (Figure 29A). After 36 hours treatment with TGF-β, the luciferase activity was measured and we observed that the induction of the CDKN1A promoter was significantly increased in cells where c-Myc expression was silenced compared with the control cells (Figure 29B). We measured also the CDKN1A mRNA levels, and we observed that TGF-β and c-Myc silencing result in synergistic induction of p21 expression (Figure 29C). This data confirmed that in our cellular model an operating c-Myc repressive mechanism mediated by TGF-β is present.

A

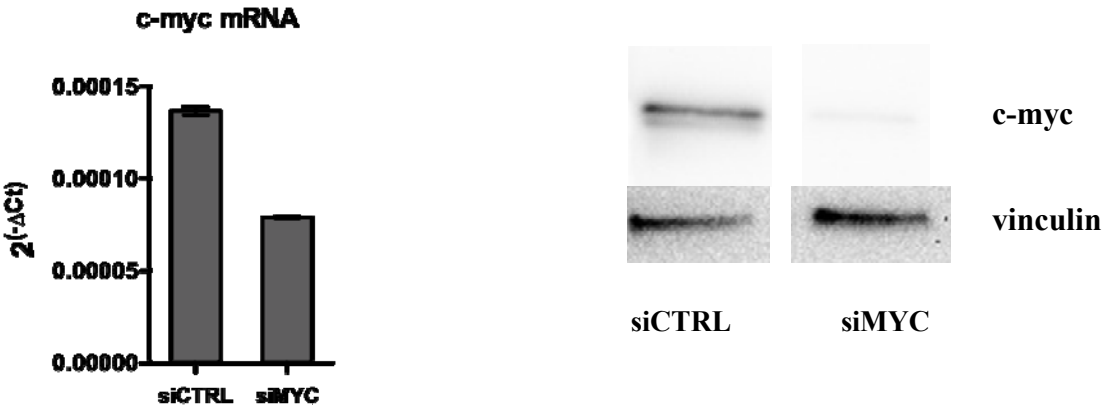

B

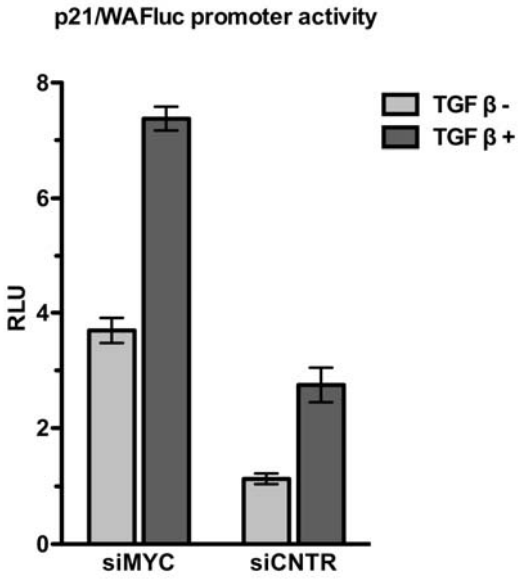

C

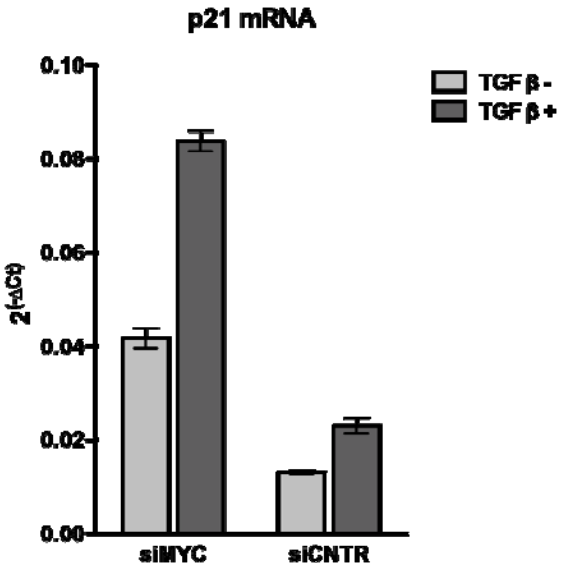

Figure 29. c-MYC silencing synergizes with TGF-β in inducing p21/WAF1 promoter activity and CDKN1A mRNA expression. (A) Transfection with 25nM of siRNA targeting c- MYC reduced significantly its mRNA and protein levels. (B) FET cells were co-transfected with a p21/WAFluc vector and siRNA duplexes against c- MYC or control siRNA and treated with TGF-β for 36 hours. Two independent experiments were performed and the luciferase activity for each condition was measured in triplicate. (C) The same conditions were used for measuring the mRNA expression of CDKN1A. The presented values are calculated as $2^{(-\Delta Ct)}$ and normalized to GAPDH. RNA from two separated experiments was used and for each sample the qPCR reaction was performed in triplicate.

3.1.15 miR-20a predicted target genes are implicated in c-MYC repression complexes

The mechanisms by which TGF-β represses c-Myc as part of its cytostatic effect are still not completely clear. Current models of TGF-β action describe that activated Smad complexes recruit transcriptional co-activators or co-repressors in the nucleus, associate with DNA binding cofactors and induce different transcriptional complexes with specificity to a particular gene, leading to its activation or repression. Such a complex is

formed between Smad-3 and the transcription factors E2F4/5, DP1 and the co-repressor p107. This complex preexists in the cytoplasm, and moves into the nucleus in response to TGF-β, associates with Smad-4 and binds the c- MYC promoter for repression, thus promoting CDKN1A transcription [61]. Besides the Smad-3/E2F4-5/p107 c-Myc repressing complex, an alternative one is formed of activated Smad-3 and KLF11. Following induction by TGF-β, KLF11 interacts with Smad-3 and recognizes the TIE of the c- MYC promoter. KLF11 binds also the Smad7 promoter and blocks its expression, disrupting the negative feedback loop of the TGF-β signaling.

When we searched for putative miR-20a targets, we identified conserved binding sites for this microRNA in E2F5, p107 and KLF11 mRNA 3'-UTRs (Table 8). We hypothesized that inhibition of these genes by miR-20a can destabilize the repression complexes, preventing the down modulation of c-Myc by TGF-β and resulting in high c-Myc levels. Schematic representation of the putative interactions of miR-20a and c-Myc repressive complexes is shown in Figure 30.

A

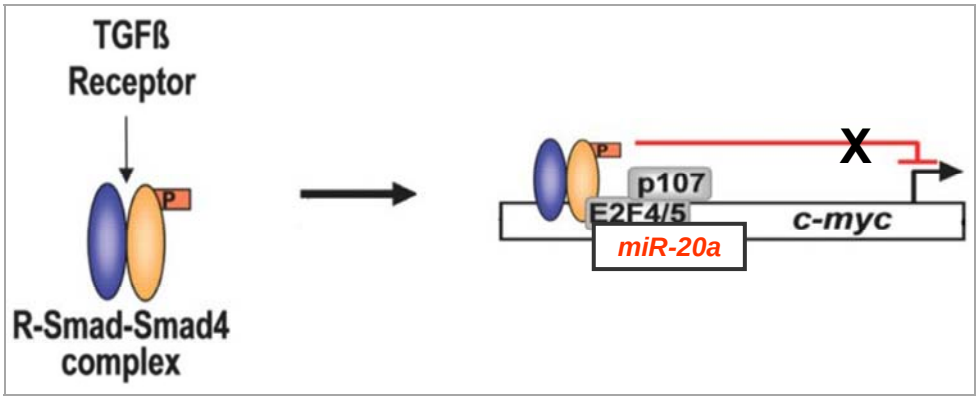

B

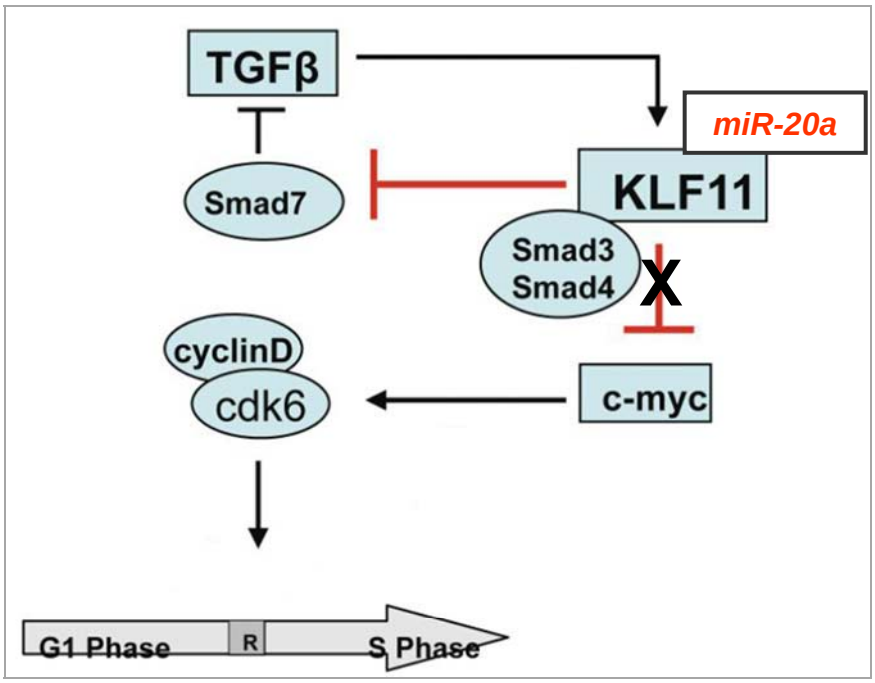

Figure 160. Schematic models representing the predicted interactions of miR-20a with genes involved in c-Myc repressing complexes mediated by TGF-β. miR-20a possess complementary binding site to the 3'-UTRs of E2F5 and p107 (A) and KLF11 (B). Putative interaction with these genes could disrupt the c-Myc repressing complexes.

3.1.16 c-Myc repression in response to TGF-β stimulation is abrogated by miR-20a

The 3'-UTR region of c-MYC lacks putative binding sites for miR-20a, and direct modulation cannot be achieved. We suggest that down modulation of the genes forming c-Myc repressive complexes (E2F5, p107 and KLF11) by miR-20a could result in high c-Myc levels thus abrogating the induction of CDKN1A transcription by the cytokine. c-Myc protein levels were analyzed in cells transfected with miR-20a or scramble precursors and stimulated with TGF-β for 36 hours. Suppression of c-Myc mediated by TGF-β was observed in the cells transfected with the negative control, while in the miR-20a

transfected cells this mechanism was abolished (Figure 31). As expected, there was no effect of miR-20a overexpression on c-Myc endogenous levels due to lack of complementary binding site. Our data suggest that miR-20a abrogates the TGF-β cytostatic program not only by direct modulation of p21, but also indirectly by abolishing the repression of c-Myc.

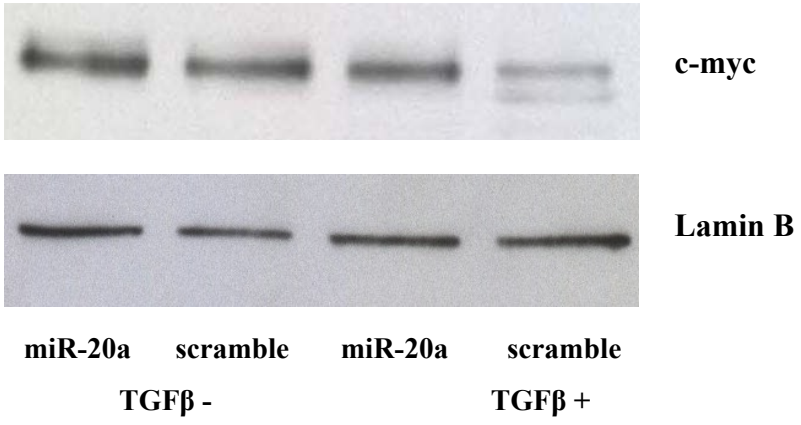

Figure 31. c-Myc down-regulation by TGF-β was abrogated by mir-20a. c-Myc protein levels were evaluated by western blotting after miR-20 overexpression and 36 hours treatment with TGF-β. 40 μg of nuclear protein were loaded and the nuclear protein Lamin B was used as a control.

3.1.17 Over-expression of miR-20a leads to decrease of E2F5 mRNA and protein levels

To establish whether miR-20a modulates E2F5, we firstly analyzed variations in its mRNA and protein levels after miR-20a transfection. For this aim, we transfected FET cells with miR-20a precursors and treated them with TGF-β for 36 hours. Then, we measured E2F5 mRNA expression by qRT-PCR and quantified its protein levels by western blotting. No significant difference in E2F5 mRNA levels was observed between miR-20a transfected and control cells, suggesting that this miRNA regulates E2F5 expression at post-transcriptional level (Figure 32A). Indeed, a reduction of E2F5 protein level by about 60%

was observed in TGF-β not treated cells, and after stimulation with the cytokine a down-modulation of about 40% was observed (Figure 32B).

A

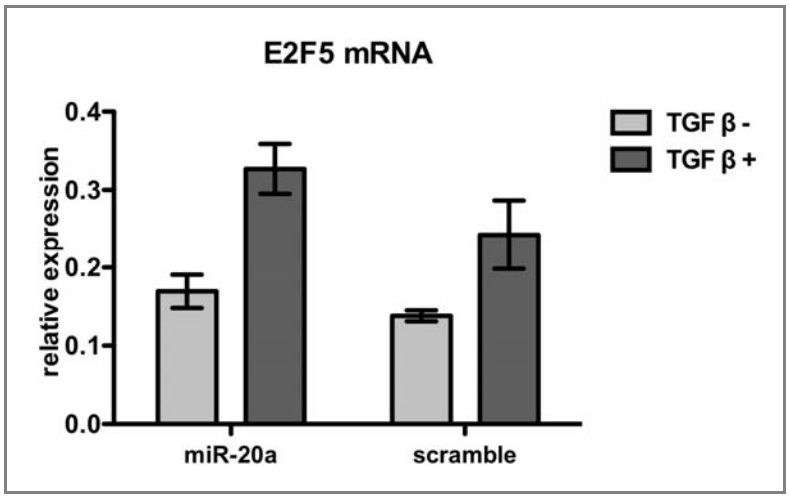

B

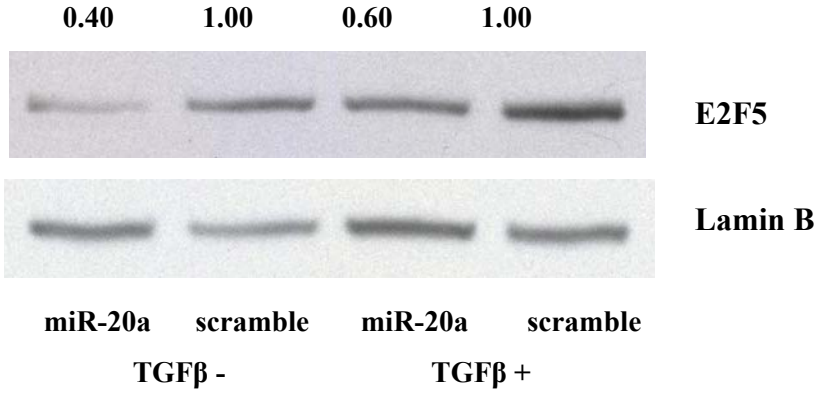

Figure 172. miR-20a does not affect E2F5 mRNA expression, but reduces its protein levels. FET cells were transfected with miR-20a or scramble and treated 36 hours with TGF-β. (A) The E2F5 expression levels detected by qRT-PCR are normalized to GAPDH and presented as $2^{(-\Delta Ct)}$. RNA from two separated experiments was used and for each sample the qPCR reaction was performed in triplicate. (B) E2F5 protein levels were detected by Western blot. 40 μg of nuclear protein were loaded and the nuclear protein Lamin B was used as a control.

3.1.18 E2F5 is a direct target of miR-20a

To validate the direct interaction between E2F5 3'-UTR and miR-20a a 206 bp fragment of the E2F5 3'-UTR, spanning from nucleotide 410 to nucleotide 615 and containing the miR-20a complementary site at position 502-509, was cloned downstream of the luciferase gene into PGL3-Promoter vector (pLuc E2F5 WT 3'-UTR). The pLuc E2F5 MUT 3'-UTR construct contains two mutated nucleotides in the miR-20a binding region and was generated using the QuickChange II XL Site-Directed Mutagenesis Kit. The induced mutations are shown in Figure 33.

miR-20a	**3'**	**GAUGGACGUGAUAUUCGUGAAAU**
		I I I I I I I
E2F5 WT 3'UTR	**5' ...**	**GTGCCTTCTGTTTTAGCACTTTA**
E2F5 mut 3'UTR	**5' ...**	**GTGCCTTCTGTTTTAGCCCTGTA**

Figure 183. Mutagenensis of the miR-20a complementary region in the 3'-UTR of E2F5. The miR-20a seed sequence GCACTTT was mutated into GCCCTGT.

Next, luciferase reporters carrying the 3' UTR of the gene with wild type (pLuc E2F5 WT 3'-UTR) or mutated miR-20a binding region (pLuc E2F5 MUT 3'-UTR) were transfected into HEK293T cells and followed by co-transfection with pre-miR-20a. The basal luciferase activity of the reporter vectors without miR-20a transfection was used for normalization. Cells were lysed 24 hours after transfection and the luciferase activity was measured.

A reduction of about 35% in luciferase activity (p-value 0.01) was observed in miR-20a and pLuc E2F5 WT 3'-UTR co-transfected cells compared to the luciferase activity measured after pLuc E2F5 MUT 3'-UTR and miR-20a co-transfection (Figure 34). These

data indicate a direct regulation of the E2F5 transcript by miR-20a and may provide a mechanism explaining the subverted down-modulation of c-Myc induced by TGF-β that we previously observed.

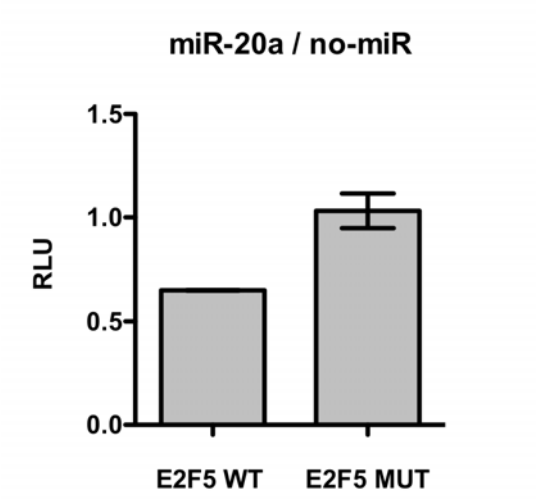

Figure 194. miR-20a modulates the E2F5 mRNA 3'-UTR reporter plasmid. Co-transfection of the E2F5 WT 3'-UTR construct with miR-20a duplexes resulted in down-regulation of luciferase activity, compared to a construct in which the miR-20a complementary sites were mutated (E2F5 MUT 3'-UTR). Averages and standard deviations are calculated from two independent experiments.

3.1.19 Attenuated E2F5 expression by miR-20a prevents its binding to the c-MYC promoter

Activation of a Smad-3/4-E2F4/5 complex on c-MYC promoter in response to TGF-β has been previously described as indispensable for the repression of its expression, a key event in growth suppression mediated by TGF-β. This complex directly binds to TIE (TGF-β inhibitory Element) on the promoter, which contains Smad binding site (TIE) and E2F consensus element. The integrity of both binding sites is required in order for TGF-β to fulfill its inhibitory effect on c-MYC transcription [61].

We investigated whether the decrease of the E2F5 protein observed in miR-20a-transfected cells could affect the binding of the Smad-3/E2F4-5/p107 complex to the c-MYC promoter and abolish its repression by TGF-β. For this aim, FET cells were transfected with a reporter construct containing the -367/+16 sequence of the c-MYC promoter upstream of the luciferase gene with intact binding sites for Smad (TIE) and E2F, or with a reporter mutated at the E2F site (E2Fm) (Figure 35A). Then, the cells were co-transfected with miR-20a and stimulated with TGF-β. Both constructs include three CAGA sequences, directly recognized and activated by Smad-3/-4, and consequently stimulation of the cells with the cytokine activates them. Therefore, we normalized the relative luciferase response (RLU) of the wild-type reporter to the relative response of the reporter containing E2Fm site (pRL-TK vector was used as an internal control), and analyzed the contribution of miR-20a for the Smad-3/E2F4-5/p107 binding to the c-MYC promoter.

As expected, TGF-β treatment decreased the activity of c-myc (-367/+16)luc in the control cells, while miR-20a transfection significantly attenuated this repression, thus subverting the implementation of the growth inhibition mediated by the cytokine (Figure 35B).

A

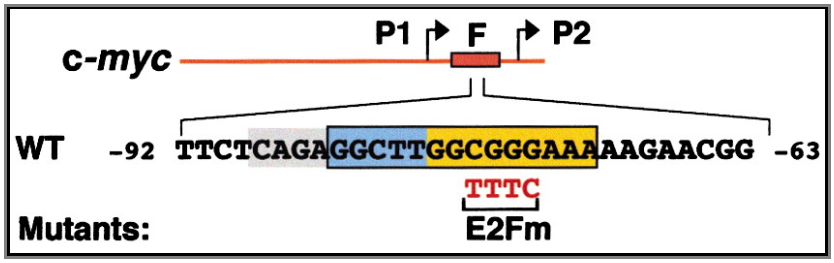

B

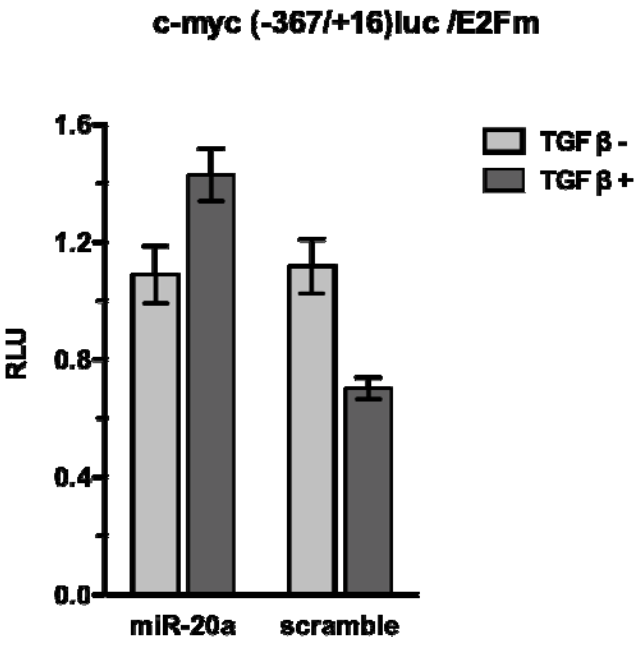

Figure 205. miR-20a overexpression abrogates TGF-β-induced repression of MYC promoter activity. (A) Schematic representation of the nucleotide sequence of TIE element (blue) and E2F binding site (yellow) in MYC promoter [modified from 61]; mutation at E2F consensus sequence (E2Fm) are shown (B) FET cells were transfected with the reporter vectors encoding the -367/+16 MYC promoter, containing intact or mutated E2F binding site, co-transfected with miR-20a or scramble precursors, and treated with TGF-β for 36 hours. Transactivation of the wild-type promoter is normalized to the E2Fm construct.

3.1.20 KLF11 is a direct target of miR-20a

In order to analyze the predicted regulation of KLF11 by miR-20a, KLF11 expression levels were analyzed after miR-20a overexpression by qRT-PCR. FET cells were transfected with miR-20a or a scramble sequence and stimulated with TGF-β for 36 hours. A significant reduction of KLF11 mRNA after miR-20a overexpression was observed: reduction of about 70% was measured in not stimulated cells and reduction of about 40% when cells were treated with the cytokine (Figure 36). Due to a lack of specific antibody we were not able to analyze the variations of the protein after miR-20a overexpression.

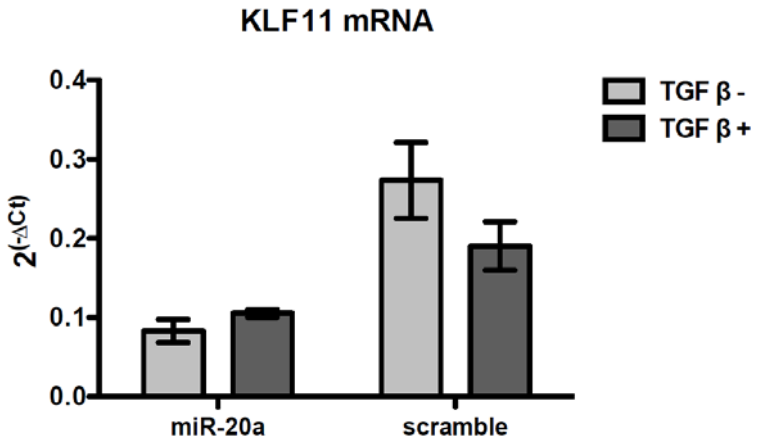

Figure 216. KLF11 mRNA expression is down-regulated after mir-20a overexpression. Relative expression levels of KLF11 were analyzed by qRT-PCR after miR-20a transfection and 36 hours TGF-β treatment. The presented values are calculated as $2^{(-\Delta Ct)}$ and normalized to GAPDH. RNA from two separated experiments was used and for each sample the qPCR reaction was performed in triplicate.

The predicted direct regulation of KLF11 transcript by miR-20a was analyzed by luciferase reporter assay using a reporter vector containing a 150 bp fragment of the KLF11 3'-UTR (from position 2049 to 2199 containing the miR-20a complementary site downstream of the luciferase gene into PGL3-Promoter vector (pLuc KLF11 WT 3'-UTR). Two nucleotides in the miR-20a binding region were mutated by QuickChange II XL Site-

Directed Mutagenesis Kit and pLuc KLF11 MUT 3'-UTR reporter vector was generated (Figure 37).

miR-20a	**3'**	**GAUGGACGUGAUAUUCGUGAAAU**
		I I I I I I I
KLF11 WT 3'UTR	**5' ...**	**GTGGGCTCCCCTCGTGCACTTTA**
KLF11 mut 3'UTR	**5' ...**	**GTGGGCTCCCCTCGTGCCCTGTA**

Figure 227. Mutagenensis sites of the miR-20a complementary region in the 3'-UTR of KLF11. The miR-20a seed sequence GCACTTT was mutated into GCCCTGT.

Next, we co-transfected HEK293T cells with pLuc KLF11 WT 3'-UTR or pLuc KLF11 MUT 3'-UTR reporter vectors and miR-20a. The influence of the endogenous miRNA levels was analyzed in the same transfection conditions without miR-20a overexpression. 24 hours after the transfection cell were lysed and luciferase activity was detected. Decrease of 30% in luciferase activity was observed in miR-20a / KLF11 WT 3'-UTR co-transfected cells compared to miR-20a / KLF11 MUT 3'-UTR co-transfection confirming a direct interaction between miR-20a and KLF11 (p-value) (Figure 38).

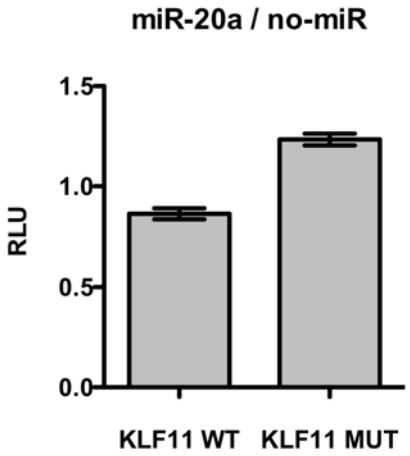

Figure 238. miR-20a modulates the KLF11 mRNA 3'-UTR reporter plasmid. Co-transfection of the KLF11 WT 3'-UTR construct with miR-20a duplexes resulted in down-regulation of luciferase activity, compared to a construct in which the miR-20a complementary sites were mutated (KLF11 MUT 3'-UTR). Averages and standard deviations were calculated from three independent experiments.

The effect of the KLF11 repression by miR-20a can have an effect of the binding of this protein to the TIE element in the c-MYC promoter, thus blocking the inhibition of the transcriptional activity of the promoter induced by TGF-β. The relevance of the KLF11 cooperation with Smad-3 was confirmed by the finding that RNA-mediated knockdown of KLF11 strongly diminished the Smad-3 binding to the c- MYC promoter TIE element. We suggest that overexpression of miR-20a could also contribute to the destabilization of the Smad-3-KLF11 interactions, and we are currently working to understand the involvement of miR-20a in this mechanism.

3.2 Analysis of TGF-β modulation on colorectal cancer deregulated miRNAs

3.2.1 Differential microRNA expression analysis in colorectal cancer specimens

We performed a miRNA profiling of 40 CRC cases matched with their normal tissue (Cohort 2) Using TaqMan Array MicroRNA Cards containing 632 microRNAs. 23 miRNAs were found significantly deregulated between tumor and normal samples (*p-value=0.05*). Eighth of them were down-modulated in tumors, while 15 showed higher expression levels when compared to normal counterparts (Figure 39).

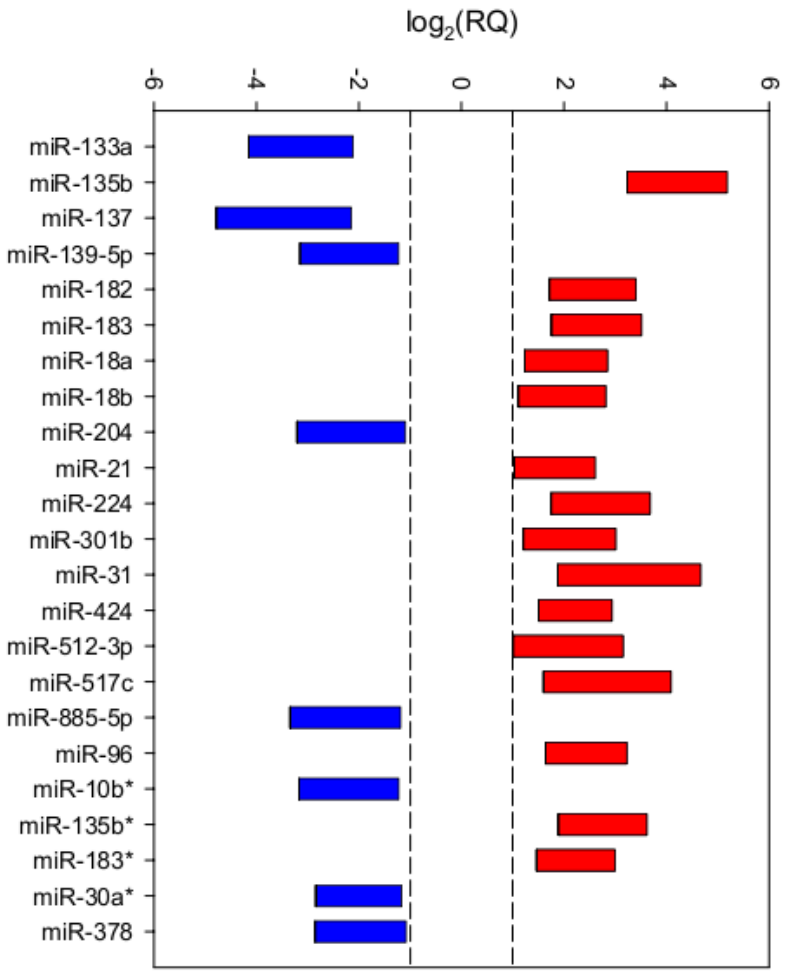

Figure 39. Differentially expressed microRNAs in 40 CRC patients (Cohort 2). The expression of each miRNA is shown as a $\log_2$ of the ratio of its expression level in the tumor samples versus its matched normal tissue (RQ: Relative Quantity). The two

horizontal dashed lines correspond to the thresholds used for considering miRNAs significantly up or down-regulated (two-fold). Each miRNA was normalized to the control RNU6B.

3.2.2 TGF-β regulated miRNAs

It was reported that Smad proteins can promote the miRNA biogenesis by facilitating the cleavage of pri-miRNA by Drosha after binding to a specific RNA-Smad binding element within the pri-miRNAs (R-SBE) [107]. We hypothesized that induction of a miRNA by TGF-β can speculate potential involvement in the TGF-β signaling pathway, thus leading to the identification of new miRNA candidates interfering with this signaling network. We decided to analyze the expression of the miRNAs previously identified as differentially expressed in our patients Cohort 2 (Figure 39) before and after stimulation with the cytokine. For this aim, we used FET cells (possessing an intact TGF-β signaling cascade) and as a control we analyzed their expression also in HT29 (cell line not responsive to TGF-β growth inhibition). The cells were treated with 5 ng/ml of TGF-β for 24 hours and RNA was extracted before and after the stimulation. The expression levels of the miRNAs were detected by qRT-PCR. We found that five of the 19 miRNAs analyzed (miR-135b, -183, -21, -424 and -96) showed a strong induction by TGF-β in FET cells, while significantly lower or no induction of their expression was observed in HT29 cells (Figure 40).

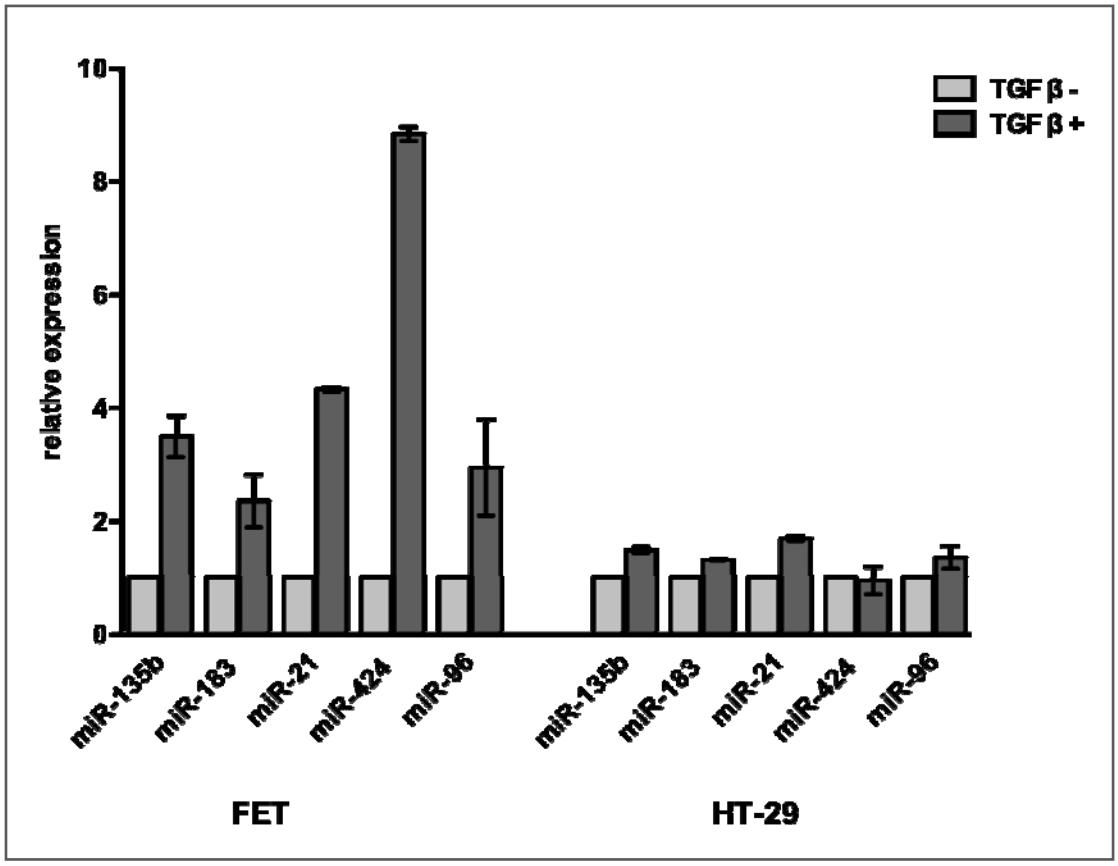

Figure 240. Alterations in the expression levels of five miRNAs (miR-135b, -183, -21, -424 and -96) in FET and HT-29 cells after TGF-β stimulation. RNA was extracted before treatment and 24 hours after treatment with TGF-β. The presented values are calculated as $2^{(-\Delta Ct)}$ and normalized to rnu6b. Relative expression was calculated by considering as value 1 the expression level before the treatment. RNA from two separated experiments was used and for each sample the qPCR reaction was performed in triplicate.

We observed detectable levels of miR-137, down-modulated in our CRC samples, only after TGF-β treatment in FET cells, while in HT29 and in FET not stimulated cells the expression of this miRNA was not detectable (data not shown). Other miRNAs frequently lost in CRC are miR-143 and miR-145, which were not included in the 23 miRNAs with highest alterations between tumor and normal specimens in our profile. We analyzed their expression before and after TGF-β stimulation and observed induction of 10 fold for miR-143 and 20 fold for miR-145 in FET cells, while their up-modulation in HT29 after TGF-β stimulation was low (Figure 41).

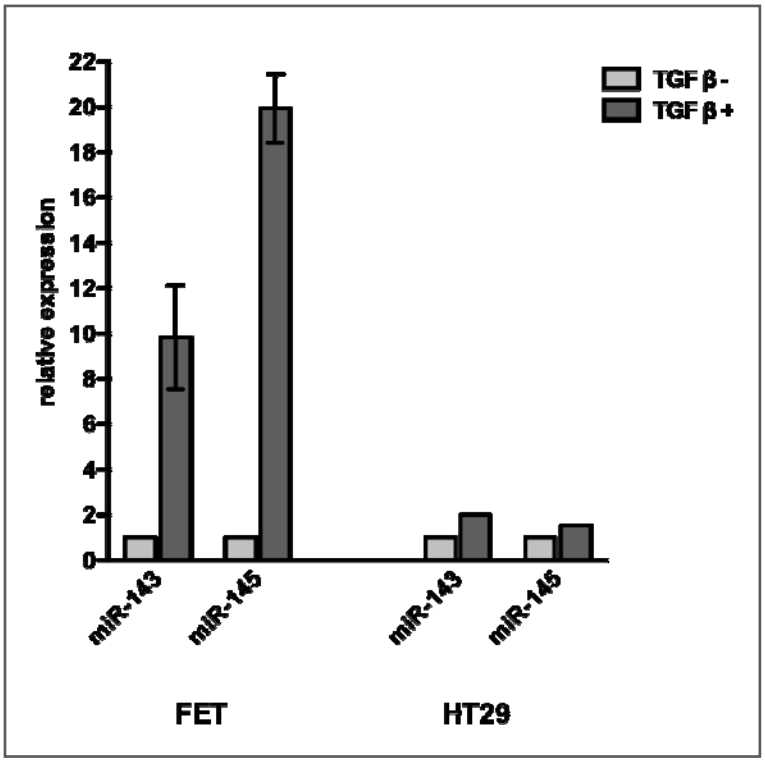

Figure 251. Alterations in the expression levels of miR-143 and miR-145 in FET and HT-29 cells after TGF-β stimulation. RNA was extracted before and 24 hours after treatment with TGF-β. The presented values are calculated as $2^{(-\Delta Ct)}$ and normalized to rnu6b. Relative expression was calculated by considering as value 1 the expression level before the treatment.

Next, we searched the putative target genes of these miRNAs in Targetscan and we found that all these miRNAs can putatively target at least one gene involved in the TGF-β signaling pathway (Table 9).

miRNA	putative target gene
miR-135b	SMAD-4
miR-183	SMAD-4
miR-21	TGFβRI
miR-424	SMAD-3, SMAD-7
miR-96	SMAD-7
miR-143	SMAD-3
miR-145	SMAD-3, SMAD-4

Table 9. The miRNAs induced by TGF-β have as putative targets genes involved in TGF-β signaling pathway. Predictions were retrieved from Targetscan.

Integration of the expression data of the miRNAs we identified as differentially expressed between normal and tumor colon samples with the results of a meta-analysis on seven public gene expression CRC datasets done comparing 229 tumors to 131 normal samples, identified 33 miRNAs that had 121 target genes belonging to CRC related pathways classified according to KEGG (Apoptosis, Cell cycle, Colorectal cancer, MAPK signaling pathway, p53 signaling pathway, TGF-β signaling pathway, Wnt signaling pathway) Putative miRNA-mRNA target pairs where included if they shared opposite patterns of expression and were significant in both the miRNA screening and the gene expression meta-analysis (Figure 39).

Four of the miRNAs that we found induced by TGF-β had targets involved in TGF-β signaling pathway with opposite pattern of expression. They showed opposite expression with genes from TGF-β signaling pathway: miR-135b and miR-183 with SMAD-4, miR-21 and TGFβRI, and miR-424 and SMAD-3 (Table 10).

miRNA	putative target gene
miR-135b	SMAD-4
miR-183	SMAD-4
miR-21	TGFβRI
miR-424	SMAD-3

Table 10. Putative interacting miRNA-gene pairs between miRNA induced by TGF-β and genes involved in this pathway. High miRNA levels corresponded with low gene expression in tumor compared to normal samples.

The reverse correlation of the expression levels of the miRNAs identified in our patients cohort with the expression levels of their predicted target genes (found in public gene expression CRC datasets) and the induction of some of them by the cytokine indicate their potential role as regulators of this signaling pathway.

4 DISCUSSION

We investigated the role of one miRNA from the miR-17-92 cluster, miR-20a, into the TGF-β signaling pathway as possible regulator of TGF-β-mediated cell cytostatic program in CRC. This cluster was identified in our previous study as localized on a region of chromosome 13, 13q31, which was highly amplified in CRC. We also confirmed concurrent over-expression of all the microRNAs from the cluster, highlighting that amplification of the region could be responsible for the over-expression of the cluster. Moreover, we identified additional microRNAs that seem to be involved in the TGF-β signaling which expression levels are modulated by the cytokine. miRNAs regulate different oncogenic and tumor suppressor pathways that are involved in the pathogenesis of cancer. Dissection of their role represent a knowledge improvement in cancer biology and could be useful for understanding the mechanisms involved in cancer progression and for the identification of novel pharmaceutical targets [136]. miRNA expression profiles can be used for prediction of prognosis and characterization of cancer sub-types and stages. Changes in the expression profiles of miRNAs have been observed in a variety of human tumors, including CRC. This tumor type is characterized by a well-defined multi-step progression, and several miRNAs are known as effectors of signaling pathways involved in the different steps of this progression. For example, there are miRNAs that regulate members of the Wnt/β-catenin and phosphatidylinositol-3-kinase (PI-3-K) pathways, KRAS, p53, extracellular matrix regulators and EMT transcriptional factors [12]. These findings significantly extend the number and type of molecules involved in the Vogelstein's model of CRC pathogenesis. However, still little is known about the role of miRNAs in the switch from intermediate adenoma to late adenoma, triggering progression. This is the time frame when loss of TGF-β growth inhibitory effect occurs giving advantages to the cells regarding their proliferation [137, 138]. Moreover, during the

carcinogenesis, the TGF-β signaling pathway achieves pro-oncogenic characteristics. The mechanisms inducing transition of tumor suppressor into oncogenic pathway are still not clear, and the contribution of the miRNAs cannot be excluded.

Previous experiments conducted in our laboratory reported the amplification of the miR-17-92 cluster in a cohort of CRC patients, and found concurrent increased expression of the miRNAs from this cluster. miR-17-92 cluster is implicated in the regulation of TGF-β response by interfering with cell-cycle arrest and apoptosis induced by the cytokine [132]. It was reported that miR-106b from the miR-106b-25 cluster (paralog of miR-20a from miR17-92 cluster) can abrogate the TGF-β mediated growth arrest in gastric cell lines by direct modulation of p21 and BIM [96]. Disruption of the tumor suppressor effect of TGF-β is observed in a large portion of the CRC [83], and we asked whether miR-20a could have a negative effect on the growth inhibition induced by the cytokine in an in-vitro model of TGF-β responsive colon carcinoma. FET cells are growth-inhibited by TGF-β and unable to grow in-vivo, unless the TGF-β signaling is artificially inactivated [139]. Defining the mechanisms abrogating TGF-β growth inhibition through miR-20a over-expression using FET, *in-vitro* cellular model of colon carcinoma, in the context of negative regulation of TGF-β response is the main goal of this project.

We have observed that miR-20a delivery to FET cells (expressing low endogenous level of this microRNA) results in decrease of endogenous p21 protein and mRNA, and after TGF-β stimulation attenuation of p21 up-regulation. We confirmed that this effect occurs after direct binding of miR-20a to CDKN1A 3'-UTR region by luciferase reporting assays containing an intact or mutated miR-20a complementary site. Reduction in the luciferase activity of 30% was observed comparing the activities of vectors containing the 3'-UTR WT vs MUT seed sequence (*p-value = 0.001*). Other groups also reported this modulation [102].

We found that, by transiently administering the miR-20a in FET cells the TGF-β mediated growth suppression is significantly inhibited. Cells transfected with a scramble oligonucleotide showed about 70% reduction in growth rates when treated with the cytokine, while miR-20a administration diminished this effect only 30%. miR-20a also negatively regulates the cell-cycle progression, inducing escape of the TGF-β- induced G1/S arrest and promoting entry into S-phase (32% cells in G1 phase in miR-20a transfected cells *vs.* 52.3% in control), suggesting that miR-20a interferes with the TGF-β signaling by subverting the G1/S arrest induced by the cytokine.

Its known that the TGF-β signaling is abrogated in presence of active MAPK signaling due to a constitutive activation of K-Ras, which is present also in our cellular model. Using a specific inhibitor of this cascade, we were able to confirm the effect of miR-20a on the p21 expression, thus showing that its effect is independent of the MAPK pathway-mediated p21 down-modulation.

Interestingly, we found also a significant reduction of CDKN1A promoter trans-activation by TGF-β after miR-20a delivery. CDKN1A is directly up-regulated by TGF-β through interactions of the Smad-3/Smad-4 complex to its proximal elements [46], while the growth promoting factor c-Myc is a direct inhibitor of its transcription [140]. C-myc down-modulation is part of the TGF-β mediated cytostatic program, and we observed abrogation of this mechanism in presence of miR-20a. c- MYC lacks a complementary binding site for miR-20a, suggesting that this miRNA negatively regulates c- MYC transcription via its promoter.

The transcriptional repression of c-MYC is mediated by a TGF-β inhibitory element located on its promoter (TIE) in proximity of an E2F site (TIE/E2F). This core sequence is recognized by a transcriptional complex composed by Smad-3, Smad-4, E2F proteins, the co-repressor p107 and other partners, which induce suppression of the promoter activity [141]. Recent works have shown than an alternative c-Myc repressive mechanism operated by KLF11 and Smad-3 exists and binds the TIE element on the c-MYC promoter. Using

bioinformatics tools we found that both E2F5 and KLF11 possess miR-20a complementary binding sites. Our analysis showed variation in their mRNA and/or protein levels after miR-20a transfection. For E2F5 no significant differences in mRNA levels were observed after miR-20a administration, but a reduction in E2F5 protein level of about 60% in TGF-β not treated cells and about 40% after stimulation with the cytokine was detected. KLF11 showed a significant mRNA reduction after miR-20a over-expression (about 70% in not stimulated cells and about 40% when cells were treated with the cytokine) suggesting that miR-20a could regulate KLF11 at transcriptional level. We functionally validated their predicted interaction with miR-20a using reporter assays containing intact or mutated complementary miR-20a sites, and we observed for E2F5 reduction in luciferase activity of 35% (3'-UTR WT vs MUT, *p-value* = 0.04) and reduction of 30% for KLF11 (*p-value* = 0.01). We suggest that down modulation of the genes forming c-Myc repressive complexes by miR-20a destabilizes them resulting in high c-Myc levels, thus allowing its transcriptional repression on the CDKN1A promoter. Indeed, we demonstrated that after miR-20a administration, the binding of E2F5 to the c-MYC promoter is abolished. We are now investigating if the KLF11 binding to the TIE is also affected by miR-20a. The participation of E2F5 and KLF11 in the miR-20a mediated deregulation of c-Myc repression will be addressed by knockdown of these transcriptional factors both separately or in combination. To understand whether miR-20a affects the assembling of the c-Myc repressive complexes, and not only their DNA binding, we are also setting the conditions for performing oligonucleotide affinity precipitation of the region of c-MYC promoter containing the TIE and E2F responsive sequences (either wild-type or mutated).

So far, our model proposes that miR-20a could modulate the TGF-β mediated cytostatic program interfering with the both branches: subverting the induction of CDKN1A by direct regulation of its 3'-UTR, and indirectly through down-modulation of E2F5 and KLF11 thus abrogating the c-Myc repression (schematically represented in Figure 42). Our

experiments indicate an oncogenic role of miR-20a in CRC model, suggesting that it could have a direct effect on loss of TGF-β growth inhibition.

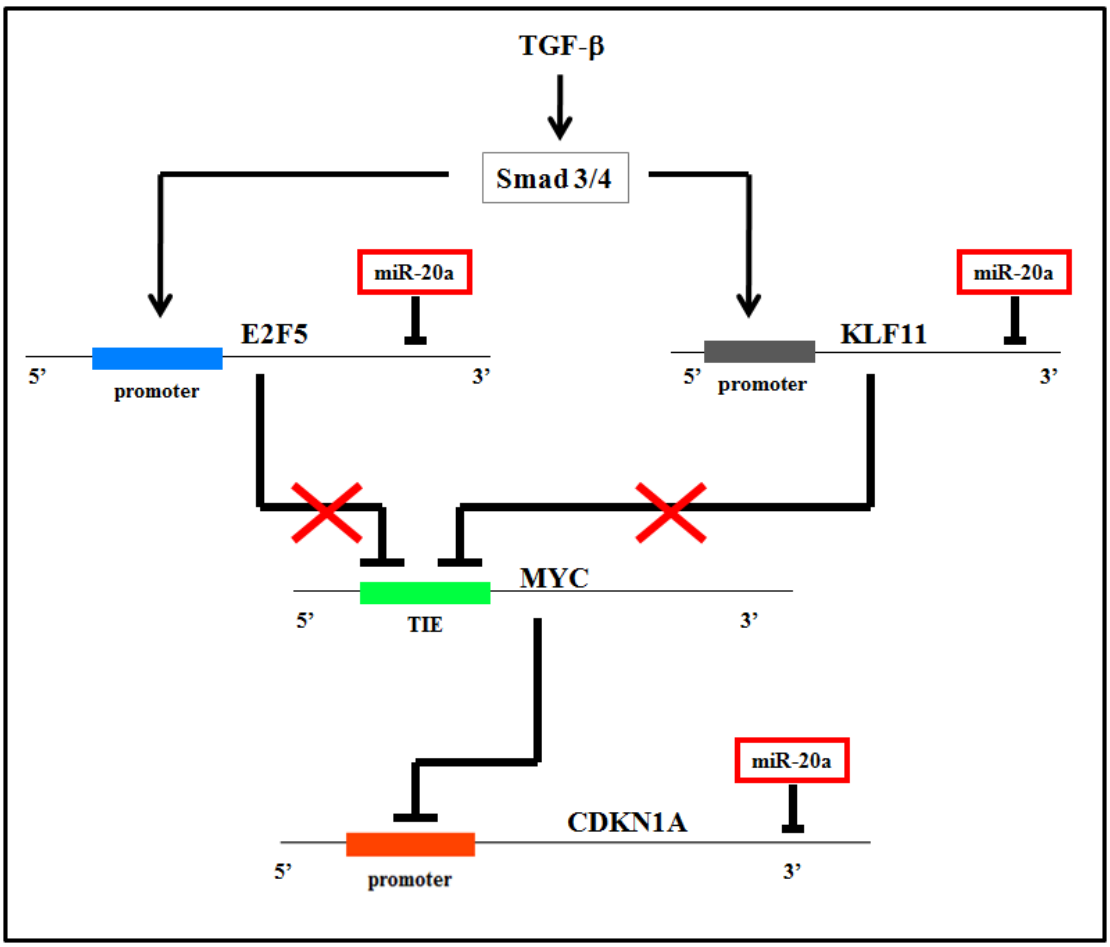

Figure 262. Schematic representation of miR-20a involvement in the TGF-β pathway. In presence of TGF-β, miR20a blocks CDKN1A, E2F5 and KLF11 by binding to their 3'-UTR. Block of E2F5 and KLF11, two repressors of c-Myc expression, increases c-Myc levels, which strongly down-modulates p21 expression, together with mir-20a, triggering cells to growth induction.

Other groups confirmed that TGFβRII, and the pro-apoptotic gene BIM are also direct targets of miR-17-92 [99] suggesting that the functional implication of miR-17-92 cluster with the TGF-β tumor suppressor pathway is even wider and affects also its pro-apoptotic function. In-vivo studies support a model in which TGF-β inhibits development of early lesions but promotes tumor progression and invasion when its suppressor activity is

overridden by oncogenic alterations. In this context, dissecting the mechanisms addressed by miR-20a should contribute to the knowledge of understanding the molecular alterations which subvert the TGF-β tumor suppressive role in cancer and provide escape from the TGF-β-dependent cell cycle arrest and apoptosis.

During the last few years a lot of information was accumulated about miRNAs regulation of crucial genes involved in carcinogenesis, but still little is known about the processes regulating the biogenesis of the miRNAs. The genomic regions which encode them are not different from the promoters of the protein coding genes and undergo the same modifications, including transcriptional regulation. Drosha processing of pri-miRNAs occurs immediately after transcription, and its association with other proteins can promote this process. It was reported that Smad proteins recognize a specific binding region within the primary stem pri-miRNA transcript called RNA Smad Binding Element (R-SBE) [106]. Mutation of this element abrogated the TGF-β mediated recruitment of Smads and Drosha impairing the processing of mature miRNAs. Not all miRNAs possess R-SBE and consequently cannot be induced by the cytokine, and currently is not yet explored what determines this selective regulation. Moreover, introduction of R-SBE into previously unregulated miRNAs by TGF-β promotes their induction by the cytokine. One of the possible theories why some genes induce miRNAs could be the necessity of extremely rapid cellular responses. The induction of multiple miRNAs in response to TGF-β, which modulate hundreds of genes, could have a strong impact on the gene expression and physiological condition of the cell.

In a study performed by our group we identified a panel of 23 miRNAs which expression is significantly altered between tumor and normal CRC specimens. Next, we analyzed their expression levels before and after TGF-β stimulation in FET cells (sensitive to TGF-β induced growth inhibition) and in the HT29 cell line (not responsive to TGF-β stimuli),

and found that five miRNAs (miR-135b, -183, -21, -424, -96) were strongly induced in FET, while in HT29 cells the induction was minimal or not present. All five miRNAs were up-regulated in our CRC tissue specimens panel. Interestingly, we found that the expression levels of miR-137, that we identified down-modulated in CRC, were detectable only after TGF-β stimulation in the responsive cell line, while this miRNA was not expressed in HT29 cells, both before and after stimulation with the cytokine. We analyzed the effects of TGF-β on the miRNAs from the 17-92 cluster and we observed only a weak down-modulation of their levels, as reported also by Petrocca et al [96]. We also found strong induction for two other miRNAs known as tumor-supressors in CRC, miR-143 and miR-145, thus demonstrating that both oncomiRs and tumor suppressor miRNAs could be up-regulated by the cytokine. The induction of four of the eight miRNAs that we found induced by TGF-β (miR-21, -424, -143 and -145) was reported in the literature [106, 107]. Moreover, each of the modulated miRNAs has as a predicted target gene at least one of the crucial effectors of the TGF-β signaling pathway. For some of the predicted pairs (miRNA/gene) we confirmed opposite correlation between the expression levels of the miRNA analyzed in our CRC panel and the expression levels of their target genes retrieved from public CRC gene expression databases. In details, we found correlation between miR-135b and miR-183 with Smad-4, miR-21 and TGFβRI, and miR-424 and Smad-3. These interactions could suggests a negative feedback loop in which through induction of specific miRNAs by the cytokine, the expression of genes directly involved in the pathway could be negatively modulated. The regulatory mechanisms between the miRNAs and the genes from the TGF-β signaling pathway are probably much more complicated, since the induced miRNAs beside the genes from the TGF-β pathway regulate the expression of hundreds of tumor suppressor and oncogenes, and this will result in a strong impact on the cellular gene expression profile. We are planning to investigate in details the mechanisms by which TGF-β induces the expression of these miRNAs (presence of R-SBE in the pri-miR

sequence), and also the possible direct modulation on the putative target genes from the pathway through direct binding to their 3'-UTR.

So far, only few reports demonstrate that Smads could induce miRNA biogenesis, and more studies are necessary to uncover the mechanisms by which these interactions occur.

The two different approaches we used to identify miRNAs involved in the TGF-β signaling network (identification of miRNAs localized on altered genomic regions and differentially expressed in CRC and identification of miRNAs whose expression is induced by the cytokine) highlighted the primary role of miRNAs in the TGF-β network their prominent potential as therapeutic targets in the cancer therapy.

The degree of miRNA alteration in cancer is measured comparing the normal tissue pattern with the malignant. Although the miRNAs largely perturbate the transcriptome and proteome in tumor cells, only some of them are deregulated in cancer. They are implemented in regulation of high number of genes involved in different signaling pathways, and unlike the protein coding genes that need to be translated, the miRNAs can modify gene expression more rapidly. Therefore, the development of therapeutic strategies to restore homeostasis by modifying miRNA expression may be more successful than targeting individual genes or proteins.

Two are the most promising strategies to target miRNA expression in cancer. Direct strategies involve the use of oligonucleotides or virus-based constructs to block the expression of oncogenic miRNAs or to rescue the loss of a tumor suppressor miRNAs. Indirect strategies involve the use of drugs to modulate miRNA expression by targeting their transcription and processing. Since the levels of the oncogenic miRNAs are upregulated in cancer, a promising strategy could be use of antisense oligonucleotides in order to block their expression. Antisense oligonucleotides act as competitive inhibitors of

miRNAs presumably by annealing to the mature miRNA strand and inducing its degradation or duplex formation. A possible problem could be represented by difficulties in introducing modifications to the chemical structure of the oligonucleotides to increase stability, binding affinity and specificity [142]. It was reported that oligonucleotides with 2'-O-methyl groups have proved to be effective inhibitors of miRNA expression in different cancer cell lines [143].

Another class of analogues nucleic acids are so called locked nucleic acids (LNA), in which the ribose ring is locked by a methylene bridge, thus assuring high affinity towards complementary single-stranded RNA and complementary single and double stranded DNA [144]. This "LNA anti-miR" constructs have been used in several *in vitro* studies to knock down specific miRNAs, and later also *in vivo* experiments using mice models confirmed the efficiency of this approach [145, 146].

Other therapeutic strategies involve the use of miRNA sponges, transcripts that contain multiple tandem-binding sites to a specific miRNA. Introduction of this construct in the cell will compete with the genes which are targets of the miRNA of interest, since possessing identical complementary binding sites. Moreover, miRNA families sharing the same seed regions were found co-repressed by the same sponge [147, 148].
miRNA-masking antisense oligonucleotides technology (miR-mask) was also proposed. miR-mask consists of single-stranded 2'-O-modified antisense oligonucleotides fully complementary to the predicted miRNA binding site in the 3'-UTR of the target mRNA. The introduced miR-mask covers the miRNA binding site protecting in this way the mRNA target from repression [149].

Since targeting multiple miRNAs using antisense oligonucleotides or mimics could be technically challenging, the indirect strategies involve several drugs that have the ability to

modulate miRNAs expression by targeting pathways that regulate miRNA encoding gene [149]. Variations in miRNA expression in response to drug treatment *in vitro* and *in vivo* have been reported [150], and miRNAs have been shown to be actively re-expressed after treatment with drugs working by DNA methyltransferase inhibition resulting in tumor suppressor gene re-expression mediated by promoter hypomethylation [151].

The development of miRNA-based therapy includes issues related to the delivery, the potential off-target effects and safety. Since "naked" oligonucleotides are rapidly degraded, the first difficult is their delivery in the cells under active forms. The second problem is their uptake by the cell, since they are negatively charged and high amounts are necessary to achieve their effect [152]. Concerning the potential off-target effects, engineering effective systems that deliver the synthetic miRNA oligonucleotides specifically to the diseased tissues or cancer cells are necessary.

The discovery of miRNAs has changed the view on gene regulation and it is now evident that deregulation of miRNAs is a key step in the development of many cancers, including CRC. A number of studies based on expression profiling have proven that there are significant changes in miRNA expression levels in CRC tissue in comparison to normal colorectal epithelium. Concerning this, the present work confirmed that increased expression of miR-20a from the miR-17-92 cluster in CRC could contribute to disruption of the TGF-β-mediated cytostatic program.

From this perspective, since TGF-β loss occurs at early stages of CRC (stage II), therapeutic strategies to restore TGF-β homeostasis by modifying miRNA expression could represent a possible therapeutic treatment for early grade of CRC. Only a small percentage of cancers detected at early stages will recur, and at present there are no markers of recurrence for these tumors, it could be interesting to verify if differences in miR-20a expression between recurrent and non recurrent stage II patients are present. miR-

20a could therefore be used as marker to identify patients with higher probability to relapse and that should be kept under strict clinical control and treatments [128].

The miRNAs field continues to evolve, a better understanding of miRNA biogenesis and function will certainly affect the development of miRNA-based therapies. The research efforts should focus on maximizing the benefit of target diversity and preventing off-target effects, thus leading to overcome of the current obstacles regarding cancer therapy.

References

1. Coleman, W.B. and G.J. Tsongalis, *Molecular mechanisms of human carcinogenesis.* EXS, 2006(96): p. 321-49.
2. Hanahan, D. and R.A. Weinberg, *Hallmarks of cancer: the next generation.* Cell, 2011. **144**(5): p. 646-74.
3. Marahatta, S.B., et al., *Cancer: determinants and progression.* Nepal Med Coll J, 2005. **7**(1): p. 65-71.
4. Ferlay, J., et al., *Estimates of worldwide burden of cancer in 2008: GLOBOCAN 2008.* Int J Cancer, 2010. **127**(12): p. 2893-917.
5. Senda, T., et al., *Adenomatous polyposis coli (APC) plays multiple roles in the intestinal and colorectal epithelia.* Med Mol Morphol, 2007. **40**(2): p. 68-81.
6. Weinberg, R.A., *The biology of cancer*. 2007, New York, NY: Garland Science. 1 v. (various pagings).
7. Cardoso, J., et al., *Expression and genomic profiling of colorectal cancer.* Biochim Biophys Acta, 2007. **1775**(1): p. 103-37.
8. Lichtenstein, P., et al., *Environmental and heritable factors in the causation of cancer - Analyses of cohorts of twins from Sweden, Denmark, and Finland.* New England Journal of Medicine, 2000. **343**(2): p. 78-85.
9. Hermsen, M., et al., *Colorectal adenoma to carcinoma progression follows multiple pathways of chromosomal instability.* Gastroenterology, 2002. **123**(4): p. 1109-19.
10. Lagerstedt, K.K., et al., *Tumor genome wide DNA alterations assessed by array CGH in patients with poor and excellent survival following operation for colorectal cancer.* Cancer Inform, 2007. **3**: p. 341-55.
11. Ried, T., et al., *Chromosomal breakpoints in primary colon cancer cluster at sites of structural variants in the genome.* Cancer Research, 2008. **68**(5): p. 1284-1295.
12. Fearon, E.R. and B. Vogelstein, *A genetic model for colorectal tumorigenesis.* Cell, 1990. **61**(5): p. 759-67.
13. Lagerstedt, K.K., et al., *The role of combined allelic imbalance and mutations of p53 in tumor progression and survival following surgery for colorectal carcinoma.* Int J Oncol, 2005. **27**(6): p. 1707-15.
14. Meijer, G.A., et al., *Multiple putative oncogenes at the chromosome 20q amplicon contribute to colorectal adenoma to carcinoma progression.* Gut, 2009. **58**(1): p. 79-89.

15. Fodde, R., et al., *Mutations in the APC tumour suppressor gene cause chromosomal instability.* Nature Cell Biology, 2001. **3**(4): p. 433-438.
16. Ionov, Y., et al., *Ubiquitous Somatic Mutations in Simple Repeated Sequences Reveal a New Mechanism for Colonic Carcinogenesis.* Nature, 1993. **363**(6429): p. 558-561.
17. Thibodeau, S.N., G. Bren, and D. Schaid, *Microsatellite Instability in Cancer of the Proximal Colon.* Science, 1993. **260**(5109): p. 816-819.
18. Frank, S.A., *Dynamics of cancer : incidence, inheritance, and evolution*. Princeton series in evolutionary biology. 2007, Princeton, N.J.: Princeton University Press. xi, 378 p.
19. Kinzler, K.W., and Vogelstein, B. 2002. Colorectal tumors. In Vogelstein, B., and Kinzler, K. W., eds., The Genetic Basis of Human Cancer (2nd edition)., pp. 583–612. McGraw-Hill, New York., ed.
20. Iafrate, A.J., et al., *Detection of large-scale variation in the human genome.* Journal of Molecular Diagnostics, 2004. **6**(4): p. 411-411.
21. Wigler, M., et al., *Large-scale copy number polymorphism in the human genome.* Science, 2004. **305**(5683): p. 525-528.
22. Cox, D.R., et al., *Whole-genome patterns of common DNA variation in three human populations.* Science, 2005. **307**(5712): p. 1072-1079.
23. Eichler, E., et al., *Fine-scale structural variation of the human genome.* Journal of Medical Genetics, 2005. **42**: p. S34-S34.
24. Altshuler, D.M., et al., *Common deletion polymorphisms in the human genome.* Nature Genetics, 2006. **38**(1): p. 86-92.
25. Scherer, S.W., et al., *Global variation in copy number in the human genome.* Nature, 2006. **444**(7118): p. 444-454.
26. Carter, N.P., *Methods and strategies for analyzing copy number variation using DNA microarrays.* Nature Genetics, 2007. **39**: p. S16-S21.
27. McCarroll, S.A. and D.M. Altshuler, *Copy-number variation and association studies of human disease.* Nature Genetics, 2007. **39**: p. S37-S42.
28. Tomlinson, I., et al., *A genome-wide association scan of tag SNPs identifies a susceptibility variant for colorectal cancer at 8q24.21.* Nature Genetics, 2007. **39**(8): p. 984-988.
29. Hudson, T.J., et al., *Genome-wide association scan identifies a colorectal cancer susceptibility locus on chromosome 8q24.* Nature Genetics, 2007. **39**(8): p. 989-994.

30. Houlston, R.S., et al., *Meta-analysis of genome-wide association data identifies four new susceptibility loci for colorectal cancer.* Nature Genetics, 2008. **40**(12): p. 1426-1435.
31. Tomlinson, I.P.M., et al., *A genome-wide association study identifies colorectal cancer susceptibility loci on chromosomes 10p14 and 8q23.3.* Nature Genetics, 2008. **40**(5): p. 623-630.
32. Massague, J., S.W. Blain, and R.S. Lo, *TGFbeta signaling in growth control, cancer, and heritable disorders.* Cell, 2000. **103**(2): p. 295-309.
33. de Caestecker, M.P., E. Piek, and A.B. Roberts, *Role of transforming growth factor-beta signaling in cancer.* J Natl Cancer Inst, 2000. **92**(17): p. 1388-402.
34. Massague, J., *TGFbeta in Cancer.* Cell, 2008. **134**(2): p. 215-30.
35. Munger, J.S., et al., *Latent transforming growth factor-beta: structural features and mechanisms of activation.* Kidney Int, 1997. **51**(5): p. 1376-82.
36. Tang, W.B., et al., *Smad anchor for receptor activation (SARA) in TGF-beta signaling.* Front Biosci (Elite Ed), 2010. **2**: p. 857-60.
37. Zawel, L., et al., *Human Smad3 and Smad4 are sequence-specific transcription activators.* Mol Cell, 1998. **1**(4): p. 611-7.
38. Nakao, A., et al., *Identification of Smad7, a TGFbeta-inducible antagonist of TGF-beta signalling.* Nature, 1997. **389**(6651): p. 631-5.
39. Afrakhte, M., et al., *Induction of inhibitory Smad6 and Smad7 mRNA by TGF-beta family members.* Biochem Biophys Res Commun, 1998. **249**(2): p. 505-11.
40. Luo, K., et al., *The Ski oncoprotein interacts with the Smad proteins to repress TGFbeta signaling.* Genes Dev, 1999. **13**(17): p. 2196-206.
41. Zavadil, J., et al., *Genetic programs of epithelial cell plasticity directed by transforming growth factor-beta.* Proc Natl Acad Sci U S A, 2001. **98**(12): p. 6686-91.
42. Seoane, J., *Escaping from the TGF beta anti-proliferative control.* Carcinogenesis, 2006. **27**(11): p. 2148-2156.
43. Hannon, G.J. and D. Beach, *p15INK4B is a potential effector of TGF-beta-induced cell cycle arrest.* Nature, 1994. **371**(6494): p. 257-61.
44. Datto, M.B., et al., *Transforming Growth-Factor-Beta Induces the Cyclin-Dependent Kinase Inhibitor P21 through a P53-Independent Mechanism.* Proceedings of the National Academy of Sciences of the United States of America, 1995. **92**(12): p. 5545-5549.

45. Kato, M., et al., *c-myc is a downstream target of the Smad pathway.* Journal of Biological Chemistry, 2002. **277**(1): p. 854-861.
46. Seoane, J., et al., *Integration of Smad and forkhead pathways in the control of neuroepithelial and glioblastoma cell proliferation.* Cell, 2004. **117**(2): p. 211-23.
47. Claassen, G.F. and S.R. Hann, *A role for transcriptional repression of p21CIP1 by c-Myc in overcoming transforming growth factor beta -induced cell-cycle arrest.* Proc Natl Acad Sci U S A, 2000. **97**(17): p. 9498-503.
48. Warner, B.J., et al., *Myc downregulation by transforming growth factor beta required for activation of the p15(Ink4b) G(1) arrest pathway.* Mol Cell Biol, 1999. **19**(9): p. 5913-22.
49. Wijchers, P.J., J.P. Burbach, and M.P. Smidt, *In control of biology: of mice, men and Foxes.* Biochem J, 2006. **397**(2): p. 233-46.
50. Chi, X.Z., et al., *RUNX3 suppresses gastric epithelial cell growth by inducing p21(WAF1/Cip1) expression in cooperation with transforming growth factor beta-activated SMAD.* Molecular and Cellular Biology, 2005. **25**(18): p. 8097-8107.
51. Eldeiry, W.S., et al., *Waf1/Cip1 Is Induced in P53-Mediated G(1) Arrest and Apoptosis.* Cancer Research, 1994. **54**(5): p. 1169-1174.
52. Eldeiry, W.S., et al., *Topological Control of P21(Waf1/Cip1) Expression in Normal and Neoplastic Tissues.* Cancer Research, 1995. **55**(13): p. 2910-2919.
53. Dotto, G.P., et al., *p21(WAF1/Cip1) suppresses keratinocyte differentiation independently of the cell cycle through transcriptional up-regulation of the IGF-I gene.* Journal of Biological Chemistry, 2006. **281**(41): p. 30463-30470.
54. Pietenpol, J.A., et al., *Transforming Growth Factor-Beta-1 Suppression of C-Myc Gene-Transcription - Role in Inhibition of Keratinocyte Proliferation.* Proceedings of the National Academy of Sciences of the United States of America, 1990. **87**(10): p. 3758-3762.
55. Alexandrow, M.G. and H.L. Moses, *Transforming Growth-Factor-Beta and Cell-Cycle Regulation.* Cancer Research, 1995. **55**(7): p. 1452-1457.
56. Grandori, C., et al., *The Myc/Max/Mad network and the transcriptional control of cell behavior.* Annual Review of Cell and Developmental Biology, 2000. **16**: p. 653-699.
57. Wanzel, M., S. Herold, and M. Eilers, *Transcriptional repression by Myc.* Trends Cell Biol, 2003. **13**(3): p. 146-50.
58. Yagi, K., et al., *c-myc is a downstream target of the Smad pathway.* Journal of Biological Chemistry, 2002. **277**(1): p. 854-861.

59. Ellenrieder, V., *TGF beta-regulated gene expression by Smads and Sp1/KLF-like transcription factors in cancer.* Anticancer Research, 2008. **28**(3A): p. 1531-1539.

60. Zhang, J.S., et al., *A conserved alpha-helical motif mediates the interaction of Sp1-like transcriptional repressors with the corepressor mSin3A.* Mol Cell Biol, 2001. **21**(15): p. 5041-9.

61. Massague, J., Y.B. Kang, and C.R. Chen, *A self-enabling TGF beta response coupled to stress signaling: Smad engages stress response factor ATF3 for Id1 repression in epithelial cells.* Molecular Cell, 2003. **11**(4): p. 915-926.

62. Lasorella, A., et al., *Id2 is a retinoblastoma protein target and mediates signalling by Myc oncoproteins (vol 407, pg 592, 2000).* Nature, 2000. **408**(6811): p. 498-498.

63. Iavarone, A. and J. Massague, *Repression of the CDK activator Cdc25A and cell-cycle arrest by cytokine TGF-beta in cells lacking the CDK inhibitor p15.* Nature, 1997. **387**(6631): p. 417-22.

64. Galaktionov, K., X. Chen, and D. Beach, *Cdc25 cell-cycle phosphatase as a target of c-myc.* Nature, 1996. **382**(6591): p. 511-7.

65. Siegel, P.M. and J. Massague, *Cytostatic and apoptotic actions of TGF-beta in homeostasis and cancer.* Nat Rev Cancer, 2003. **3**(11): p. 807-21.

66. Ikushima, H. and K. Miyazono, *Cellular context-dependent "colors" of transforming growth factor-beta signaling.* Cancer Sci, 2010. **101**(2): p. 306-12.

67. Jang, C.W., et al., *TGF-beta induces apoptosis through Smad-mediated expression of DAP-kinase.* Nature Cell Biology, 2002. **4**(1): p. 51-58.

68. Kim, S.G., et al., *Transforming growth factor-beta 1 induces apoptosis through Fas ligand-independent activation of the Fas death pathway in human gastric SNU-620 carcinoma cells.* Molecular Biology of the Cell, 2004. **15**(2): p. 420-434.

69. Ohgushi, M., et al., *Transforming growth factor beta-dependent sequential activation of Smad, Bim, and caspase-9 mediates physiological apoptosis in gastric epithelial cells.* Molecular and Cellular Biology, 2005. **25**(22): p. 10017-10028.

70. Iwasaki, H. and T. Suda, *Cancer stem cells and their niche.* Cancer Science, 2009. **100**(7): p. 1166-1172.

71. Gorelik, L. and R.A. Flavell, *Immune-mediated eradication of tumors through the blockade of transforming growth factor-beta signaling in T cells.* Nature Medicine, 2001. **7**(10): p. 1118-1122.

72. Bernabeu, C., et al., *Synergistic cooperation between hypoxia and transforming growth factor-beta pathways on human vascular endothelial growth factor gene expression.* Journal of Biological Chemistry, 2001. **276**(42): p. 38527-38535.

73. Pertovaara, L., et al., *Vascular Endothelial Growth-Factor Is Induced in Response to Transforming Growth-Factor-Beta in Fibroblastic and Epithelial-Cells.* Journal of Biological Chemistry, 1994. **269**(9): p. 6271-6274.

74. Shimo, T., et al., *Involvement of CTGF, a hypertrophic chondrocyte-specific gene product, in tumor angiogenesis.* Oncology, 2001. **61**(4): p. 315-322.

75. Yin, J.J., et al., *TGF-beta signaling blockade inhibits PTHrP secretion by breast cancer cells and bone metastases development.* J Clin Invest, 1999. **103**(2): p. 197-206.

76. Derynck, R., R.J. Akhurst, and A. Balmain, *TGF-beta signaling in tumor suppression and cancer progression.* Nature Genetics, 2001. **29**(2): p. 117-129.

77. Yang, G. and X. Yang, *Smad4-mediated TGF-beta signaling in tumorigenesis.* Int J Biol Sci, 2010. **6**(1): p. 1-8.

78. Kretzschmar, M., et al., *A mechanism of repression of TGFbeta/ Smad signaling by oncogenic Ras.* Genes Dev, 1999. **13**(7): p. 804-16.

79. Moses, H.L., et al., *Interdependent SMAD and JNK signaling in transforming growth factor-beta-mediated transcription.* Journal of Biological Chemistry, 1999. **274**(52): p. 37413-37420.

80. Goggins, M., et al., *Genetic alterations of the transforming growth factor beta receptor genes in pancreatic and biliary adenocarcinomas.* Cancer Res, 1998. **58**(23): p. 5329-32.

81. Villanueva, A., et al., *Disruption of the antiproliferative TGF-beta signaling pathways in human pancreatic cancer cells.* Oncogene, 1998. **17**(15): p. 1969-78.

82. Grady, W.M., et al., *Mutational inactivation of transforming growth factor beta receptor type II in microsatellite stable colon cancers.* Cancer Research, 1999. **59**(2): p. 320-324.

83. Grady, W.M. and S.D. Markowitz, *Genetic and epigenetic alterations in colon cancer.* Annu Rev Genomics Hum Genet, 2002. **3**: p. 101-28.

84. Parsons, R., et al., *Microsatellite instability and mutations of the transforming growth factor beta type II receptor gene in colorectal cancer.* Cancer Res, 1995. **55**(23): p. 5548-50.

85. Biswas, S., et al., *Transforming growth factor beta receptor type II inactivation promotes the establishment and progression of colon cancer.* Cancer Research, 2004. **64**(14): p. 4687-4692.

86. Pasche, B., et al., *T beta R-I(6A) is a candidate tumor susceptibility allele.* Cancer Research, 1999. **59**(22): p. 5678-5682.

87. Salovaara, R., et al., *Frequent loss of SMAD4/DPC4 protein in colorectal cancers.* Gut, 2002. **51**(1): p. 56-9.
88. Eppert, K., et al., *MADR2 maps to 18q21 and encodes a TGF beta-regulated MAD-related protein that is functionally mutated in colorectal carcinoma.* Cell, 1996. **86**(4): p. 543-552.
89. Uchida, K., et al., *Somatic in vivo alterations of the JV18-1 gene at 18q21 in human lung cancers.* Cancer Res, 1996. **56**(24): p. 5583-5.
90. Xu, J. and L. Attisano, *Mutations in the tumor suppressors Smad2 and Smad4 inactivate transforming growth factor beta signaling by targeting Smads to the ubiquitin-proteasome pathway.* Proc Natl Acad Sci U S A, 2000. **97**(9): p. 4820-5.
91. Takaku, K., et al., *Intestinal tumorigenesis in compound mutant mice of both Dpc4 (Smad4) and Apc genes.* Cell, 1998. **92**(5): p. 645-656.
92. Bartel, D.P., *MicroRNAs: Genomics, biogenesis, mechanism, and function.* Cell, 2004. **116**(2): p. 281-297.
93. Garzon, R., G. Marcucci, and C.M. Croce, *Targeting microRNAs in cancer: rationale, strategies and challenges.* Nat Rev Drug Discov, 2010. **9**(10): p. 775-89.
94. Hutvagner, G., et al., *A cellular function for the RNA-interference enzyme Dicer in the maturation of the let-7 small temporal RNA.* Science, 2001. **293**(5531): p. 834-838.
95. Gu, S., et al., *Biological basis for restriction of microRNA targets to the 3' untranslated region in mammalian mRNAs.* Nat Struct Mol Biol, 2009. **16**(2): p. 144-50.
96. Croce, C.M., et al., *E2F1-regulated microRNAs impair TGF beta-dependent cell-cycle arrest and apoptosis in gastric cancer.* Cancer Cell, 2008. **13**(3): p. 272-286.
97. Ivanovska, I., et al., *MicroRNAs in the miR-106b family regulate p21/CDKN1A and promote cell cycle progression.* Mol Cell Biol, 2008. **28**(7): p. 2167-74.
98. Tanzer, A. and P.F. Stadler, *Molecular evolution of a microRNA cluster.* Journal of Molecular Biology, 2004. **339**(2): p. 327-335.
99. Volinia, S., et al., *A microRNA expression signature of human solid tumors defines cancer gene targets.* Proc Natl Acad Sci U S A, 2006. **103**(7): p. 2257-61.
100. Ventura, A., et al., *Targeted deletion reveals essential and overlapping functions of the miR-17 through 92 family of miRNA clusters.* Cell, 2008. **132**(5): p. 875-86.
101. Fontana, L., et al., *Antagomir-17-5p abolishes the growth of therapy-resistant neuroblastoma through p21 and BIM.* PLoS One, 2008. **3**(5): p. e2236.

102. Trompeter, H.I., et al., *MicroRNAs MiR-17, MiR-20a, and MiR-106b act in concert to modulate E2F activity on cell cycle arrest during neuronal lineage differentiation of USSC.* PLoS One, 2011. **6**(1): p. e16138.

103. Mendell, J.T., *miRiad roles for the miR-17-92 cluster in development and disease.* Cell, 2008. **133**(2): p. 217-22.

104. Dews, M., et al., *The myc-miR-17~92 axis blunts TGF{beta} signaling and production of multiple TGF{beta}-dependent antiangiogenic factors.* Cancer Res, 2010. **70**(20): p. 8233-46.

105. Schultz, N., et al., *Off-target effects dominate a large-scale RNAi screen for modulators of the TGF-beta pathway and reveal microRNA regulation of TGFBR2.* Silence, 2011. **2**: p. 3.

106. Davis, B.N., et al., *Smad proteins bind a conserved RNA sequence to promote microRNA maturation by Drosha.* Mol Cell, 2010. **39**(3): p. 373-84.

107. Davis, B.N., et al., *SMAD proteins control DROSHA-mediated microRNA maturation.* Nature, 2008. **454**(7200): p. 56-61.

108. Mendell, J.T., et al., *c-Myc-regulated microRNAs modulate E2F1 expression.* Nature, 2005. **435**(7043): p. 839-843.

109. Sylvestre, Y., et al., *An E2F/miR-20a autoregulatory feedback loop.* J Biol Chem, 2007. **282**(4): p. 2135-43.

110. Woods, K., J.M. Thomson, and S.M. Hammond, *Direct regulation of an oncogenic micro-RNA cluster by E2F transcription factors.* J Biol Chem, 2007. **282**(4): p. 2130-4.

111. Lin, W.C., F.T. Lin, and J.R. Nevins, *Selective induction of E2F1 in response to DNA damage, mediated by ATM-dependent phosphorylation.* Genes Dev, 2001. **15**(14): p. 1833-44.

112. Xiang, J. and J. Wu, *Feud or Friend? The Role of the miR-17-92 Cluster in Tumorigenesis.* Curr Genomics, 2010. **11**(2): p. 129-35.

113. Dews, M., et al., *Augmentation of tumor angiogenesis by a Myc-activated microRNA cluster.* Nature Genetics, 2006. **38**(9): p. 1060-1065.

114. Xiao, C., et al., *Lymphoproliferative disease and autoimmunity in mice with increased miR-17-92 expression in lymphocytes.* Nat Immunol, 2008. **9**(4): p. 405-14.

115. Lu, Y., et al., *Transgenic over-expression of the microRNA miR-17-92 cluster promotes proliferation and inhibits differentiation of lung epithelial progenitor cells.* Dev Biol, 2007. **310**(2): p. 442-53.

116. Yu, Z., et al., *A cyclin D1/microRNA 17/20 regulatory feedback loop in control of breast cancer cell proliferation.* J Cell Biol, 2008. **182**(3): p. 509-17.
117. Zhang, L., et al., *microRNAs exhibit high frequency genomic alterations in human cancer.* Proc Natl Acad Sci U S A, 2006. **103**(24): p. 9136-41.
118. Yang, L., N. Belaguli, and D.H. Berger, *MicroRNA and colorectal cancer.* World J Surg, 2009. **33**(4): p. 638-46.
119. Wang, C.J., et al., *Suppression of microRNA-31 increases sensitivity to 5-FU at an early stage, and affects cell migration and invasion in HCT-116 colon cancer cells.* BMC Cancer, 2010. **10**.
120. Schepeler, T., et al., *Diagnostic and prognostic microRNAs in stage II colon cancer.* Cancer Res, 2008. **68**(15): p. 6416-24.
121. Nagel, R., et al., *Regulation of the adenomatous polyposis coli gene by the miR-135 family in colorectal cancer.* Cancer Research, 2008. **68**(14): p. 5795-5802.
122. Schetter, A.J., et al., *MicroRNA Expression Profiles Associated with Prognosis and Therapeutic Outcome in Colon Adenocarcinoma.* Tumor Biology, 2008. **29**: p. 19-19.
123. *ATCC*. [cited; Available from: http://www.lgcstandards-atcc.org/.
124. Brattain, M.G., et al., *Heterogeneity of human colon carcinoma.* Cancer Metastasis Rev, 1984. **3**(3): p. 177-91.
125. Ramasamy, A., et al., *Key issues in conducting a meta-analysis of gene expression microarray datasets.* PLoS Med, 2008. **5**(9): p. e184.
126. Barrett, T., et al., *NCBI GEO: archive for functional genomics data sets-10 years on.* Nucleic Acids Research, 2011. **39**: p. D1005-D1010.
127. Reid, J.F., et al., *Integrative approach for prioritizing cancer genes in sporadic colon cancer.* Genes Chromosomes Cancer, 2009. **48**(11): p. 953-62.
128. Locker, G.Y., et al., *ASCO 2006 update of recommendations for the use of tumor markers in gastrointestinal cancer.* Journal of Clinical Oncology, 2006. **24**(33): p. 5313-5327.
129. Duffy, M.J., et al., *Tumour markers in colorectal cancer: European Group on Tumour Markers (EGTM) guidelines for clinical use.* European Journal of Cancer, 2007. **43**(9): p. 1348-1360.
130. *miRBase*. [cited; Available from: http://www.mirbase.org/.
131. *Targetscan*. [cited; Available from: www.targetscan.org.

132. Croce, C.M., F. Petrocca, and A. Vecchione, *Emerging Role of miR-106b-25/miR-17-92 Clusters in the Control of Transforming Growth Factor beta Signaling.* Cancer Research, 2008. **68**(20): p. 8191-8194.
133. *DAVID*. [cited; Available from: http://david.abcc.ncifcrf.gov/.
134. *Sanger*. [cited; Available from: http://www.sanger.ac.uk/.
135. De Bosscher, K., C.S. Hill, and F.J. Nicolas, *Molecular and functional consequences of Smad4 C-terminal missense mutations in colorectal tumour cells.* Biochem J, 2004. **379**(Pt 1): p. 209-16.
136. Aslam, M.I., et al., *MicroRNAs are novel biomarkers of colorectal cancer.* Br J Surg, 2009. **96**(7): p. 702-10.
137. Yu, F., et al., *let-7 regulates self renewal and tumorigenicity of breast cancer cells.* Cell, 2007. **131**(6): p. 1109-23.
138. le Sage, C., et al., *Regulation of the p27(Kip1) tumor suppressor by miR-221 and miR-222 promotes cancer cell proliferation.* EMBO J, 2007. **26**(15): p. 3699-708.
139. Ye, S.C., et al., *Contextual effects of transforming growth factor beta on the tumorigenicity of human colon carcinoma cells.* Cancer Res, 1999. **59**(18): p. 4725-31.
140. Seoane, J., H.V. Le, and J. Massague, *Myc suppression of the p21(Cip1) Cdk inhibitor influences the outcome of the p53 response to DNA damage.* Nature, 2002. **419**(6908): p. 729-34.
141. Massague, J., et al., *E2F4/5 and p107 as Smad cofactors linking the TGF beta receptor to c-myc repression.* Cell, 2002. **110**(1): p. 19-32.
142. Weiler, J., J. Hunziker, and J. Hall, *Anti-miRNA oligonucleotides (AMOs): ammunition to target miRNAs implicated in human disease?* Gene Ther, 2006. **13**(6): p. 496-502.
143. Garzon, R., et al., *Distinctive microRNA signature of acute myeloid leukemia bearing cytoplasmic mutated nucleophosmin.* Proc Natl Acad Sci U S A, 2008. **105**(10): p. 3945-50.
144. Vester, B. and J. Wengel, *LNA (Locked nucleic acid): High-affinity targeting of complementary RNA and DNA.* Biochemistry, 2004. **43**(42): p. 13233-13241.
145. Sampson, V.B., et al., *MicroRNA let-7a down-regulates MYC and reverts MYC-induced growth in Burkitt lymphoma cells.* Cancer Research, 2007. **67**(20): p. 9762-9770.

146. Elmen, J., et al., *Antagonism of microRNA-122 in mice by systemically administered LNA-antimiR leads to up-regulation of a large set of predicted target mRNAs in the liver.* Nucleic Acids Research, 2008. **36**(4): p. 1153-62.

147. Sharp, P.A., M.S. Ebert, and J.R. Neilson, *MicroRNA sponges: competitive inhibitors of small RNAs in mammalian cells.* Nature Methods, 2007. **4**(9): p. 721-726.

148. Xiao, J., et al., *Novel approaches for gene-specific interference via manipulating actions of microRNAs: examination on the pacemaker channel genes HCN2 and HCN4.* J Cell Physiol, 2007. **212**(2): p. 285-92.

149. Schier, A.F., W.Y. Choi, and A.J. Giraldez, *Target protectors reveal dampening and balancing of nodal agonist and antagonist by miR-430.* Science, 2007. **318**(5848): p. 271-274.

150. Jones, P.A., et al., *Specific activation of microRNA-127 with downregulation of the proto-oncogene BCL6 by chromatin-modifying drugs in human cancer cells.* Cancer Cell, 2006. **9**(6): p. 435-443.

151. Baylin, S.B., O. Galm, and J.G. Herman, *The fundamental role of epigenetics in hematopoietic malignancies.* Blood Reviews, 2006. **20**(1): p. 1-13.

152. Aagaard, L. and J.J. Rossi, *RNAi therapeutics: principles, prospects and challenges.* Adv Drug Deliv Rev, 2007. **59**(2-3): p. 75-86.